Extracellular Matrix Stiffness Dictates Changes in Gene Expression During Breast Cancer Progression

By

Esteban R. Carrillo

A dissertation submitted in fulfillment of

the requirement for the degree of

Doctor of Philosophy

Cellular and Molecular Biology

at the

UNIVERSITY OF WISCONSIN-MADISON

2016

Date of final oral examination: 12/17/2015

The dissertation is approved by the following members of the Final Oral Committee:

Dr. Patricia Keely, Professor, Cell and Regenerative Biology
Dr. William Bement, Professor, Zoology
Dr. Anna Huttenlocher, Professor, Medical Microbiology and Immunology
Dr. Mark Burkard, Associate Professor, School of Medicine and Public Health
Dr. Pamela Kreeger, Assistant Professor, Biomedical Engineering

ACKNOWLEDGEMENTS

As with any endeavor that lasts more than 6 years, there are numerous people I have encountered along my graduate career that have left a positive impression. First, I would like to thank all the past and current members of the Keely Laboratory, especially Suzanne Ponik and Madeline Gore for their constant support. I have enjoyed all of our scientific and non-scientific discussions over beer Friday and our multiple lab outings. I truly appreciate the friendships, along with the camaraderie, that make up a delightful work place that I look forward to come to.

Second, Patti, my advisor, has provided me with the ideal lab environment. Although there was always her expertise at my disposal, I felt as though I needed to explore things for myself, and Patti encouraged me to do so. I tried and failed countless times, which I believe has turned me into a better researcher. Patti has supported me along the way by always being enthusiastic about my data and being an excellent personal cheerleader. Like myself, Patti is a parent and truly understands that having a strong family support was essential for me and the ability to balance work and home. I am very grateful for her understanding. I had the good fortune of working directly along with Dr. Bement and Dr. Kreeger when I rotated in their labs and felt their passion for good relevant, science. During my undergraduate studies, I took Dr. Bement's Cell Biology course where my interest was piqued and my passion solidified in this discipline. My committee members' comments were invaluable because they have prepared me to become a better scientist with helpful suggestions. I always eagerly anticipated meetings with Dr. Huttenlocher because she provided me with great scientific guidance and was able to give new perspectives to my data. I appreciated Dr. Burkard for meeting with me in person on a

handful of occasions where we discussed science in a more relaxed venue in which I was able to talk though many of my shortcomings and struggles. Thank you all very much.

Third, I would like to thank my parents and siblings. My parents have always encouraged me to push forward and promoted within me the notion that I am the only one responsible for my own actions. Thank you for instilling your passion for work and teaching me to face every project with enthusiasm. I would like to offer gratitude to my siblings for always bringing my ego down to earth and constantly motivating me to reach new achievements.

Finally, I have to thank my girls; my daughters Anya and Elia, and my wife, Abby, for their unconditional love and support. Cliché or not, they have been there for me at my lowest low and revitalized me when I thought I could no longer continue. Being a parent has been the greatest gift of all and being called “dad” is still my biggest privilege. Abby is undoubtedly my better half and has constantly motivated me and pushed me to improve upon every facet of my personal and professional life. I love you.

To Abby:

Roses are red, violets are blue,

I dedicate my thesis to you.

ABSTRACT

MATRIX STIFFNESS DICTATES CHANGES IN GENE EXPRESSION DURING BREAST CANCER PROGRESSION

Esteban R. Carrillo

under the supervision of Dr. Patricia Keely

at the University of Wisconsin - Madison

The greatest independent risk factor for women to develop breast cancer is mammographic density. Density in the breast is the result of high concentrations of collagen rendering the tissue stiff around the mammary ducts. Highly-aligned collagen fibers during breast cancer progression has been shown to promote metastasis and is a marker of poor patient survival. Although some molecular mechanisms have been elucidated with regards to how matrix stiffness regulates breast cancer progression, it still remains a topic that it is not well understood. Mammary epithelial cells engage with the extracellular matrix by integrin binding and FAK activation, especially under mechanically stiff conditions, that elicit changes in gene expression. FAK knock-out in the murine mammary gland inhibited tumor metastasis demonstrating that regulatory pathways under FAK merit further analysis. Downstream of FAK activity in stiff matrices are two novel pathways through MRTF-A and DDR2. Matrix stiffness regulates transcriptional activity of MRTF-A and induces the production of DDR2. MRTF-A and p53 are oppositely regulated by FAK in both normal and carcinoma cells. p53 knock-down elevates the levels of MRTF-A indicating a transcriptional repression. On the other hand, DDR2 expression correlates with the activity of FAK and the expression levels of a known transcription factor, ATF4. While DDR2 expression has been implicated in increased invasiveness there has not been a selective inhibitor

to target DDR2 to understand its functional role as a collagen receptor. In this study, we use a pharmacological inhibitor, WRG-28, to prevent DDR2 activity upon collagen binding, hereby blocking downstream interactions that may lead to proliferation and invasion. Restricting DDR2 hinders migration and the alignment of collagen fibers that further stimulate migration. Taken together, these data describe that a stiff microenvironment elicit alterations in mechanosensing through FAK, MRTF-A and DDR2. Administering inhibitors to FAK to increase p53 production and blocking DDR2 to block migration may become of crucial relevance in the battle to cure breast cancer.

TABLE OF CONTENTS

LIST OF FIGURES

Chapter 1: Introduction

Breast Cancer

Cancer typically results from mutations in genes associated with growth and development leading to uncontrolled cell proliferation and swelling of the tissue called a tumor. Tumors can be characterized as benign or malignant. Benign tumors are noncancerous groupings of cells that do not multiply at heightened rates nor spread to nearby tissues. Malignant tumors, on the other hand, proliferate at abnormally high levels. As malignant tumors develop and progress, cancer cells may metastasize, or migrate to other areas of the body and initiate tumor growth [1].

Breast cancer is the second most common cancer diagnosed in women. In the United States, 1 in 8 women will develop breast cancer at some point in their lifetime. Several factors that influence the development of breast cancer include genetic factor variants, aging, family history, environmental changes, lifestyle choices, and mammographic density. It is widely-accepted that lifestyle choices of diet, alcohol consumption, smoking, physical activity, and obesity, can have an impact on the risk of developing most cancers [1]. As a society we have made great strides to combat breast cancer. In 1975, for instance, the incidence rate for breast cancer in the United States was 105 new cases for every 100,000 women in the population and the mortality rate was 31 deaths for every 100,000 women. Since 2007, the mortality rate has declined to 23 deaths, and the trend seems to be continually decreasing. More importantly, between 1975 and 1977, 75% of women survived at least for 5 years after diagnosis. Specifically, white women survival rate was 76%, while African American women had a 62% survival rate. In 2007, of women diagnosed with breast cancer, 90% were expected to survive at least 5 years,

and white women's relative survival rate was 91% and for black women was 78% [2]. This increase in survival can be attributed to better screening techniques and improved treatment.

Many other advances in patient treatment have reduced breast cancer mortality. Examples include, breast-conserving surgery, called lumpectomy, with the addition of local radiation to replace total mastectomy, mammographic screenings as the standard for early breast cancer detection, and adjuvant chemotherapies before surgery to increase the rate of breast-conserving surgery over mastectomies. Additionally, hormonal therapy targeted for women with estrogen receptor-positive breast cancer, and antibody blocking treatment that targets HER2 (human epidermal growth factor receptor-2) to reduce its production in highly-aggressive cancers have also added to the rise in survival rates. Finally, use of genetic screening for mutated genes such as BRCA1 (Breast Cancer 1) and BRCA2 (Breast Cancer 2) has allowed for early detection of breast cancer and accurate prophylactic removal [2].

Despite all the recent improvement to treatments and screening methods, continued efforts are still necessary to enhance the quality of life for patients diagnosed with breast cancer. Although there are avenues of treatment for patients such as HER-2 positive breast cancers, there are also patients unable to receive hormonal therapy because they lack the appropriate receptors. Triple-negative breast cancers (TNBC) lack estrogen receptor (ER), progesterone receptor (PR) and HER2. TNBC are biologically more aggressive, recur at a higher rate, and women diagnosed with TNBC have a poor prognosis than other cancer subtypes. TNBC is diverse and gene profile analysis have described 6 TNBC subtypes: Basal like 1 and 2 (BL1 and BL2), immunomodulatory (IM), mesenchymal (M), mesenchymal-stem like (MSL), and a luminal androgen receptor (LAR) [3].

Cancer genomics and new findings in cell biology have the potential to lead to the identification of breast cancer before it becomes malignant. In addition, personalized medicine can be of great importance because the disease is heterogeneous with many subtypes and no single treatment can be utilized on all patients [3]. Knowing the genetic makeup of tumors via biopsies can only aid the field in the development of better individualized treatments that can be more effective and less toxic [2].

Collagen Alignment as a prognostic marker

Of interest to our lab is the diagnosis of breast cancer arising from mammographically dense tissue. Women who have over 60% collagen-dense breast tissue are four to six times more likely to develop cancer than women who have tissue of little to no density [4, 5]. This dense tissue is highly fibrous with an elevated rate of proliferation in the epithelial tissue [6]. In biopsies of these breast tissues, growth factors are found to be abundant, which adds to the likeliness of developing cancer. Of importance, collagen type I is the major contributor to mammographic density [7, 8]. Collagen can function, not only as a biochemical ligand, but as mechanical signal for mammary epithelial cells. Our lab and others have provided evidence that collagen density results in increased breast cancer aggressiveness [9].

As the tumor continues to grow, the orientation of the collagen fibers alters. The different collagen arrangements can be classified into three stages. The first is Tumor Associated Collagen Signature-1 (TACS-1) where the tumor is dense with unaligned collagen. The second is TACS-2, where collagen straightens across the tumor, which is now increased in size. In the final stage, TACS-3, the straightened collagen fibers align radially around the tumor

perpendicular to its boundary. This last step aids invasion of cancer cells to other areas of the body [10]. A human patient study was conducted to study the correlation of these collagen signatures with patient survival. Of consequence, the final stage of TACS-3 has a strong correlation with poor patient survival. Therefore, analysis of collagen fibers alignment may be an efficient predictor of human breast cancer survival [11].

Relevance of *in vitro* and *in vivo* models for understanding breast density and cancer progression

Collagen dense mouse model

The stromal tissue surrounding the ducts and lobules in the breast is comprised primarily of type-I collagen and provides the mechanical cues to maintain normal cell behavior. When collagen density in the stroma is altered it can greatly influence carcinoma development [12]. However, the cellular mechanisms involved in cancer progression within the context of a dense-collagen microenvironment remain unclear. Therefore, the field has strived to generate a model to study the effect of collagen density on normal and cancer cells. For *in vivo* murine models, Dr. Rudolph Jaenish created a transgenic mouse strain in which there is a copy of the collagen I alpha 1 gene that renders a mutated collagen 1a1 chain at the collagenase cleavage site to produce a protein resistant to collagenase. This mouse, Col1a1^{tm1Jae} , exhibits a high density phenotype due to the inability of collagenase to cleave collagen resulting in a three-fold increase in stromal collagen [9, 13]. To study tumor formation in the mammary glands, Col1a1^{tm1Jae} were crossed with a transgenic mouse strain, Polyomavirus middle-T, under the control of the mammary specific MMTV promoter (PyVT). This cross created tumor-bearing animals within a

collagen-dense stromal tumor microenvironment. PyVT/Col1a1 mice increased tumor formation by three-fold, as well as producing three-fold more metastases to the lung than PyVT/wild type (wt) [9]. This pivotal study in a murine model recapitulated the observations made in human patients that link collagen-dense environments, tumor formation, and invasiveness.

Collagen 3D gels

Although it is convenient to passage and propagate cells on tissue-culture treated dishes, in reality, mammary epithelial cells are surrounded by many proteins and cell types in a three-dimensional (3D) environment. Studies investigating mammary gland development have demonstrated that the tissue microenvironment and its remodeling sustains normal cell behavior and also promotes tumor formation along with tumor progression [14-16]. Our laboratory, among others, has developed and mastered an *in vitro* model of a native 3D microenvironment.

This *in vitro* model will benefit researchers as we make an effort to further understand how cells respond to a dense or stiff microenvironment. Our research uses collagen matrices as a 3D representation of the *in vivo* microenvironment [17]. In these 3D matrices, collagen can be manipulated to increase its density and, therefore, its stiffness, which reproduces the conditions encountered by mammary epithelial cells (MECs) in dense breast tissue. MECs, namely T47D and MCF10A, are able to contract the matrix and differentiate into tubules when they encounter matrices that are soft, low-density collagen gels. In contrast, this phenotype is no longer existent when the matrix is stiff or the gel density is high. This results in the loss of tubule formation as cells develop into a different, invasive phenotype [18-20].

MECs that are embedded in a high-density collagen environment are unable to use the cell's contraction ability to modify the collagen gel. Although changing the concentration of

collagen can inherently make the matrix stiff, one could argue that ligand concentration is also increased making it hard to differentiate whether the downstream signaling events are due to mechanical stiffness or ligand density. To circumvent this issue, we have also used collagen gels of the same density at different stiffnesses to avoid the introduction of cross-linking molecules [21]. We produce a stiff matrix in cell culture by pouring a collagen gel and allowing it to polymerize for 2 hours at room temperature. After this time, we can either choose to release the gel by gently sliding a pipette tip around the gel or leaving the sides of the gel attached to the non-tissue culture plate well. The latter produces a stiff environment in which cells are pulling on the matrix but unable to contract it, while the released or soft matrix can be contracted and modified.

Breast cancer progression models

Human breast carcinomas are typically thought to evolve when transformations occur from normal epithelium to benign hyperplasia to atypical hyperplasia to ductal carcinoma *in situ* to malignant/invasive tumors. In order to analyze this sequence of events, Santner *et al.* derived a model that uses this progression from a common genetic background [22]. The researchers implanted xenografts of premalignant human MECs that produced carcinomas and were later isolated. These cell lines were cultured and tested for experimental and spontaneous metastasis to assess their metastatic potential. The progression ranged from the normal epithelial to ductal carcinoma *in situ* to invasive carcinoma or MCF10A, MCF10-DCIS, MCF10-Ca1d, respectively [22].

Even though the MCF10-Ca1d lineage resembles a metastatic cell line, it does not offer some of the characteristics that reflect the spectrum of metastatic disease in breast cancer. The

increased death rate in human patients with cancer is due to the metastatic growth in distal sites that eventually impair the function of such vital organs. Some cancer cells may leave the tumor after acquiring genetic and epigenetic mutations that allows them to degrade the surrounding basement membrane. Tumor cells invade into the stroma where they will interact with collagen fibers, fibroblasts and immune cells that will collaborate to intravasate the endothelial lining. Here, metastatic cells may reside in the bone marrow to proliferate or remain dormant. Tumor cell dormancy relates to the state in which tumor cells pause their physiological activities and become quiescent. At this stage, the disease is asymptomatic as cells are in cell cycle arrest and have not yet colonized any particular organ [23].

Aside from bone, tumor cells can be dormant in lymph nodes or in the surrounding vasculature of a target organ before extravasation. Tumor cells have then four fates at this stage: undergo apoptosis, enter a dormancy state as single cells, enter a quiescent arrest as a micrometastatic lesion, or restart proliferation [23]. After treatment of breast cancer by mastectomy, 20-45% of patients suffered from cancer recurrence even 10 years after relapse with the majority of patients relapsing in the first 5 years [24]. Cancer dormancy has been an elusive field of study due to the lack of a dependent model and the inability to isolate disseminated cells that will become dormant. Despite having the ability of having isogenic cell lines that are non-metastatic (normal) vs. metastatic, it does not encompass the gamut of the disease in humans.

Invasion, intravasation, dissemination, transport, extravasation, and proliferation are the stages tumor cells have to go through to be considered metastatic. If tumor cells fail to progress into metastatic stages they are deemed non-metastatic carcinoma cells. Subpopulations of tumor cells that summarize these stages were isolated from a single, spontaneous tumor in BalB/C

mouse strain and the progression subset of cell lines were derived from this original tumor are briefly described [25]. 67NR cells fail to leave the primary tumor site. 168FAR cells can reach lymph nodes, but fail to progress into further stages. 4T07 cells are highly-tumorigenic and disseminate consistently as they can be found in the blood and lung; however, they fail to metastasize as visible macro metastases never form. Lastly, the highly-invasive 4T1 cell line metastasizes to the lung, liver, bone, and brain via vasculature dissemination [25]. It is unknown what restarts proliferation of dormant cells that produces metastases years after the original diagnosis. Aguirre-Guiso *et al* (1999), showed in head and neck carcinoma that the microenvironment (fibronectin) relayed signals that were essential to drive tumorigenesis. When the mechanotransduction pathway via fibronectin was blocked, cells became dormant in *in vivo* demonstrating that the ECM may drive cells out of dormancy [26]. Collagen stiffness has been documented to drive tumor growth and metastasis in a mouse transgenic model [9]. Since invasive, non-metastatic cells are constantly interacting with collagen either at the tumor site or target organs, it is unknown whether dormant cells can convert these biophysical signals from the ECM into an exit out of dormancy and toward proliferation.

FAK and ERK are essential players in mechano-signal transduction

Mechanotransduction is the process where cells elicit a response after sensing mechanical signals or forces and convert these into biochemical signaling pathways. These signaling pathways are comprised of myriads of complex protein interactions that regulate processes such as gene expression, proliferation, migration, dormancy, differentiation and apoptosis [27]. Signaling pathways can stem from sites of focal adhesion that are formed due to integrin binding

to the ECM receptors for cell adhesion. Although integrins are not the only receptors for the ECM they adhere more robustly than other receptors and are the most well-studied [28]. Integrins are transmembrane protein heterodimers containing α and β subunits. The exact combination of α and β subunits determines the specificity of which ECM protein is bound, resulting in downstream signaling events. Integrins possess extracellular domains, single transmembrane helices, and cytoplasmic tails that mediate cytoskeletal interactions. Their activation is modified by a change in conformation that relate to low- and high-affinity states depending on the type of stimuli. Conformational changes display either an active state where these receptors are fully extended allowing the extracellular domain to bind ligands or an inactive state, in which the binding portion is bent and is in a compact, closed configuration.

In the mammary gland, fibrillar collagen type I is the primary ECM protein and the integrin receptor for this collagen type, α2β1 integrin, is expressed on mammary epithelial and mesenchymal cells, which are components of the breast microenvironment [7]. Applying a force to integrin ligands fortifies the interaction between integrins and the cytoskeleton, and amplifies integrin clustering forming focal adhesions [29, 30]. Mechanical matrix rigidity drives numbers of focal adhesion sites and enhances integrin-cytoskeletal forces [31]. There are many central building blocks in the mechanically induced intracellular signaling cascade, which include two hubs of signaling interactions: focal adhesion kinase (FAK) and extracellular signal-regulated kinase (ERK). FAK is a non-receptor tyrosine kinase that functions as a critical signaling molecule and localizes to sites of focal adhesion to influence cell proliferation, survival and migration. Subsequent to integrin activation, focal adhesions assemble by recruitment of cytoplasmic partners to complex including talin, vinculin and α-actinin [32]. Along these

proteins, FAK is also recruited to the focal adhesion complex. FAK is phosphorylated at several Tyr residues, starting with Tyr397, site of autophosphorylation or p-FAK. This creates an SH2 binding site for Src, SHC, PI3K, Grb7 and PLCγ [33]. Src is another non-receptor tyrosine kinase; when bound to p-FAK-Y397, Src further phosphorylates FAK in the kinase domain to increase its activity, and phosphorylates FAK at Tyr925, creating a binding site for Grb2-SOS complex [33].

Grb2 docking prompts a signaling cascade that leads to the activation of Ras, Raf, MEK, and ERK, which then is able to modify gene expression and promote cell proliferation [34]. ERK is part of the mitogen-activated protein kinase (MAPK) family and it has been well documented as it is involved in proliferation, differentiation, survival, and apoptotic events [35]. It has been well established in seminal research studies that activation of FAK after integrin engagement signals to the RAS/ERK pathway [36, 37]. The small G-protein, Ras, recruits Raf kinases to the plasma membrane for activation after Ras exchanges its GDP for GTP. Raf kinase, a MAP3K, further phosphorylates MAPKK tier proteins, MAPK/ERK kinases (MEKs). The linear MEKs cascade is characterized as MEKs being phosphorylated on two Ser residues (Ser218 and Ser222) and becoming activated. MEKs are dual-specificity Tyr/Thr kinases that phosphorylate ERKs (p-ERK), thereby activating ERK1 and ERK2. ERK1/2 are 44kDa and 42kDa proteins responsible for further phosphorylating several transcription factors that control proliferation. The series of kinases from RAF to MEK to MAPK provide opportunities for feedback regulation and signal amplification [35].

A stiff microenvironment activates ERK in normal mammary epithelial cells, while basal levels are observed on soft matrices [34, 38]. While cells in a stiff matrix have more protrusions,

the inhibition of ERK via MEK reverts this phenotype resembling to what is observed in soft matrices [34]. As ERK controls proliferation, the activity levels of ERK is low in cells cultured in a soft collagen matrix, it is hypothesized that a soft matrix does not support a proliferative, invasive environment. Several growth factor receptors also signal to p-FAK and p-ERK, including platelet-derived growth factor (PDGF), epidermal growth factor (EGF), hepatocyte growth-factor (HGF) [39]. Interestingly in 3D soft matrices, the addition of HGF to either normal or transformed mammary epithelial cells promotes cell invasion indicating that HGF may enhance integrin/FAK/paxillin complex [34]. In 3D *in vitro* environments, ERK activation is regulated by using a dominant negative FAK, FRNK, which inhibits FAK function and reduces p-ERK responsiveness to stiffness in non-carcinoma cell lines. And, thus, the field of 3D matrix biology is attempting to unveil the connections between these two pivotal molecules that will elucidate how proliferation is regulated in both normal and carcinoma cells.

Collagen and DDR2

Discoidin domain receptors are an understudied group of receptor tyrosine kinases (RTKs) that are activated by collagen. The transmembrane proteins discoidin domain receptors, DDR1 and DDR2 contain a discoidin homology (DS) domain in the extracellular region. The ectodomains of DDRs consist of: an N-terminal DS domain and a second globular domain (Discoidin 2) that is unique to DDRs. A single transmembrane domain links the extracellular region to the cytoplasmic region, which contains the C-terminal kinase domain, connected to a juxtamembrane region. DDRs are special RTKs as they form dimers regardless of the ligand state unlike other inactive monomeric RTKs [40]. DDRs get their name from *Dictyostelium*

discoideum, as the DS portion is homologous to a protein from this organism; however, the DDRs differ in function as they contain a collagen binding domain that specifically mediates attachment to different types of collagen [41]. DDR1 and DDR2 are predicted to be post-translationally modified by *N*- or *O*-glycosylation, although there is no evidence as to how it may affect, if at all, its activation (Figure 1-1).

Furthermore, DDRs are activated by an ECM protein, collagen, in contrast to other RTKs that are activated by cytokines, peptide-like growth factors [42]. DDR1 is mostly found in epithelial cells, and DDR2 is primarily expressed in mesenchymal cells [43]. DDRs have a wide range of collagen-binding partners, but they do require a native, triple-helical collagen conformation, as heat-denatured collagen does not bind to neither DDR [42]. Though, DDR1 and DDR2 have preferences for collagens, both will bind to collagens I-III and V. DDR1 selectively binds to IV and DDR2 to X [44]. This suggests that migrating cells may employ different DDRs during invasive processes depending on the collagen matrix cells may encounter [45]. The primary binding site for both DDR1 and DDR2 in collagens is identified as the GVMGFO motif (where O is hydroxyproline). Once DS domains in DDRs bind to collagen, it activates the cytosolic kinase domain by autophosphorylation due to a possible conformational change, although this is not completely known [46].

Interestingly, DDR activation is slow, reaching full potential after 18h in some cell types, unlike other typical RTKs that are activated within seconds [42]. Classical RTKs respond to stimuli by negative feedback loops that include receptor internalization, degradation or phosphatase activation. After DDR activation, though, their phosphorylation levels linger for days [42]. One hypothesis to the persistent activity of DDRs is to counteract and recycle the

activity of other RTKs and integrins. Integrins and FAK activation occurs within minutes of collagen binding, DDRs might have evolved to down-regulate these signals; however, many questions remain as to the basis for this persistent activation [44]. Upon collagen binding and DDR activation, downstream signals impact matrix remodeling by controlling matrix metalloproteinases (MMPs) expression [47, 48]. A proto-oncogene, Src, is required for full DDR phosphorylation, and these phosphorylation sites serve as docking sites to other molecules (SchA and Nck2) [42]. ERK, a pivotal signaling molecule, is also regulated by DDR activation, although it is either activated or inhibited depending on the cell type [44]. In pancreatic cancer cells, N-cadherin expression up-regulation that leads to epithelial-mesenchymal transition (EMT) is controlled by DDR1/Pyk2, while in MDCK (Madin-Darby Canine Kidney) cells, DDR1 form a complex with E-cadherin, indicating that DDR1 interacts and modulates other membrane molecules important for cell-cell contact [49, 50]. EMT is characterized as epithelial cells undergo a loss in cell polarity and cell-cell adhesion (E-cadherin) and gain migratory and invasive properties (N-cadherin). In monkey kidney epithelial cells (COS1), DDR1 can have its ectodomain cleaved by MMPs with or without collagen I-induction. This ectodomain shedding can have a powerful effect on the the downstream activation of DDR1 as it will restrict further signaling from DDR1. Although, the consequences of this cleavage are not completely determined, shedding of DDR2 is unknown, which suggests selectivity in the pool of receptors that control collagen-induced signaling [51]. In osteoblasts, Runx2, a transcription factor, is activated by p38 MAPK downstream of DDR2 [52].

DDRs are phosphorylated independent of β1 integrins and their cross-talk is not well-understood in terms of cross-activation and possible interplay [53]. What it is known is that both

integrins and DDRs recognize, with no overlap, distinct specific amino acid sequences in collagen, and DDR expression permits more secure cell adhesions suggesting a positive regulation by enhancing integrin activation [54].

DDR2 and disease

While DDR1 is functionally similar to DDR2, the latter has been shown to be more involved in disease progression. For instance, in vascular smooth muscle cells (VSMCs) hypoxic environments drive the expression of DDR2 and MMP-2. DDR2 expression is regulated the stress signal p38-MAPK and the binding of Myc-Max to the DNA promoter region of DDR2. Hypoxia in this system regulates proliferation and migration, suspected by the increase of DDR2 protein levels, although the mechanisms are not known [55]. In hepatic stellate (HS) cell activation, miR-29b over-expression initiates cell quiescence as this controls DDR2 and collagen Type I, among others. Knowing that DDR2 is an "invasive" marker, miR-29b could be a marker for suppressing the activation of HS cells and subsequent liver fibrosis [56]. In squamous cell carcinoma (SCC) in the lung, analysis of patient tyrosine kinome it was found that a mutated DDR2 was sensitive to a multi-purpose kinase inhibitor. It was determined that a gain-of-function DDR2 in SCC may be a target of interest [57].

Furthermore, in breast cancer, DDR2 was identified to be a marker for prognosis while looking at 122 patient tumor samples. Ren *et al.* (2013) demonstrated that the relative mRNA levels of DDR2 and expression patterns by immunohistochemistry were increased by six-fold when compared to DDR1 in paired samples of tumorigenic versus normal tissue. In a study of patient survival, negative expression of DDR2 was found to be correlated with better disease-free survival [58]. Also, MDA-MB-231 ectopically expressing a constitutively active DDR2 in

xenografts was found to be more aggressive as more metastases were found and it drastically decreased survival in contrast to WT DDR2-bearing animals. At the same time, breast cancer cells that were DDR2-depleted harbored less metastases, although tumor growth was not inhibited [59]. Moreover, DDR2 expression has been associated with regulating levels of Snail and E-cadherin, markers responsible for EMT, in both human and murine cancer cell lines [59, 60].

While many advances have been made regarding the kinetics of DDR2 after collagen stimulation, as well as submitting that DDR2 elevated expression associates with many cancers, the molecular mechanisms and the repercussions of how DDR2 expression is controlled remains unknown. Namely, *in vitro* experiments have not shifted to appreciate the contribution of DDR2 as collagen receptor in a 3D architectural context.

RhoA and MRTF-A signaling as a link between mechanical cues and gene expression

Rho is a small GTPase that acts as a molecular 'switch', depending on the stimuli [61]. Rho can either be active by binding to GTP or inactive by being GDP bound. Following the exchange of GDP for GTP, Rho becomes active and is prone to interact with downstream effectors such as Rho kinase (ROCK). Rho-GTP activates ROCK by inducing a conformational change in the molecule, subsequently ROCK phosphorylates myosin light chain (MLC) and an inactivation of MLC phosphatase, which generates an increase in actomyosin contractility [62, 63]. Rho/ROCK signaling is one of the known mechanisms by which the cells sense ECM stiffness signaling [19, 64]. RhoA activity is higher in a stiff 3D collagen matrix than when cells are plated in a soft 3D matrix and RhoA/ROCK inhibitors block contraction and tubule

differentiation in soft matrices [19, 20].

One cellular process already introduced, by which cells respond to stiffness of the microenvironment is through activation of integrins and FAK. Subsequently, FAK regulates Rho activity potentially through activation or inactivation of Rho regulators. To determine the mechanism by which FAK regulates RhoA in response to increased matrix stiffness, FAK was knocked down in cells cultured in soft and stiff collagen gels. It was also established that in FAK-depleted cells RhoA and RhoA-regulators were being down-regulated [20]. Demonstrating how signal transduction affects transcriptional activity which leads to an increase in RhoA is highly significant because it will allow us to further understand signaling mechanisms that govern cell contractility.

RhoA activation alters actin dynamics, by specifically targeting the assembly of actin stress fibers that are formed by the polymerization of globular actin (g-actin) into stable filamentous actin (f-actin) [65]. Because RhoA activity is elevated in stiff matrices, f-actin/g-actin ratio is also higher, aided by the ROCK/LIM kinase-cofilin pathway [20, 66].

Links between Rho-GTPase and transcriptional regulation

RhoA regulates a handful of transcription factors, pointing to possible mechanisms by which RhoA could regulate gene transcription. RhoA influences the activity of serum response factor (SRF), a transcriptional activator of immediate early genes and skeletal muscle genes [67-69]. It was determined that actin dynamics, including mDia1, effect on fiber stabilization, directly affect the expression of SRF target genes, including SRF itself, under serum-induced conditions [66, 70].

RhoA also regulates a member of the myocardin family of cardiac transcription factors, myocardin-related transcription factor-A (MRTF-A). MRTF-A binds to g-actin, which serves to inhibit its functionality, and thus it is subject to release from the cytoskeleton upon actin polymerization. Moreover, MRTF-A binds tightly to SRF as a co-activator to regulate gene transcription after SRF binds to a CArG DNA sequence also known as the serum response element (SRE) [68, 71, 72]. While SRF can also interact with members of the ternary complex factor (TCF) family by MAP kinase phosphorylation, during RhoA activation SRF exclusively binds to MRTF-A [67, 73, 74]. TCFs are phosphorylated in the nucleus by ERK via the MAPK pathway and activate SRF target genes. However, this activation can be repressed upon serum stimulation since this activates the RhoA/ROCK pathway; similarly, ERK activation enhances MRTF-A phosphorylation and release from SRF [75, 76]. This triggers the export of MRTF-A out of the nucleus by increasing the affinity to g-actin [76]. RhoA activates effectors that lead to an increase in f-actin, shuttling of MRTF-A to the nucleus and increase in the SRF transcriptional activity. In addition to binding to SRF, TCF carries a DNA recognition binding site that attaches to DNA upstream of the SRE, while MRTF-A, on the other hand, lacks such domain and binds directly to SRF (Figure 1-2).

Once in the nucleus MRTF-A forms a complex with SRF through basic and Q-rich domains and activates downstream genes through its transcriptional activation domain [68, 77]. Most of the work on MRTF-A has involved the study of gene expression in myofibroblasts and smooth muscle differentiation in 2D matrices, though some investigators are starting to explore the role of MRTF-A in mechanical signaling [74, 78-82]. Still, it is not completely understood as to how MRTF-A is controlled by 3D stiffness both at the activity and expression levels as cells

respond to stiffness by FAK/Rho/ERK regulation [34]. The signaling cascades that define these co-activators of SRF differ will be of significance as we try to discern the transcriptional activity that is contributed from each of these pathways.

Stiff-collagen stroma increases the risk of breast cancer [83]. Even though we have found that stiffness of the microenvironment has an impact in the Rho/ROCK pathway, the cellular events as to why this increase in stiffness promotes cancer progression is unknown. RhoA-GTP levels are dramatically increased when cells encounter stiff matrices, especially in metastatic cells [19, 64, 84]. The transcriptional function and expression of MRTF-A, in turn, may be imperative to control expression of genes that are regulators of proliferation, migration and colonization during breast cancer metastasis. In addition, the link between Rho activity, actin dynamics, and gene transcription is relevant because it directly ties ECM mechanical cues to adaptations in gene expression.

Hypothesis

Mammary epithelial cells that encounter a mechanically stiff collagen environment transmit signals via engagement of integrins and FAK activation. The up-regulation of these events aid in the progression of breast cancer and are controlled by matrix stiffness. In response to altered matrix density, the signaling pathways controlled by integrins and the FAK complex that elicit proliferation and invasion are not well understood. **Here, we propose to explore two signaling cascades through MRTF-A and DDR2, which are regulated by FAK activation in response to a stiff collagen matrix.** Matrix stiffness enhances RhoA activity, which is known to regulate upstream effectors of MRTF-A activity. Similarly, a stiff matrix promotes cell invasiveness and in human invasive breast cancer tissues, the expression of DDR2 is amplified compared to normal breast tissue. Thus, ***I hypothesize that under stiff collagen matrix conditions, mammary carcinoma/epithelial cells activate FAK, which subsequently regulates both MRTF-A and DDR2 resulting in invasiveness and proliferative behaviors.*** The following chapters will address this hypothesis (Figure 1-3).

Figure 1-1. Structural features and domains of DDR2

Discoidin domain receptor 2 (DDR2) is identified as a collagen receptor that interacts via its DS (Discoidin 1) domain on its extracellular domain. It binds native, triple-helical collagen fibers and is activated by collagens I, II, III, V, and X. The DS domain on its N-terminus is followed by a DS-like (Discoidin 2) domain and extracellular juxtamembrane (JM) region. Single-pass transmembrane (TM) domain is followed by a cytoplasmic JM and the kinase domain with a short C-terminus tail. Post translational modifications predicted *N*-glycosylation sites are depicted by red dots and predicted *O*-glycosylation sites are indicated by blue dots. Mutated DDR2 residues (black), which were identified in samples of non-small cell lung carcinomas. This figure is adapted from [85].

Figure 1-1. Structural features and domains of DDR2

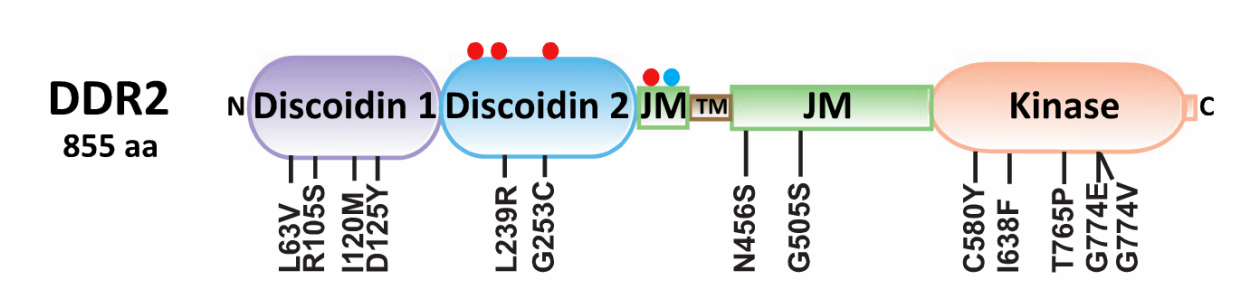

Figure 1-2. Transcriptional activity induction of MRTF-A by RhoA

Myocardin related transcription factor A (MRTF-A) is a co-activator that is transcriptionally active upon serum-induction. In this model, lysophosphatidic acid (LPA) in serum stimulates G-protein-coupled receptors that subsequently activates RhoA. RhoA-GTP forms and stabilizes filamentous actin (f-actin) by polymerizing monomeric/globular actin (g-actin) via two pathways: ROCK/cofilin and mDia1. MRTF-A is bound to g-actin in the cytoplasm and its release is regulated by f-actin formation. MRTF-A contains a nuclear localization signal that enables its entry into the nucleus to form a complex with serum response factor (SRF) transcription factor. MAPK/ERK pathway can also elicit a response from SRF by the binding of a member of the ternary complex factor (TCF) family of transcription factors. ERK can regulate the binding of SRF/MRTF-A complex by phosphorylating MRTF-A in the nucleus to initiate its release from SRF and its nuclear export by increasing g-actin binding. This figure was adapted from [76]

Figure 1-2 Transcriptional activity induction of MRTF-A by RhoA

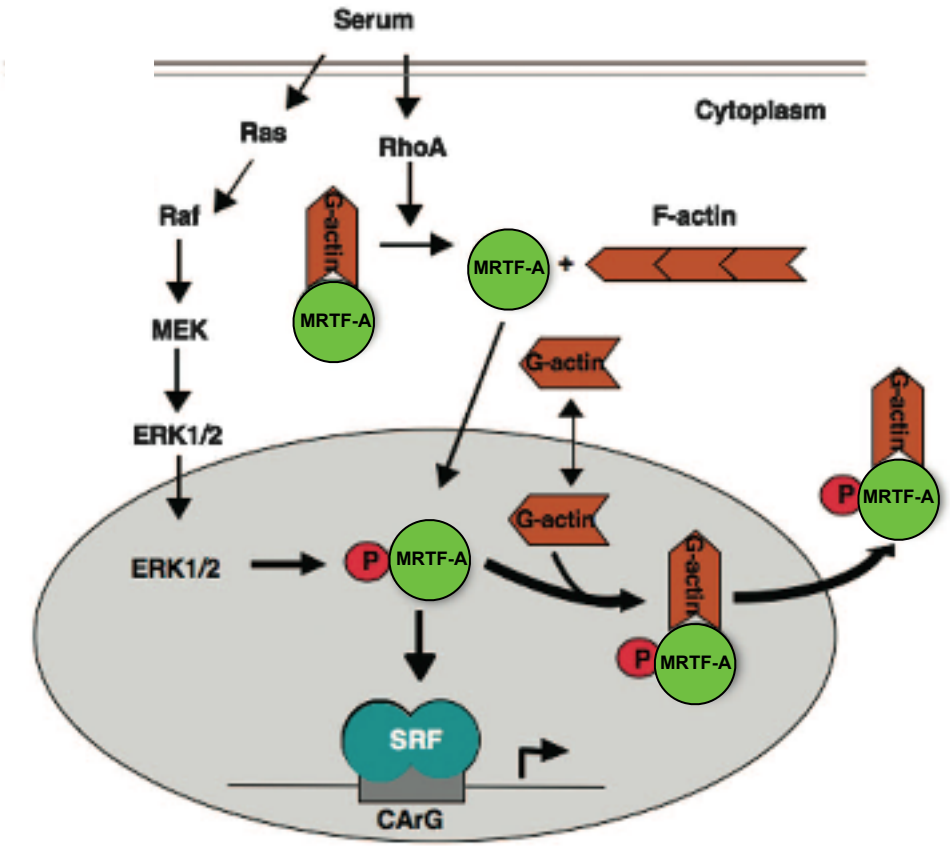

Figure 1-3. A stiff environment modulates FAK activity and downstream pathways

My thesis work will delve into exploring two signaling events downstream of FAK activation: MRTF-A and DDR2. Matrix stiffness enhances RhoA activity, which frees MRTF-A into the nucleus via MLC and mDia mechanisms as g-actin polymerizes. Likewise, a stiff microenvironment promotes cell invasive behavior and EMT. DDR2 aids in this transition and its over-expression has been measured in breast cancer tissues when compared to normal breast tissue. FAK, a crucial focal adhesion molecule, subsequently regulates both MRTF-A and DDR2. Solid lines= already known and published. Dashed lines= Work contained in this thesis.

Figure 1-3. Model of regulation downstream of FAK

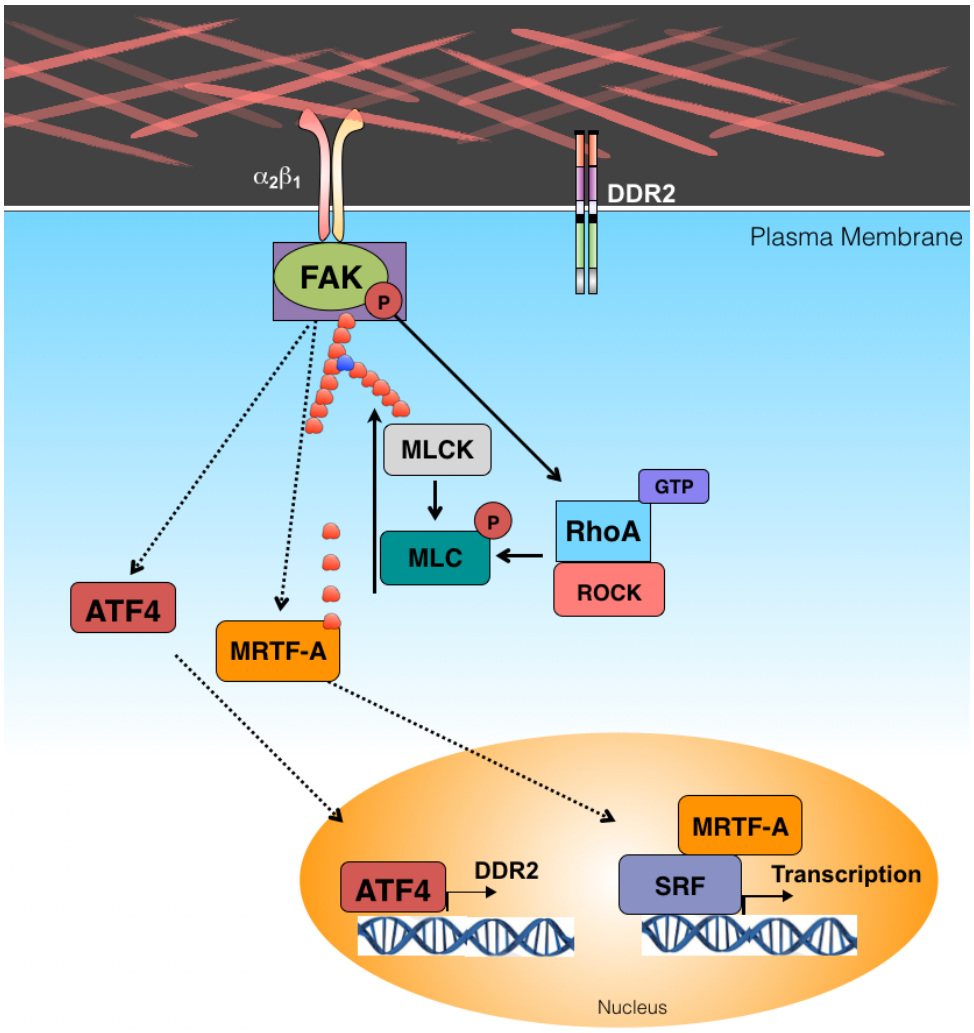

Chapter 2: MRTF-A activity in stiff matrices

Title: MRTF-A, an SRF co-activator, is regulated by FAK and p53 in 3D collagen environments.

ABSTRACT

Mammary epithelial cells that engage the ECM via integrin-FAK activation relay a cascade of signals that transduce changes in cell behavior. Essential changes that contribute to the progression of breast cancer including cell proliferation, survival, and migration are due to the tight regulation of gene expression. In breast cancer progression the ECM is remodeled by alignment of collagen fibers, which become intrinsically stiffer. The stiffness of the ECM drives Rho-mediated contraction, integrin clustering, and formation of focal adhesions in the cell. Activity of FAK in response to a dense matrix becomes a hub for transducing outside-in signaling that enables Rho activation and p53 regulation. Targeted FAK knock-out in the mammary gland of a murine mouse model reduced metastases and tumor burden mass. Here, we examined the role of the transcription factor, MRTF-A, in controlling gene expression in response to FAK activation within a 3D collagen environment. The activity of MRTF-A was significantly higher in stiff matrices and is regulated by FAK. Additionally, the endogenous MRTF-A targets, SRF and TnC, were up-regulated at the mRNA level in non-carcinoma epithelial cells. FAK inhibition led to an increase in p53 production, and MRTF-A contains a transcriptional binding site for p53. In normal MECs, p53 knock-down increased MRTF-A production contributing to the transcriptional regulation. Thus, FAK activity differentially

regulates downstream targets in normal versus carcinoma epithelial cells by targeting MRTF-A and p53.

INTRODUCTION

Increased mammographic density tissue, which is comprised primarily of type-1 collagen, has been shown to increase the likelihood for women to develop breast cancer four- to six-fold [4, 5, 83]. Collagen type I is the most abundant protein in the body, and in the breast, it surrounds the mammary gland as part of the extracellular matrix (ECM) milieu [7]. Collagen is a component of the ECM known to interact with cell surface integrins in mammary gland development and in tumor progression [14, 16]. We have previously found that increased stromal collagen in mouse mammary tissue significantly increases tumor formation and pulmonary metastases [9]. Furthermore, collagen has an essential role in the activation of focal adhesion kinase (FAK) in human mammary epithelial cells. In addition, FAK over-expression is measured in many tumors including breast, colon, melanomas, thyroid, and others [86, 87]. The exact mechanisms by which FAK mediates these responses are not well understood. Targeted knock-down of FAK in the mammary epithelium significantly reduced tumor growth compared to a wild-type control in a transgenic murine model [34, 88]. Notably, although there were fewer tumors, FAK-/- tumors did form, but were neither invasive nor metastatic. Comparison of gene expression profiles demonstrated hundreds of genes whose expression was altered upon loss of FAK, many of them regulated by the transcriptional regulator, p53.

A widely known tumor suppressor, p53 has been identified as a critical target for many genetic alterations in human cancers. p53, as a transcription factor, tightly controls cell death under the induction of cell stress, hypoxia, and DNA damage [89]. p53 also regulates genes such

as p21, cyclin G and Bax that control cell cycle arrest and cell death [89]. Moreover, p53 binds to the promoter region of FAK *in vivo,* and ectopic over-expression of p53 blocks FAK expression at the mRNA and protein levels [90, 91]. FAK itself may be a transcriptional regulator upon loss of adhesion, wherein it translocates to the nucleus and associates with p53 to facilitate p53 turnover via a ubiquitin-dependent manner [92]. These findings suggest that p53 mis-regulation along with FAK activation may promote cancer progression. However, a viable treatment for human patients to regulate cell death and control proliferation through FAK-p53 has not been addressed.

Interestingly, the myocardin related transcription factor-A (MRTF-A) has been linked to tumor metastases in a murine model of breast cancer [93, 94]. In breast cancer cell lines in culture, depletion of MRTF-A leads to a reduction in cell adhesion, spreading, invasion, and motility without affecting proliferation or inducing apoptosis [95]. MRTF-A is a member of the myocardin family of transcriptional coactivators that regulate serum response factor (SRF) activity during cell growth, migration, and myogenesis [96-99]. The actin-sensitivity of SRF activity is reportedly due to sequestration of MRTF-A in the cytoplasm by direct binding to g-actin [66, 100]. Decreased monomeric actin and increased actin polymerization in response to RhoA signaling results in the translocation of MRTF-A to the nucleus, and the consequent activation of SRF by its binding to a DNA region in target genes at the serum response element (SRE) [101-103]. Moreover, extracellular signal-regulated kinase (ERK) activation regulates SRF transcriptional activity by the binding of proteins from the ternary complex factors (TCF) family [104, 105]. Thus, SRF is ultimately regulated by RhoA and ERK pathways due to its association with different transcriptional activators.

Taken together, these findings suggest that MRTF-A and SRF may be controlled by a stiff environment through FAK and ERK. Here, we sought to identify how the activity of MRTF-A is influenced by collagen stiffness and the link between FAK-p53-MRTF-A in breast cancer progression. We find that stiff matrices regulate RhoA transcriptional activity via SRF/MRTF-A and that p-FAK controls this activity. Additionally, we show for the first time that p-FAK inhibition negatively controls p53 expression in both normal and carcinoma cell lines.

RESULTS

Transcriptional activity of SRF is dependent on matrix stiffness

We first assessed the role of matrix stiffness on gene regulation by using a reporter construct carrying a luciferase gene downstream of an SRE element that can be recognized by SRF [106]. SRF can respond to either MAPK pathway (ERK) or RhoA activation; both of which are activated in stiff matrices [19, 20, 70, 73]. To examine SRF regulation in normal human mammary epithelial cells (MECs), we used the MCF10A cell line. MCF10A cells were transfected with the luciferase construct, pSRE-luc, and a *Renilla* vector for normalization. MCF10A cells were then seeded in collagen gels at concentrations that the cells could contract (1.3mg/mL, soft) and increasing until MCF10A cells were no longer able to contract the gel, creating a stiff environment at 3mg/mL collagen. As the collagen concentration increased, SRE luciferase activity was also increased (Figure 2-1A), indicating that SRF activation increases with matrix stiffness.

RhoA and ERK signaling pathways both control downstream gene expression via SRF, but have different known effectors. SRF contains a protein interaction domain that has high affinity for both a member of the ternary complex factor (TCF) family or MRTF-A, but not

simultaneously [70, 73]. These two proteins compete for SRF's binding, but this competition can be ameliorated depending on how the cell is stimulated and the cell type [74, 107]. To test whether RhoA and/or ERK activity were essential for the up-regulation of SRF-dependent gene expression, we used pharmacological inhibitors. Cells were treated with cell-permeable C3 Exoenzyme to block Rho activity, H-1152 which perturbs ROCK kinase activity, or U0126 to block MEK activation thus, blocking ERK phosphorylation. All three treatments decreased luciferase levels, demonstrating that SRF transcriptional activity was dependent on both RhoA and ERK pathways when cells were presented with a stiff matrix (Figure 2-1B).

Increased collagen density activates SRF downstream of RhoA activation

RhoA and ERK pathways control the binding of SRF to the SRE DNA sequence using different upstream pathways. Both TCFs and MRTF-A compete for binding SRF, making SRF the limiting factor for controlling subsequent gene expression [108]. To examine the mechanoregulation that MCF10A cells exhibit in stiff matrices, we investigated the contribution of the RhoA pathway using a modified luciferase vector, pSRF-RE, which carries a mutation on the DNA binding site for TCF, abolishing any binding of TCF with this reporter. After we verified that pSRF-RE luciferase activity was also regulated by collagen density, we examined whether it only responds to RhoA activation (Figure 2-2A). We probed this by using the pharmacological inhibitors, C3 Exoenzyme and U0126. When compared to untreated conditions we measured an expected down-regulation of pSRF-RE when gels were treated with C3 Exoenzyme. On the other hand, U0126 did not inhibit pSRF-RE reporter levels, and actually increased its activation, indicating that transcription measured by the reporter is not stimulated by MEK/ERK, but rather by the Rho/MRTF-A pathway (Figure 2-2A). Furthermore, given that

MRTF-A relies on actin polymerization to become a functional transcriptional factor, we tested this by treatment with drugs that stabilize (Jasplakinolide) or inhibit (Cytochalasin D) actin filaments and confirmed that MRTF-A activation depends on the pool of g-actin [66, 100, 109] (Figure 2-2B).

SRF activity is regulated by heterotypic mechanical coupling between fibroblasts and epithelial cells

Next, we tested whether the co-culture with human mammary fibroblasts (HMFs) have an impact on the SRF/MRTF-A activity in MCF10A cells. MCF10A cells could not contract the stiff matrix gels, but when co-cultured with highly-contractile HMFs, the matrix was contracted by the fibroblasts, which may be mechanically regulating MRTF-A activity. HMFs can contract gels that are 4mg/mL of collagen, a density that MCF10A mammary epithelial cells encounter as too stiff to contract. MCF10A and HMF cells were co-cultured in MCF10A-stiff collagen gels (3mg/mL). We observed a down-regulation of MRTF-A transcriptional activity compared to a mono-culture of MCF10A cells in a stiff matrix, despite the different numbers of HMFs that were plated (Figure 2-3A). The transcriptional activity was not due to the HMFs, which were not transfected with the reporter construct. After 48h, the co-culture in stiff gels contracted in a similar fashion to the contraction observed in a mono-culture of MCF10As (13% decrease in diameter) in a soft environment.

One possible explanation for the regulation of MRTF-A transcriptional activity is that HMFs were secreting factors that prevented the activation of MRTF-A/SRF; however, HMFs secrete collagen or TGF-β1 that may induce the up-regulation of MRTF-A activity via RhoA activity, consequently this regulation may be mechanical and not cytokine-driven [110]. To test

whether secreted factors regulated MRTF-A transcriptional activity, HMFs and MCF10A cells were cultured together with equal parts of their growth media for 48h in a stiff matrix, then conditioned media was removed. MCF10A cells were cultured in a stiff matrix in this conditioned media for 48h to assess whether ligands secreted by the fibroblasts induced the inhibition of MRTF-A/SRF activity. The reporter activity did not differ between MCF10A cells cultured with the control media compared to those cultured with conditioned media originating from the co-culture of HMF and MCF10A cells (Figure 2-3B). This suggests that there was not a soluble factor secreted by the HMF cells that triggered this down-regulation of SRF activity in MCF10A cells, but rather the contraction power of fibroblasts that diminish the contraction load in MCF10A cells.

mRNA levels of MRTF-A endogenous targets are regulated by stiffness

Since transcriptional regulation is complex due to its dependence on many transcription factors, we next analyzed known endogenous targets regulated by MRTF-A, serum response factor (SRF) itself and tenascin-C (TnC) to corroborate luciferase reporter data [111-113]. To understand further how MRTF-A transcriptional activity may differ between normal cells and breast carcinoma, we also analyzed the carcinoma subclone, MCF10CA-1d (hereafter, CA1d). We surveyed the expression levels of SRF and TnC in MCF10A and CA1d cells cultured in stiff vs soft matrices. Similar to our luciferase results, the relative expression levels of SRF and TnC in MCF10A cells were increased in stiff matrix conditions. (Figure 2-4A). However, in Ca1d cells, the expression level of the SRF and TnC in stiff matrices was greatly reduced compared to MCF10A cells (Figure 2-4B). These data suggest that MRTF-A transcriptional activity in some carcinoma cells may be mis-regulated and does not follow the response to matrix stiffness in the

same manner as non-carcinoma breast epithelial cells.

FAK inhibition regulates MRTF-A transcriptional activity

To understand other factors that may impinge upon the MRTF-A pathway, and knowing that stiff matrices influence integrin clustering and focal adhesion formation, we probed for expression of MRTF-A while inhibiting the activity of FAK. For these experiments we used a selective, ATP competitive inhibitor, PF-562,271, to target FAK and decrease its kinase activity. The transcriptional activity of pSRF-RE was significantly reduced by the addition of PF-562,271 (Figure 2-5A). We assessed FAK phosphorylation after 24h and confirmed levels of FAK-Y397 were diminished as well as the protein production of MRTF-A by immunoblot on both normal (MCF10A) and carcinoma (Ca1d) MECs (Figure 2-5B-D). This identifies FAK as a regulator of transcriptional activity of MRTF-A targets by controlling the expression of MRTF-A itself.

FAK activity is critically involved in p53 production

To further explore the regulation of MRTF-A by FAK, we analyzed the 5' UTR of MRTF-A to identify transcription factors that may be downstream of FAK. We surveyed the promoter sequence of MRTF-A using TRANSFAC and noted that p53 had many predicted binding sites along the promoter region of MRTF-A [114]. p53 expression and protein stability regulates FAK; however, there has not been a link between FAK inactivation and p53 production [16, 91, 115]. We quantified the levels of p53 on both MCF10A and Ca1d cells in the presence or absence of PF-562,271 by immunoblotting and observed a substantial up-regulation of p53 when FAK activity is inhibited (Figure 2-6A-D). This dramatic increase in p53 occurred regardless of the matrix stiffness.

p53 knock-down enhances MRTF-A protein production in MCF10A

The above results are consistent with a model where p53 can function as a transcriptional repressor by binding to the promoter region of MRTF-A. To investigate this supposition, we compared control and p53-depleted normal MECs to confirm that p53 represses MRTF-A expression. To establish stable cell lines, we used lentiviral shRNA that were either empty or anti-p53 vectors. After we discovered that p53 protein production was depleted in MCF10A cells (Figure 2-7A,C), we found by immunoblotting that protein production of MRTF-A was significantly higher in p53-depleted cells (Figure 2-7B). This suggests that p53 represses MRTF-A expression and that the presence of p53 may inhibit MRTF-A's target, TnC, from being transcribed [113].

Other studies have suggested that ERK activity is intensified in stiff matrices and that this correlates with high proliferation levels [34, 38]. Indeed, in normal MCF10A cells we observed a heightened ERK activity due to matrix stiffness compared to soft conditions. This activity was not disturbed with the addition of PF-562,271 or the depletion of p53 in MCF10A cells (Figure 2-7A,D). Inhibition of ERK, via U0126, had no effect on p53 or MRTF-A (Supplementary Fig. 2-S1). As confirmed earlier, FAK inhibition led to a noticeable p53 up-regulation in the shRNA-Empty set (Figure 7A,C). However, treating with PF-562,271 in shRNA-p53 cells did not rescue the production of MRTF-A as expected, and we still detected that PF-562,271 treatment depletes MRTF-A. These results indicate that FAK is upstream of both p53 and MRTF-A, yet FAK does not control MRTF-A through p53. Collectively, these findings demonstrate that p53 represses MRTF-A expression and that FAK activity does not coordinate MRTF-A through p53.

FAK inhibition amplifies ERK signaling in Ca1d

After identifying that MRTF-A regulation of endogenous targets may be mis-regulated in Ca1d cells (Figure 4B), we next investigated whether p53 knockdown affected MRTF-A expression in these cells. Ca1d cells were stably transfected with an empty vector or shRNA-p53. Inhibition of FAK activity showed that p53 levels were augmented in the shRNA Empty and p53-depleted cells showed noticeable p53 reduction (Figure 8A,C). Unlike MCF10A cells, the protein production of MRTF-A in Ca1d carcinoma cells was not influenced by p53 knock-down and MRTF-A was critically regulated by FAK inhibition (Figure 8A,B). This may represent a mechanism that differs between normal and tumorigenic cancer cells. Interestingly, ERK regulation due to matrix stiffness was lost on both shRNA-Empty and shRNA-p53 sets and it was unchanged regardless of matrix stiffness, which is strikingly different of what we detected in normal epithelial, MCF10A cells (Figure 8A,D). In contrast to MCF10A cells, phosphorylation of ERK in PF-562,271-treated Ca1d cells was considerably higher than the untreated cells and this effect was observed regardless of the stiffness or p53 status (Figure 2-8A,D). Finally, we inhibited ERK kinase activity by U0126 administration, but observed no differences by immunoblotting for both MRTF-A and p53 levels (Supplementary Fig. 2-S2). Taken together, these findings identify carcinoma cells use FAK to regulate ERK, as well as p53 to regulate MRTF-A. These data are consistent with the notion that breast cancer cells acquire genetic and epigenetic transformations that foster uncontrolled growth and contribute to cell invasiveness.

FIGURES

Figure 2-1. SRF activity increases as collagen density increases

Measurement of RhoA/ERK luciferase reporter expression in MCF10A. MCF10A cells were transfected using with an SRF reporter, pSRE-luc, and a Renilla luciferase, pRL-TK (for normalization). A) After 24h following transfection, cells were lifted and seeded into different collagen gel densities for 48h before lysis. B) 24h after plating, stiff collagen gels were treated overnight with either DMSO, C3 (CT04) at 1μg/mL, H-1152 10μM and U0126 10μM. Reporter plasmid expression levels are shown relative to Renilla luciferase controls and normalized to soft (1.3mg/mL) or untreated, mean±SEM, $n \geq 3$, $*p<0.05$, $**p<0.01$

A)

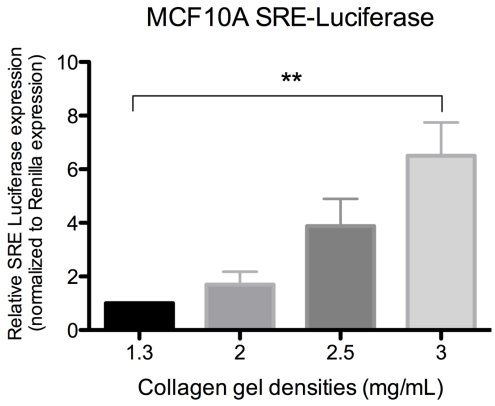
MCF10A SRE-Luciferase
Relative SRE Luciferase expression (normalized to Renilla expression)
10
8
6
4
2
0
**
1.3
2
2.5
3
Collagen gel densities (mg/mL)

B)

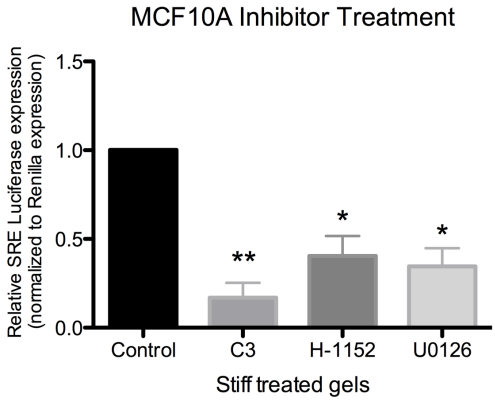
MCF10A Inhibitor Treatment
Relative SRE Luciferase expression (normalized to Renilla expression)
1.5
1.0
0.5
0.0
**
*
*
Control
C3
H-1152
U0126
Stiff treated gels

Figure 2-2. Rho-specific transcriptional reporter for SRF is not regulated by ERK

MCF10A cells were transfected with pSRF-RE, Rho-specific reporter for SRF, and a Renilla luciferase, pRL-TK, for normalization. A) MCF10A cells were plated in soft (1.3mg/mL) for normalization and stiff (3mg/mL) ±C3 (CT04) at 1μg/mL or U0126 10μM. After 24h following treatment gels were lysed. B) Collagen gels were treated with either DMSO, Jasplakinolide (0.5μM) or Cytochalasin D (2μM). Reporter plasmid expression levels are shown relative to Renilla luciferase controls and normalized to soft DMSO (1.3mg/mL), mean±SEM, n=3, *$p<0.05$, ***$p<0.001$.

A)

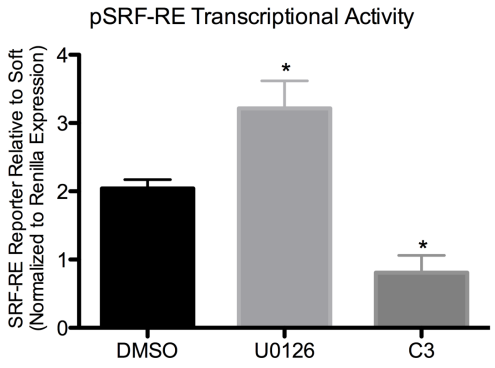
pSRF-RE Transcriptional Activity
SRF-RE Reporter Relative to Soft (Normalized to Renilla Expression)
0
1
2
3
4
*
*
DMSO
U0126
C3

B)

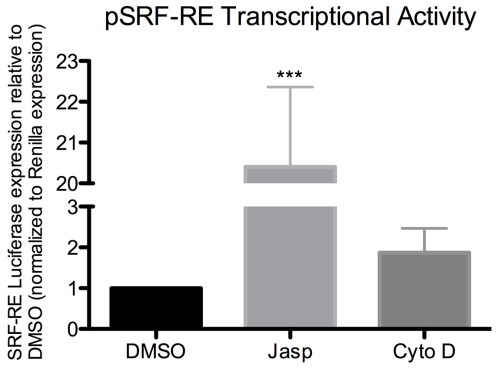
pSRF-RE Transcriptional Activity
SRF-RE Luciferase expression relative to DMSO (normalized to Renilla expression)
0
1
2
3
20
21
22
23
***
DMSO
Jasp
Cyto D

Figure 2-3. SRF activity is regulated by heterotypic mechanical coupling between fibroblasts and epithelial cells

MCF10A cells were transfected with pSRF-RE (Promega) and pRL-TK prior to co-culture. Following 24h after transfection, MCF10A were co-cultured in stiff matrices with A) $1.5x10^4$ $3x10^4$ and $4.5x10^4$ HMFs. B) Conditioned media from MCF10A and HMF cells was used in monoculture MCF10A stiff gels. Transcriptional activity was measure after 48h. Reporter plasmid expression levels are shown relative to Renilla luciferase controls and normalized to stiff (3mg/mL), mean±SEM, n=4, **p<0.01.

A)

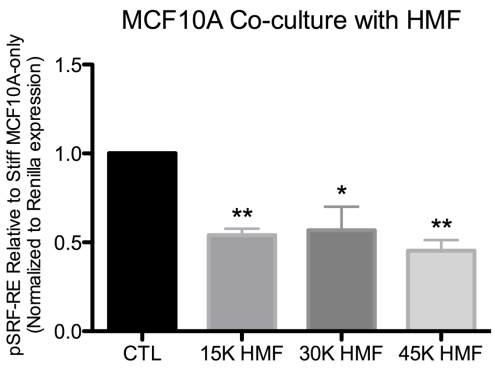
MCF10A Co-culture with HMF
pSRF-RE Relative to Stiff MCF10A-only
(Normalized to Renilla expression)
1.5
1.0
0.5
0.0
**
*
**
CTL
15K HMF
30K HMF
45K HMF

B)

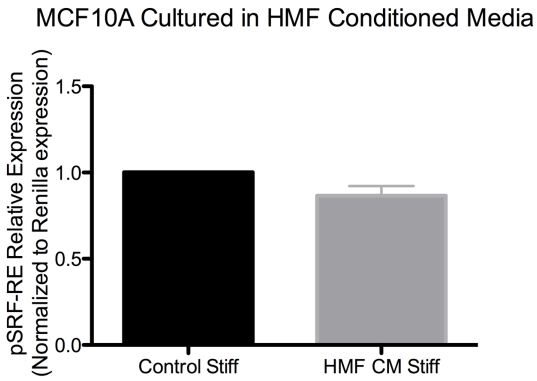
MCF10A Cultured in HMF Conditioned Media
pSRF-RE Relative Expression
(Normalized to Renilla expression)
1.5
1.0
0.5
0.0
Control Stiff
HMF CM Stiff

Figure 2-4. MCF10A and Ca1d have different regulatory mechanisms for MRTF-A's endogenous targets in 3D stiff environments

A) $5x10^5$ MCF10A (1.3 or 3mg/mL) and B) $4x10^5$ Ca1d (2 or 3.5mg/mL) were plated for 24h on either soft or stiff matrices before RNA extraction followed by cDNA synthesis. qRT-PCR was performed using GAPDH as the normalizing gene to measure transcript levels. mRNA levels were normalized to soft. The ΔΔCt method was applied and Pfaffl efficiency was incorporated to calculate the relative quantity of mRNA expression levels. Ct is defined as the threshold cycle where the amplification of template begins determined by the software. Pfaffl Relative levels= $[(E_{target})^{\Delta CPtarget(control-sample)}]/ [(E_{ref})^{\Delta CPref(control-sample)}]$. Data presented are the mean ± SEM, n=3, *p<0.05, **p<0.01.

A)

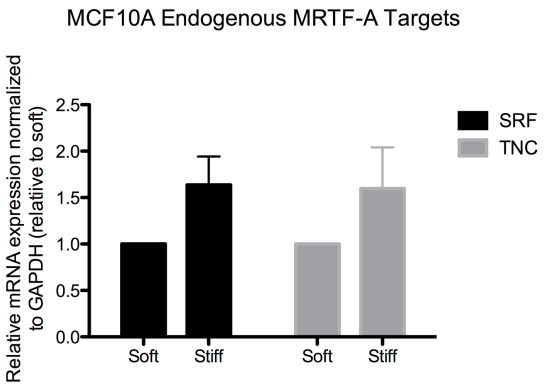
MCF10A Endogenous MRTF-A Targets
Relative mRNA expression normalized to GAPDH (relative to soft)
2.5
2.0
1.5
1.0
0.5
0.0
Soft
Stiff
Soft
Stiff
SRF
TNC

B)

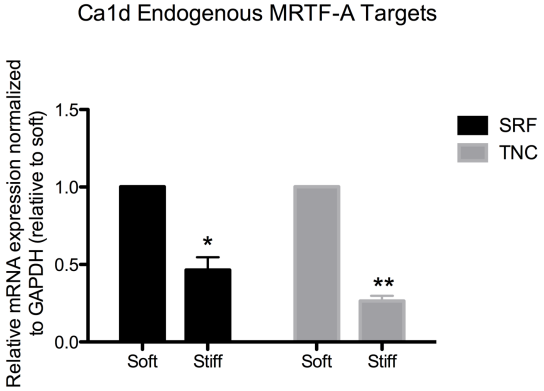
Ca1d Endogenous MRTF-A Targets
Relative mRNA expression normalized to GAPDH (relative to soft)
1.5
1.0
0.5
0.0
*
**
Soft
Stiff
Soft
Stiff
SRF
TNC

Figure 2-5. MRTF-A reporter activity and protein production are reduced in soft and stiff collagen gels after addition of FAK inhibitor, PF-562,271

MCF10A cells were transfected with pSRF-RE and pRL-TK for normalization. MCF10A (1.3 or 3mg/mL) cells with collagen were treated ±PF-562271 (10μM) for 24h before A) transcriptional activity was measured using luminescence reporter construct. For protein analysis, MCF10A and Ca1d (2 or 3.5mg/mL) cells were plated ±PF-562,271 (10μM) and lysed after 24h. Representative immunoblots are displayed (B,C), and the mean ±SEM band densitometry relative to GAPDH are shown. $n \geq 3$, * $p<0.05$, ** $p<0.01$, *** $p<0.001$.

A)

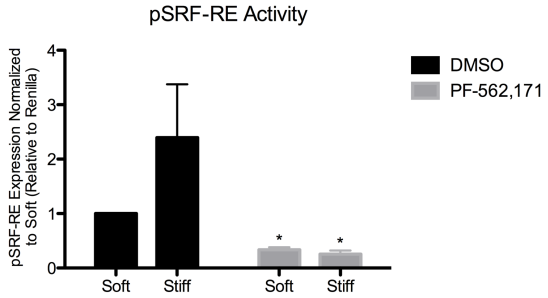

B) **MCF10A** **C)** **Ca1d**

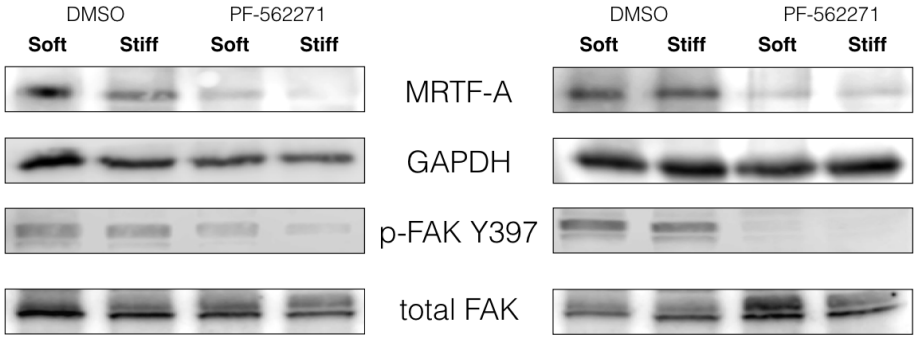

D) **E)**

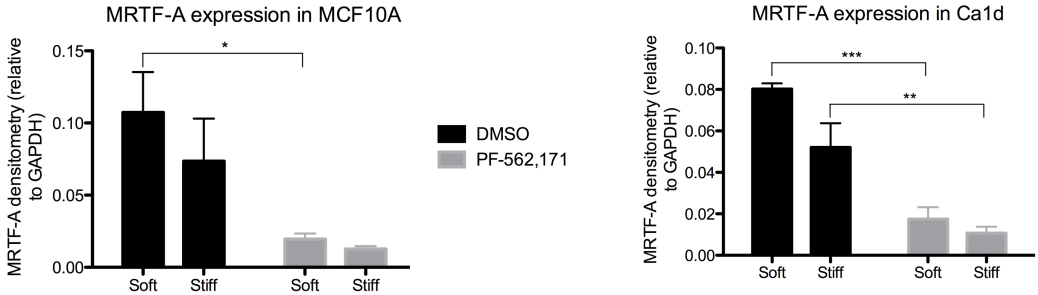

Figure 2-6. p53 protein levels are increased when FAK activity is inhibited in both MCF10A and Ca1d cells

MCF10A AND CA1D Cells were cultured in soft or stiff matrices: MCF10A (1.3 or 3mg/mL) and Ca1d (2 or 3.5mg/mL) with ±PF-562,271 (10μM) for 24h before lysis for Western blotting. Representative immunoblots are displayed (C,D) and the mean ± SEM relative to GAPDH and normalized to control are charted (A,B). $n \geq 4$, * $p<0.05$, ***$p<0.001$.

A) **MCF10A**

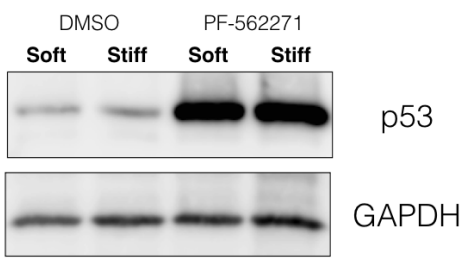

B) **CA1D**

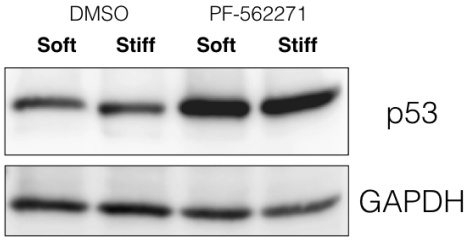

C)

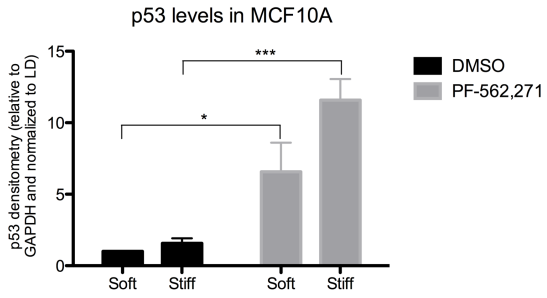

D)

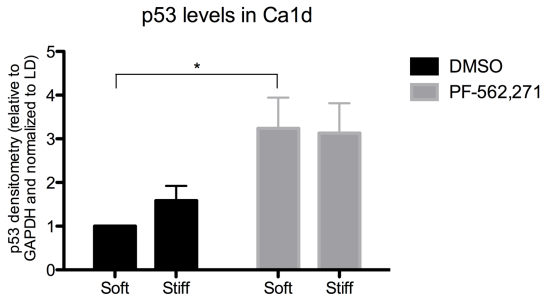

Figure 2-7. MRTF-A levels in MCF10A in response to p53 knock-down

MCF10A cells were cultured in soft (1.3mg/mL) or stiff (3mg/mL) collagen gels for 24h. MRTF-A, ERK activation and p53 levels were measured ±PF-562271 (10μM) and ±shRNA p53. Representative immunoblots are displayed (A) and densitometry of mean±SEM are shown relative to GAPDH for B) MRTF-A, C) p53. D) Active ERK is shown relative to total ERK. n=3, * $p<0.05$, ** $p<0.01$, ***$p<0.001$ vs. respective control.

A)

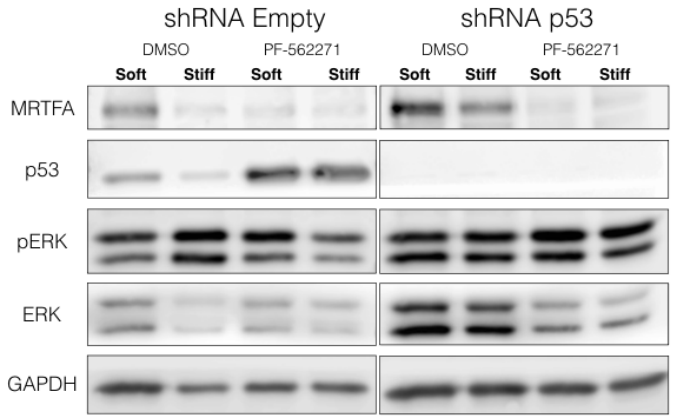
shRNA Empty
shRNA p53
DMSO
PF-562271
DMSO
PF-562271
Soft
Stiff
Soft
Stiff
Soft
Stiff
Soft
Stiff
MRTFA
p53
pERK
ERK
GAPDH

B)

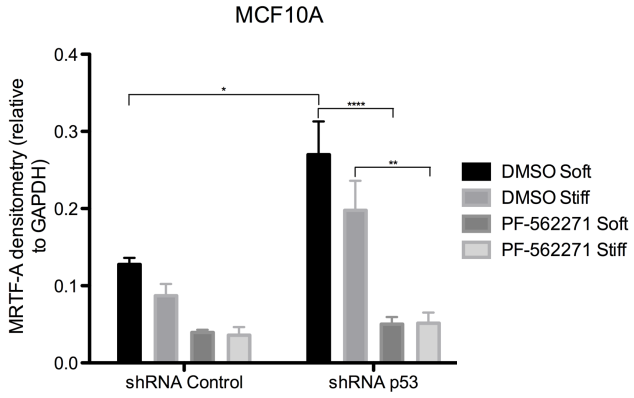
MCF10A
MRTF-A densitometry (relative to GAPDH)
0.4
0.3
0.2
0.1
0.0
*
****
**
shRNA Control
shRNA p53
DMSO Soft
DMSO Stiff
PF-562271 Soft
PF-562271 Stiff

C)

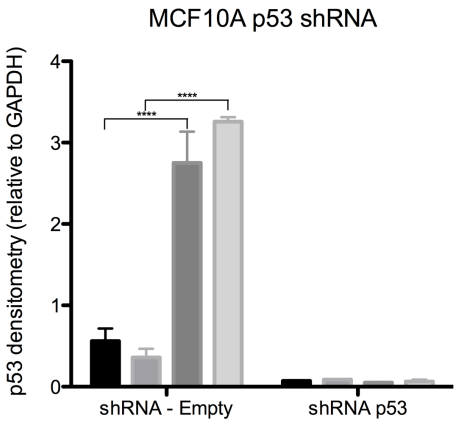
MCF10A p53 shRNA
p53 densitometry (relative to GAPDH)
4
3
2
1
0
****
****
shRNA - Empty
shRNA p53

D)

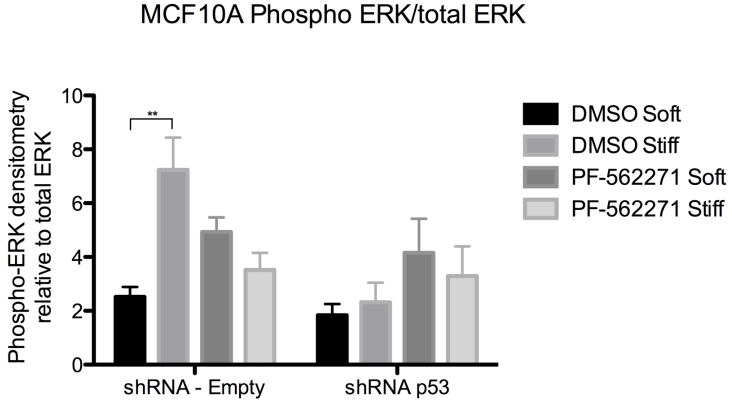
MCF10A Phospho ERK/total ERK
Phospho-ERK densitometry relative to total ERK
10
8
6
4
2
0
**
shRNA - Empty
shRNA p53
DMSO Soft
DMSO Stiff
PF-562271 Soft
PF-562271 Stiff

Figure 2-8. MRTF-A production in Ca1d in response to p53 knock-down and stiffness

Ca1d cells were cultured in soft (2mg/mL) or stiff (3.5mg/mL) collagen gels for 24h. MRTF-A, ERK activation and p53 levels were measured ±PF-562271 (10μM) and ±shRNA p53. Representative immunoblots are displayed (A) and densitometry of mean±SEM are shown relative to GAPDH for B) MRTF-A, C) p53. D) Active ERK is shown relative to total ERK. n=3, * $p<0.05$, ** $p<0.01$, ***$p<0.001$ vs. respective control.

A)

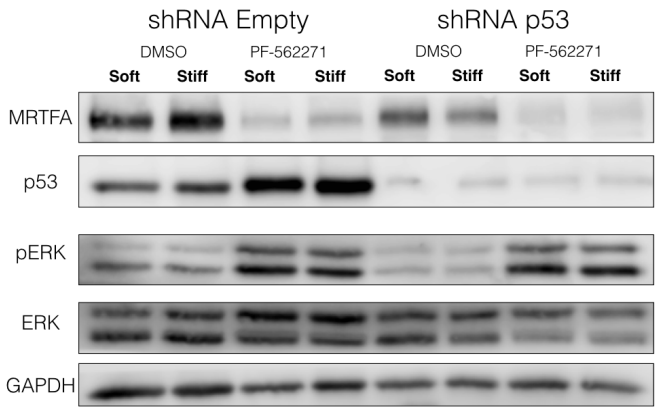
shRNA Empty
shRNA p53
DMSO
PF-562271
DMSO
PF-562271
Soft
Stiff
Soft
Stiff
Soft
Stiff
Soft
Stiff
MRTFA
p53
pERK
ERK
GAPDH

B)

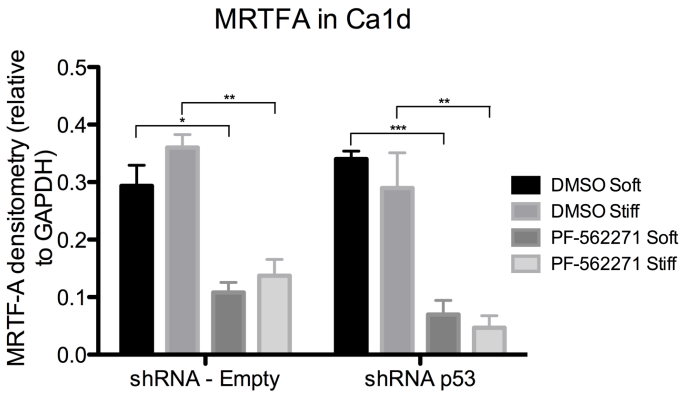
MRTFA in Ca1d
MRTF-A densitometry (relative to GAPDH)
0.5
0.4
0.3
0.2
0.1
0.0
shRNA - Empty
shRNA p53
DMSO Soft
DMSO Stiff
PF-562271 Soft
PF-562271 Stiff

C)

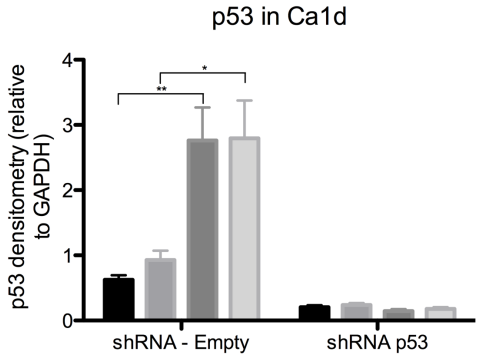
p53 in Ca1d
p53 densitometry (relative to GAPDH)
4
3
2
1
0
shRNA - Empty
shRNA p53

D)

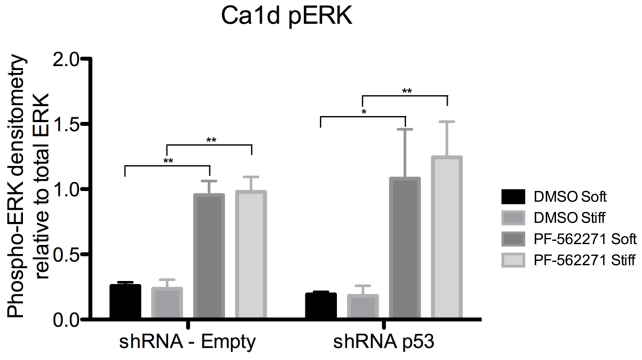
Ca1d pERK
Phospho-ERK densitometry relative to total ERK
2.0
1.5
1.0
0.5
0.0
shRNA - Empty
shRNA p53
DMSO Soft
DMSO Stiff
PF-562271 Soft
PF-562271 Stiff

DISCUSSION

Myocardin related transcription factor-A, MRTF-A, binds SRF to initiate transcriptional activity [97, 116]. Rho-GTPase activity in stiff matrices is elevated when compared to soft microenvironments [19]. Here, we discovered that SRF/MRTF-A activity is up-regulated when cells encounter a stiff matrix. This regulation is controlled by FAK activation as it diminishes MRTF-A protein and as a consequence transcriptional activity of MRTF-A. FAK inhibition negatively regulates p53 on both normal and carcinoma cell lines, indicating that FAK activation is essential to cell proliferation by regulating p53 levels.

In the mammary gland, stiffness drives tumorigenesis by turning on cascade of signals downstream of integrin-FAK clusterings [16, 34, 38]. Moreover, FAK is over-expressed in breast tumors, and it is transcriptionally regulated by p53 [86, 87, 90]. Loss of p53 is a hallmark of carcinogenesis by promoting cell survival and proliferation [89, 91]. In this study, we find that collagen stiffness regulates serum response factor (SRF) activity in normal mammary epithelial cells and is controlled by Rho and ERK (Figure 1). We used a Rho-specific reporter to address MRTF-A activity and confirmed that stiffness and Rho, but not ERK, control this activity in MCF10A cells (Figure 2). MCF10A cells are not highly-contractile and are unable to pull on the matrix as readily as human mammary fibroblasts (HMFs). Co-culture of HMFs and MCF10A cells down-regulated MRTF-A/SRF activity, and this is mechanically-induced because conditioned media did not influence reporter activity (Figure 3). This finding represents a heterotypic mechano-coupling that differ in their matrix-contractility potential by triggering RhoA transcriptional activity.

MRTF-A and SRF act together to transcribe many target genes in breast cancer cells [93].

We decided to measure mRNA levels of SRF itself by qPCR as a common target of MRTF-A/SRF and tenascin-C as a relevant marker of proliferation in the metastatic niche in breast cancer cells [113, 116]. In MCF10A cells, gene expression levels were higher in stiff matrices while Ca1d cells did not follow this trend and SRF and TnC mRNA levels were markedly down-regulated under stiff conditions (Figure 4A,B).

Furthermore, MRTF-A/SRF activity is positively controlled by FAK, a key regulator of proliferation and tumorigenesis [47, 48]. FAK activity controls the expression and transcriptional activity of MRTF-A in both MCF10A and Ca1d cell lines (Figure 5). Blocking FAK activity by PF-562,271 treatment enhances p53 protein levels is higher on both normal and carcinoma cell lines (Figure 6). This negative regulation of FAK and p53 may address the mechanism in a murine model where FAK knock-out in mammary glands retards tumor growth and metastasis, although this remains to be seen [88].

As p53 and MRTF-A are regulated by FAK, we found that p53 has predicted binding sites in the promoter region of MRTF-A using bioinformatics [114]. To test whether p53 affects MRTF-A production, we knocked-down p53 in both MCF10A and Ca1d cell lines and assessed MRTF-A protein levels. In Figure 7, we show the complete depletion of p53 in MCF10A cells and the striking up-regulation of MRTF-A. This result demonstrates that p53 could act as a transcriptional repressor of MRTF-A as p53 has been shown to repress other genes including FAK [115]. However, p53 was not directly downstream of FAK to regulate MRTF-A because MRTF-A levels were reduced in PF-562,271-treated regardless of p53 status.

Normal breast epithelial cells become invasive and increase their metastatic potential by acquiring mutations, altering epigenetic events, and amplifying proliferation and survival

pathways. Ca1d cells are a model that represents this transition because they originated from normal epithelial cells and are capable of colonizing pulmonary regions in experimental metastasis [22]. In Figure 8, we analyzed whether p53 knock-down alters the MRTF-A response of carcinoma cells, in contrast to MCF10A cells, MRTF-A production remains unchanged when p53 is knocked down. We observed an almost complete reduction of MRTF-A on shRNA-Empty and shRNA-p53 when treated with PF-562,271, while p53 protein on shRNA-Empty remained up-regulated. Also different from MCF10As, was the hyper-activation of ERK in FAK-inhibited cells (Figure 8D). This finding could signify that carcinoma cells possess the advantage of controlling another survival/proliferation pathway (ERK) when a tumor suppressor, in this case p53, is elevated or a crucial ECM-activated kinase is inhibited (FAK). Carcinoma cells may act in this manner to prevent cell apoptosis, and it may indicate why cancer cells are so resilient to cell death.

Figure 2-S1. MRTF-A levels in MCF10A cells after inhibition of FAK and/or ERK activity in soft matrices

MCF10A cells were cultured under stiff (3mg/mL) conditions for 24h. MRTF-A, ERK activation and p53 levels were measured after PF-562,271 (10μM) and/or U0126 (10μM) addition. Representative immunoblots are displayed (A) and densitometry of mean±SEM are shown relative to GAPDH for B) MRTF-A, C) p53. D) Active ERK is shown relative to total ERK. n=3, * $p<0.05$, *** $p<0.001$ vs. Stiff DMSO.

A)

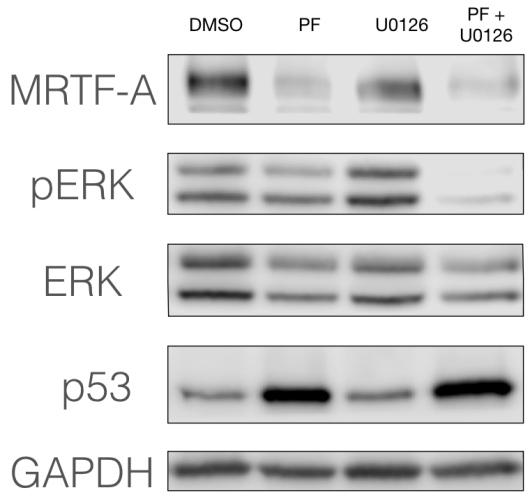
DMSO
PF
U0126
PF + U0126
MRTF-A
pERK
ERK
p53
GAPDH

B)

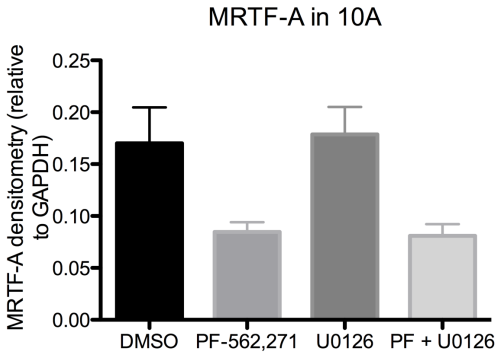
MRTF-A in 10A
MRTF-A densitometry (relative to GAPDH)
0.25
0.20
0.15
0.10
0.05
0.00
DMSO
PF-562,271
U0126
PF + U0126

C)

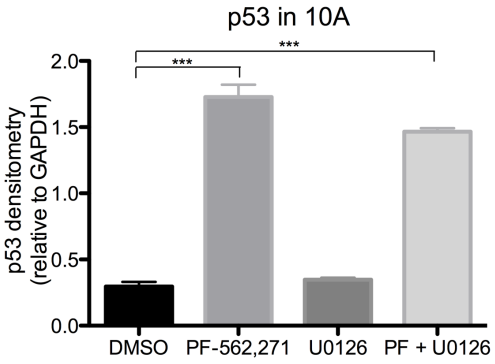
p53 in 10A
***
***
p53 densitometry (relative to GAPDH)
2.0
1.5
1.0
0.5
0.0
DMSO
PF-562,271
U0126
PF + U0126

D)

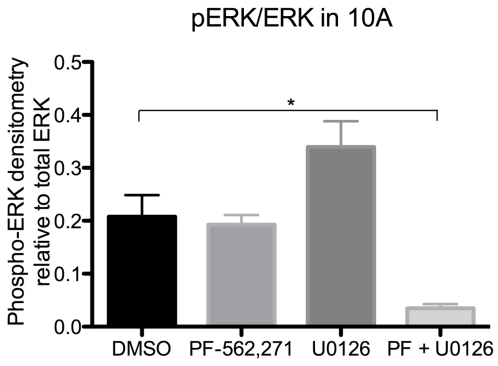
pERK/ERK in 10A
*
Phospho-ERK densitometry relative to total ERK
0.5
0.4
0.3
0.2
0.1
0.0
DMSO
PF-562,271
U0126
PF + U0126

Figure 2-S2. MRTF-A production in Ca1d cells after FAK and/or ERK inhibition

Ca1d cells were cultured under stiff (3.5mg/mL) conditions for 24h. MRTF-A, ERK activation and p53 levels were measured after PF-562,271 (10μM) and/or U0126 (10μM) addition. Representative immunoblots are displayed (A) and densitometry of mean±SEM are shown relative to GAPDH for B) MRTF-A, C) p53. D) Active ERK is shown relative to total ERK. n=3, * $p<0.05$, ***$p<0.001$ vs. Stiff DMSO.

A)

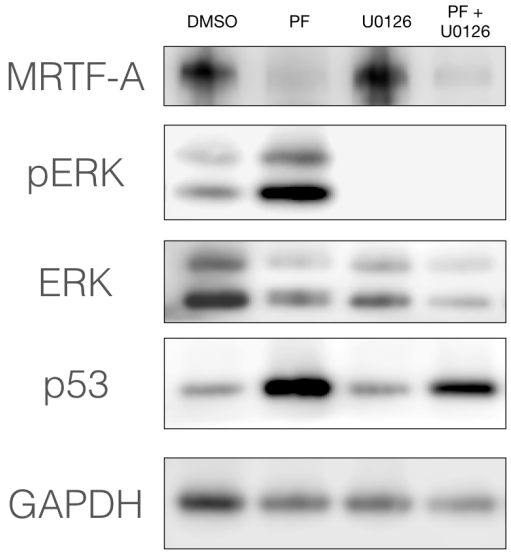
DMSO
PF
U0126
PF + U0126
MRTF-A
pERK
ERK
p53
GAPDH

B)

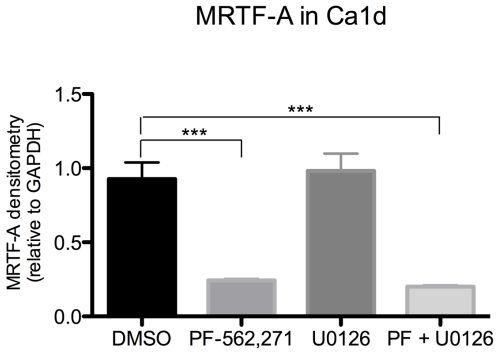
MRTF-A in Ca1d
MRTF-A densitometry (relative to GAPDH)
1.5
1.0
0.5
0.0
***
***
DMSO
PF-562,271
U0126
PF + U0126

C)

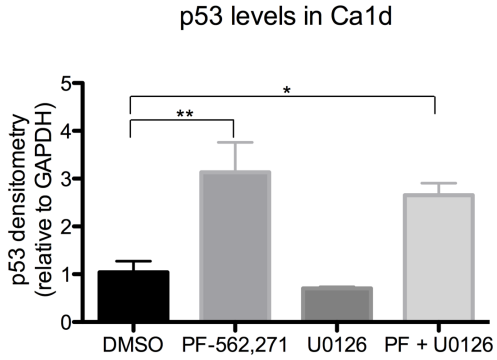
p53 levels in Ca1d
p53 densitometry (relative to GAPDH)
5
4
3
2
1
0
**
*
DMSO
PF-562,271
U0126
PF + U0126

D)

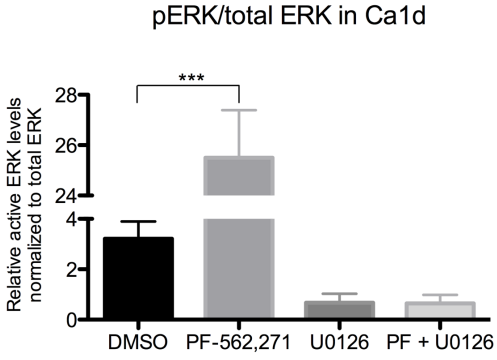
pERK/total ERK in Ca1d
Relative active ERK levels normalized to total ERK
28
26
24
4
2
0
***
DMSO
PF-562,271
U0126
PF + U0126

MATERIAL AND METHODS

Cell lines, cell culture and stable shRNA transfection

The MCF10A and MCF10-Ca1d (Ca1d) cell lines were used as representative models of normal and malignant breast epithelial [22, 117]. The MCF10A cell line was a kind gift from Dr. Alan C. Rapraeger (University of Wisconsin-Madison) and MCF10-Ca1d was purchased through the Barbara Karmanos Cancer Institute (Detroit, MI). Cells were cultured in compliant (1.3 mg/mL MCF10A, 2mg/mL Ca1d) or stiff (3mg/mL MCF10A, 3.5mg/mL Ca1d) type I collagen gels as previously described [118, 119]. In brief, collagen was mixed thoroughly with equal volume of neutralization solution containing 100mM HEPES in 2x PBS (pH 7.4) and placed on ice. Determined collagen concentrations as listed in the manuscript were added to cells suspended in complete media. Complete media contained 50% DMEM with high glucose (Gibco Life Technologies, Grand Island, NY), 50% F-12 Nutrient mix (Gibco), 5% horse serum (Gibco), 10μg/mL bovine insulin (Cell Applications, Inc., San Diego, CA), 0.5mg/mL hydrocortisone (Sigma-Aldrich, St. Louis, MO), and 20 ng/mL epidermal growth factor (EMD Millipore/ Calbiochem, Darmstadt, Germany). Cells and media were thoroughly mixed with neutralized collagen. A total volume of 1mL cells/media/collagen was dispensed to one well of a 6-well non-tissue culture treated plate (BD Falcon™, Franklin Lakes, NJ) and incubated at RT for 10min. The plate was transferred to a 5% CO_2, 37°C incubator for 2h. The gels were then released from the plate by gently sliding a 200μl pipet tip around the outer edge of the gel and 2mL of complete media was added to the gel prior to returning the plate to a 5% CO_2, 37°C incubator.

For drug treatments, cells were subjected to 10μM FAK ATP inhibitor PF-562271 (Selleckchem, Houston, TX) or 10μM U0126 (Promega, Madison, WI), 1μM H-1152 (EMD Millipore/ Calbiochem, Darmstadt, Germany), 1μg/mL C3 Exoenzyme (Cytoskeleton, Denver, CO), 2μM Cytochalasin D (Millipore/Calbiochem, Darmstadt, Germany), 0.5μM Jasplakinolide (Millipore/Calbiochem, Darmstadt, Germany)

p53-depleted MCF10A and Ca1d cell lines were produced by stably transfecting with either the control vector (pGIPZ) or with an shRNA-p53 (GE Dharmacon, Lafayette, CO).

Luciferase Reporter assay

The plasmids containing the luciferase driven by serum response element (SRE) and Renilla were a kind gift from Dr. Michele A. Wozniak, University of Pennsylvania. The serum response factor-response element (SRF-RE) was purchased from Promega (Madison, WI). Cells were lifted and plated ($5x10^5$) in a 100mm tissue culture dish (BD Falcon™, Franklin Lakes, NJ) for 24h and transfected with 8 μg of luciferase plasmid, 4 μg of Renilla plasmid and 30 μl of Lipofectamine® 2000 Transfection Reagent (Invitrogen Life Technologies, Carlsbad, CA). After transfecting for 24h, cells were lifted and cultured in collagen gels ± 10 μM PF-562271 (Selleckchem, Houston, TX), 10 μM U0126 (Promega, Madison, WI), 1μM H-1152 (EMD Millipore/Calbiochem, Darmstadt, Germany) or 1μg/mL C3 Exoenzyme (Cytoskeleton, Denver, CO). Gels were rinsed with PBS, placed in 250 μl Glo Lysis Buffer (Promega, Madison, WI) and repeatedly passed through an 18 gauge needle. Cell lysates were centrifuged at high speed for 1min to clear lysate. Supernatant was used and dispensed in duplicate to a 96-well Microfluor® white flat bottom plate (Thermo Electron Corporation, Milford, MA). Luminescence was assessed via the Dual-Glo® Luciferase Assay System (Promega) and

incubating substrates/lysates for 15min per substrate before readings. Plates were read on a Fluoroskan Ascent® FL (Thermo Scientific) plate reader. Activity in each sample was measured and duplicates were averaged in each experiment from at least three independent experiments.

Immunoblots

Cells cultured in collagen gels were washed in PBS and lysed in 300 μL 2X RIPA buffer (50 mM Tris [pH 7.4], 150 mM NaCl, 2 mM Na_2EDTA, 2% NP-40, 0.5% deoxycholic acid, 2 mM NaF, 1 mM Na_3VO_4). The lysate was repeatedly passed through an 18-gauge needle and incubated on ice for 10min. Lysates were centrifuged (15,800xg, 10min, 4°C) to separate the collagen from the cell lysate. The aqueous solution was saved and mixed with 10X sample buffer (100 mM Tris [pH 8], 7.5 mM EDTA, 100 mM dithiothreitol, 10% sodium dodecyl sulfate, 30% glycerol, 1% bromophenol blue) for a 1X sample buffer final concentration. Protein samples were boiled (8min), loaded onto an SDS-PAGE gel, transferred to a 0.45 mm Immobilion-P polyvinylidene difluoride membranes (Millipore). Blots were cut for multiple detection and incubated with antibodies raised against MRTF-A HPA030782 (Sigma Aldrich, Saint Louis, MO), p-FAK(pY397) (Life Technologies, 44624G), total FAK (Millipore, 05-537), p44/42 MAPK, p-p44/42 MAPK (pT202/Y204) (Cell Signaling Technology, Beverly, MA), p53 sc-126, MRTF-A, sc-21558, and GAPDH sc-25778 (Santa Cruz Biotechnology, Santa Cruz, CA). Blots were washed and subsequently incubated with HRP-conjugated secondary antibodies (Jackson Immunolabs, West Grove, PA). Bound secondary antibody was visualized following incubation of the membrane with SuperSignal West chemiluminescent HRP substrate (Thermo Scientific Pierce, Waltham, MA) and using a LI-COR Odyssey (LI-COR, Lincoln, NE) for imaging. Luminescence was quantified and evaluated using LI-COR's ImageStudio Software.

RNA Extraction from 3D collagen gels

Collagen gels were washed with PBS and RNA was isolated using 400µL of TRIzol reagent (Invitrogen) and then, followed manufacturer's instructions. Briefly, media was removed and the gels were washed with once with PBS before TRIzol. We used an 18-gauge needle to homogenize collagen gels and centrifuge at 12,000 x g for 10min to pellet the collagen. We added chloroform and followed incubation and centrifugation steps. Aqueous phase containing RNA was removed by pipetting and transferred to a new tube and isopropanol was added. RNA was the incubated at RT for 10min and centrifuged. RNA pellet was carefully washed twice with 75% ethanol. After isolation, RNA cleanup was performed using an RNeasy Kit (Qiagen, Valencia, CA) and was later quantified and its purity analyzed with a ND-1000 spectrophotometer (NanoDrop, Wilmington, DE).

Quantitative Real-time Polymerase Chain Reaction

1µg of RNA was then treated with DNase I (Invitrogen). RNA was reversely transcribed into cDNA using SuperScript III First-Strand Synthesis (Invitrogen) using 50ng of random hexamers. mRNA levels were measured using SYBR GreenER for ABI Prism (Invitrogen) at a final concentration of 1X in an ABI 7900HT Real-Time PCR system (Applied Biosystems, Foster City, CA) using 2µl of template in a 20µl reaction and ran in triplicate. Samples were then incubated at 50°C for 2min (UDG incubation), 95°C for 10min (UDG inactivation and DNA pol activation) followed by 45 cycles of 95°C for 15 s, 55°C for 30 s and 68°C for 20 s. Primer efficiencies were measured for both cell lines and values ranged from 91% to 108% efficiency. GAPDH was used as the reference gene and quantification of mRNA levels was calculated using the Pfaffl method. Roche qPCR primer design was used for the majority of the primers and

target specificity was confirmed through *in silico* qPCR (genome.uscs.edu). Cycles to determine threshold of targets were normalized to GAPDH. Results are expressed in relative fold change in mRNA levels relative to Soft Untreated. Blank and no template controls were also analyzed. Melt-curve analysis was also performed after each experiment.

Sequences of primers pairs used are as follows:

TnC Human (75 nt): Forward: 5- CGG GGC TAT AGA ACA CCA GT; Reverse: 5- AAC ATT TAA GTT TCC AAT TTC AGG TT

SRF Human (80 nt): Forward: 5- AGC ACA GAC CTC ACG CAG A; Reverse: 5- GTT GTG GGC ACG GAT GAC

GAPDH Human (66 nt): Forward: 5- AGC CAC ATC GCT CAG ACA C; Reverse: 5- GCC CAA TAC GAC CAA ATC C

Chapter 3: ECM Stiffness induces up-regulation of DDR2

Title: Stiff collagen matrices induce DDR2 expression and its inhibition disrupts collagen alignment.

Esteban R. Carrillo, Whitney R. Grither, Madeline L. Gore, Joseph M. Szulczewski, Kevin Eliceiri, Greg D. Longmore, and Patricia J Keely

This chapter is in preparation for submission to Molecular Biology of the Cell. I performed the experiments and analysis contained in this chapter, with some assistance on cell migration studies by Madeline Gore. Whitney Grither and Greg Longmore provided the DDR2 blocking reagent. Joseph Szulczewski assisted with multi photon imaging acquisition. Patricia Keely, Greg Longmore, and Kevin Eliceiri provided guidance and input on experimental design and imaging.

ABSTRACT

Women with collagen-dense breast tissue are four to six times more likely to develop breast cancer in their lifetime. DDR2 is a tyrosine kinase transmembrane receptor that is activated by triple-helical collagen and is abundant on the stromal cells surrounding tumors in the breast. Here, we investigated the regulation of DDR2 by a stiff matrix and its role in establishing and responding to collagen alignment. Increasing the stiffness of the collagen matrix results in an up-regulation of DDR2, which is positively regulated by p-FAK, but negatively regulated by p-ERK. Using a novel inhibitor for DDR2, WRG-28, we discovered that in a 3D migration plug assay, cells fail to align collagen at the boundary of the cell plug, which leads to a significant reduction in cell migration. These results suggest that DDR2 inhibition could be used as a therapeutic target to inhibit metastasis in breast cancer.

INTRODUCTION

One in eight women will develop breast cancer during the course of their lifetime. While this disease is attributable to both environmental and genetic contributions, the greatest

independent risk factor for developing breast cancer is increased mammographic density [4, 5]. This increased mammographic or breast density has been correlated to increased deposition of the extracellular matrix (ECM) protein, collagen [8]. In women with dense breast tissue of greater than 60% collagen they are four to six times more likely to develop cancer in the future [4]. These patients also often have more advanced stages of the disease at diagnosis, and more rapid disease progression .

Collagens are a diverse and important family of ECM proteins that are best known for their structural contributions to the architecture of the tissue or organ. In the mammary duct, fibrous Type I collagen is a principle component of the stroma where they lend support to the underlying ductal epithelium [12, 14]. An underappreciated role for this collagen, however, is related to its vast functions in cellular signaling. The increased presence or concentration of collagen has been correlated with increased metastatic potential of tumors, and changes in collagen density are sufficient to induce more invasive cellular phenotypes, higher rates of proliferation, and broad changes to gene expression [7, 9, 34, 38, 88].

These observations pose an interesting overarching question. That is, how does the cell sense, respond, and remodel to its local environment? Collagen can be a ligand for specific receptors, but it also can provide a rich source mechanical cues or stimuli [15, 16]. Increased collagen deposition or cross-linking has been shown to result in a stiffer ECM [120]. The fibrous nature of collagen also exists in a continuum from randomly organized to regions with a high degree of alignment [10]. The significance of this organization can be profound as localized regions of enhanced alignment can further stiffen the local ECM microenvironment, but could also provide a mechanism for cells to escape and migrate [10, 121]. Cancer cells demonstrate

increase directional migration and persistence when offered these ‘highways’ of aligned collagen [121, 122]. Indeed, the direction and alignment of collagen fibers generates a stiffer environment compared to random fiber orientations [121].

There are several signaling cascades that are thought to mediate the sensing of the stiffness or architecture of the local ECM microenvironment [9, 15, 19]. One of the leading candidates is through integrin binding and focal adhesion kinase (FAK). Integrins are the physical link between extracellular microenvironment and the internal contractile machinery [32]. FAK has been shown to be more active in stiff matrices, and plays a pivotal role in linking the ECM to changes in adhesion, proliferation, motility, and gene expression [39, 123, 124]. In addition, FAK knock-out mice have a reduced tumor burden and metastasis occurrence in the mammary gland [88].

While integrins and FAK almost certainly play an important role in the signaling response to collagen density, many other receptors or signaling pathways are likely to also contribute to this complex regulation. One potentially interesting class of receptors are the discoidin domain receptors (DDRs). DDRs are categorized as receptor tyrosine kinases (RTKs), and are unique because of their collagen binding in the ECM [125, 126]. A fibrillar, triple-helical structure of collagen is necessary in order to act as a ligand for the activation of DDRs [125, 126].

DDRs are known to play a role in the regulation of many typical cell activities such as adhesion, proliferation, and migration [127]. Within this class of collagen receptors there are two different types, DDR1 and DDR2. DDR1 is common in epithelial cells with a wide range of collagen binding activity, while DDR2 is usually found in mesenchymal cells, with specific

binding to collagens I and III [43, 125]. DDR2 is found to be abundant on breast stromal cells surrounding the tumor, and may be linked to metastasis, as well as function as a prognostic marker for breast cancer patients [58-60, 87]. DDR2 has also been shown to be an invasive marker, induce proliferation and migration in prostate, melanoma, human umbilical vein endothelial cells, hepatoma, and carcinoma cells [128-130]. While this receptor has been studied for its activity upon collagen binding, no work in breast cancer cells has been performed to understand whether DDR2 expression changes upon exposure to increasing stiffness of the 3D environment. In our research, we investigated whether changes in collagen stiffness regulate DDR2 expression and examined the signal mechanism that cancer cells may use to trigger its up-regulation and its role in collagen fiber alignment.

RESULTS

Mechanical Stiffness induces the up-regulation DDR2

To assess the expression of DDR1 and DDR2 in a 3D collagen environment, we made use of three different breast cancer cell lines: human breast cancer MCF7 cells were chosen because they have moderate proliferation and migration and allow us to assess either increases or decreases in proliferative and migratory ability. We also made use of mouse mammary carcinoma 4T1 and 4T07 cells, which were chosen because they are derived from the same parental line and differ in metastatic capability such that both 4T1 and 4T07 cells grow in the mammary fat pad as tumors, but only 4T1 cells robustly form metastases in lungs [25].

MCF7 cells were cultured in a low-density (1.3mg/mL) or a high-density (3mg/mL) collagen gel to mimic a soft or stiff microenvironment, respectively (Figure 3-1A). After 24h, DDR2 protein levels were higher in the stiff than the soft environment, while DDR1 levels

remain unchanged (Figure 3-1B,C). As a control for effects of changing the ligand density, we also used an additional means to create a soft or stiff environment, in which soft collagen gels are floated into the media or left attached to the culture dish. Attached (stiff) gels up-regulate Rho activation and phosphorylation of FAK in human breast cancer cells compared to soft gels [19]. These attached collagen gels show similar phenotypes to high density gels and are not contracted even after the course of several days [19]. Both 4T07 and 4T1 demonstrated an up-regulation of DDR2 in the attached (stiff) collagen gel (Figure 3-1E,F). The same results were obtained when we generated stiff substrata using collagen-coated polyacrylamide gels that had different stiffnesses ranging from 2kPa (soft) to 31kPa (stiff), where stiff substrata resulted in increased DDR2 levels (Supplementary Fig 3-S1).

DDR2 becomes phosphorylated on tyrosines following activation through collagen stimulation [42]. Not only were the protein levels of this receptor increased in the stiffer gels, the amount of DDR2 activation was also enhanced. (Supplementary Fig. 3-S2).

DDR2 is regulated by α2 integrin.

We next sought to understand the mechanisms involved in DDR2 regulation in response to increased matrix stiffness. It is well established that integrins are receptors for the extracellular matrix (ECM). Since α2β1 integrin mediates collagen response in mammary epithelial cells, we chose to prevent its activation via treatment with an α2 integrin (CD49b) blocking antibody [131]. 4T07 and 4T1 cells were cultured in a soft or stiff collagen matrix and then treated with anti-CD49b. In control conditions, increased matrix stiffness activated FAK by increasing phosphorylation at Y397 and elevated DDR2 protein levels (Figure 3-2A). As

expected, treatment with the integrin blocking antibody decreased FAK activation. Importantly, blocking the α2 integrin subunit reduced DDR2 levels (Figure 3-2A,B).

One of the known means by which DDR2 expression is regulated is through activating transcription factor 4 (ATF4) [52]. Notably, protein levels of ATF4 also increased under stiff matrix conditions and were inhibited by CD49b treatment (Figure 3-2C). These findings suggest that α2 integrin activation is upstream of DDR2, and implicate ATF4 as a mediator of this up-regulation.

DDR2 is regulated by p-FAK and negatively regulated by p-ERK

Since FAK is a crucial signaling molecule that relays the signal from integrin binding and focal adhesion formation and maturation, we blocked the activity of FAK with the ATP-competitive inhibitor, PF-562,271. Treatment with PF-562,271 greatly reduced the catalytic activity and the autophosphorylation levels of FAK (Figure 3-3A). Consequently, it also reduced the levels of DDR2 at both the protein and mRNA levels when cells were cultured in either soft and stiff collagen environments (Figure 3-3 A,B and Figure 3-5) To control for off-target effects, we tested another FAK inhibitor, TAE-226. Although its mechanism is not well documented, this drug does not have the same mode of action as PF-562,271 according to the manufacturer. Treatment of cells with TAE-226 also down-regulated the levels of DDR2 protein (Figure 3C,D).

To further test whether activating FAK was sufficient to elevate the levels of DDR2, we used a hyper-active FAK (SuperFAK) that enhances downstream signaling [132]. 4T07 and 4T1 cell lines were stably transfected with SuperFAK, and cultured in soft or stiff collagen gels. Expression of SuperFAK resulted in p-FAK levels that were strikingly higher than control cells.

DDR2 were also highly up-regulated in SuperFAK-transfected cells, even in soft matrices, indicating that FAK activation can drive DDR2 expression (Figure 3-3 E,F).

Upon FAK autophosphorylation, binding of Src leads to phosphorylation of other tyrosine residues on FAK, which creates binding sites for additional downstream signaling events. Specifically Y925 on FAK creates a binding site for Grb2, which can dock SOS and subsequently activates the Ras/ERK pathway [34, 37]. ERK activation has been implicated in cellular events including proliferation, migration and survival, and thus its activity has been considered a marker for such processes [35]. Seeing that DDR2 expression is correlated with increased proliferation, we sought to understand whether ERK activity modulation disrupts DDR2 expression.

While p-FAK levels were increased in 4T07 and 4T1 cells in stiff matrices, we found that p-ERK levels were lower under these conditions compared to cells cultured in soft matrices (Figure 3-4). ERK was inhibited by blocking its upstream activator, MEK, with MEK inhibitor, U0126, which resulted in an increase in DDR2 protein levels (Figure 3-4). We then sought to understand whether FAK could override ERK's impact on DDR2. PF-562,271 caused DDR2 down-regulation even after the addition of U0126 suggesting that the effect of ERK is not downstream of FAK in this system (Figure 3-4). Messenger RNA levels after U0126 treatments were minimally different than controls, suggesting the regulation of DDR2 by ERK is possibly at the post-transcriptional level (Figure 3-5).

DDR1 knock-down leads to up-regulation of DDR2

DDR1 is related to DDR2, but is largely expressed in epithelial cells in normal tissues, while many murine and human cancer cells have higher levels of DDR2 than DDR1 [133]. We

tested whether the loss of DDR1 might affect DDR2 levels using a short hairpin RNA (shRNA) directed to DDR1. Stable cell lines with either an empty vector, shControl (pGIPZ), or with an shRNA-DDR1 were created. We cultured them on soft and stiff collagen gels and detected that DDR2 protein was significantly greater when DDR1 was knocked down than in cells expressing the control vector (Figure 3-6 B,C). Moreover, ATF4 levels were also increased upon expression of shRNA-DDR1 in cells (Figure 3-6 B,C). These data suggest that DDR1 expression negatively regulates DDR2, which may have implications for their expression during epithelial-mesenchymal transition (EMT) [60, 133, 134].

Inhibition of DDR2 reduces cell proliferation

A specific peptide inhibitor was used to prevent downstream signaling. WRG-28 is a non-competitive inhibitor of DDR2 that is believed to block the binding of collagen to DDR2. It has shown efficacy in preventing DDR2 autophosphorylation (Greg Longmore, personal communication). Upon treatment with WRG-28, DDR2 levels and phosphorylation of FAK were significantly increased only in 4T07 cells, but not in 4T1 cells (Figure 3-7A,B).

As DDR2 presence has been linked to proliferation, we determined the effect of DDR2 inhibition on cell proliferation [129, 135]. Here, 4T07 cells treated with WRG-28 had significantly lower proliferative rates after 48h than vehicle-treated cells (Figure 3-7C). Expression of SuperFAK or DDR2 over-expression resulted in higher proliferation rates (Figure 3-7D).

Inhibition of DDR2 reduces migration and ability of cells to align collagen

We previously demonstrated that cells in a 3D collagen gel will align the collagen between two cell-dense plugs, and preferentially invade onto the aligned region [122]. This

assay was used to test the role of DDR2 in collagen alignment and subsequent cell invasion (Supplementary Fig. 3-S3). A dense drop of cells was seeded on each side of a collagen gel creating two "cell plugs". The cell plugs were cultured for 48h allowing time for cells to migrate out of the plug. Treatment of 4T07 cells with WRG-28 diminished their ability to move along the collagen fibers, even though their protrusions were much longer (Supplementary Movie S1A,C). Not only was the number of cells that traveled out of the plug reduced, but their distance traveled was greatly diminished (Figure 3-9C). Moreover, the inhibition of DDR2 in 4T1 cells significantly decreased the invasive nature of this metastatic cell line (Figure 3-8 F,H). Time-lapse imaging showed a notable reduction in the number of invasive cells and the distance traveled for these cells (Supplementary Movie. 3-S1B,D).

Using Second Harmonic Generation (SHG), we were able to detect a change in the collagen alignment around the periphery of the cell plug. Remarkably, 4T07 and 4T1 cells were not able to align the collagen fibers outside of the plug when DDR2 was inhibited with WRG-28 (Figure 3-8 A-D).

FIGURES

Figure 3-1. Endogenous DDR2 protein is regulated by matrix stiffness

A) Model of 3D collagen gels for MCF7 cells. Cells were mixed in with neutralized collagen at either 2mg/mL (Soft) or 3.5mg/mL (Stiff) for 24h before cell lysis and examined by immunoblot for DDR2 and DDR1. B) Representative blot for DDR1 and DDR2 and C) densitometry quantification are displayed as the mean normalized to the control (Soft) and p190B as a reference protein. D) Cartoon representation of soft vs. stiff matrices with same collagen concentration. 4T07 and 4T1 were cultured in 2mg/mL of collagen. Stiff matrices were not released from the sides of the well and E) representative blot is shown. Mammary epithelial cells were cultured for 24h before cell lysis and F) densitometry of DDR2 is normalized to GAPDH. $n \geq 4$, mean ±SEM, $^{**}p \leq 0.01$ vs respective soft control.

A)

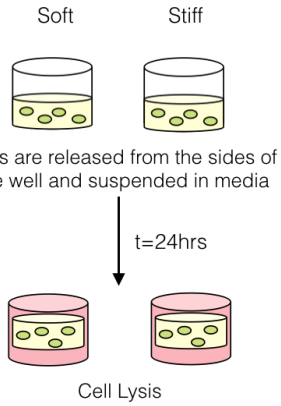
Soft
Stiff
Gels are released from the sides of the well and suspended in media
t=24hrs
Cell Lysis

B)

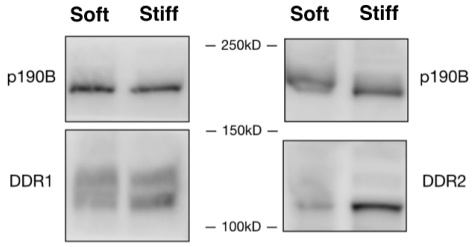
Soft
Stiff
Soft
Stiff
p190B
DDR1
250kD
150kD
100kD
p190B
DDR2

C)

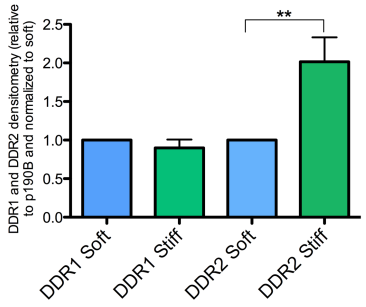
DDR1 and DDR2 densitometry (relative to p190B and normalized to soft)
2.5
2.0
1.5
1.0
0.5
0.0
**
DDR1 Soft
DDR1 Stiff
DDR2 Soft
DDR2 Stiff

D)

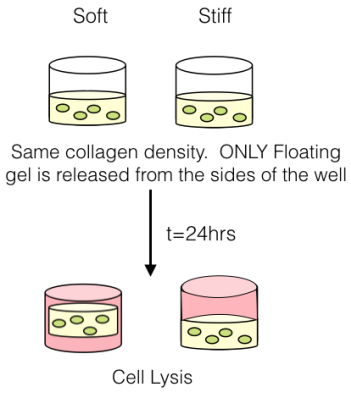
Soft
Stiff
Same collagen density. ONLY Floating gel is released from the sides of the well
t=24hrs
Cell Lysis

E)

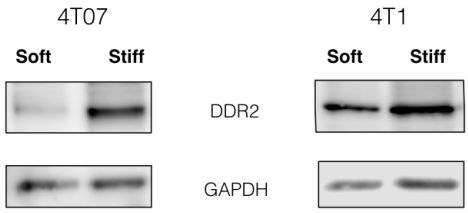
4T07
4T1
Soft
Stiff
Soft
Stiff
DDR2
GAPDH

F)

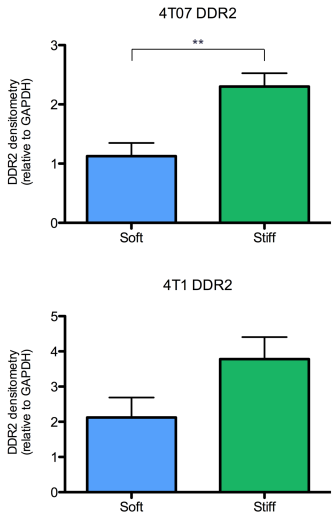
4T07 DDR2
**
DDR2 densitometry (relative to GAPDH)
3
2
1
0
Soft
Stiff
4T1 DDR2
DDR2 densitometry (relative to GAPDH)
5
4
3
2
1
0
Soft
Stiff

Figure 3-2. Blocking α2 integrin decreases FAK phosphorylation, DDR2 and ATF4

A) 4T07 and 4T1 cells were cultured in either soft or stiff collagen gel environments ± IgG control or CD49b (10μg/mL) for 24h before cell lysis and assessing (B) DDR2 and (C) ATF4 protein production. Representative immunoblots are displayed for 4T07 and densitometry is measured relative to GAPDH levels and normalized to soft. n=3, mean ±SEM, *$p \leq 0.05$, ***$p \leq 0.001$ vs respective control.

A)

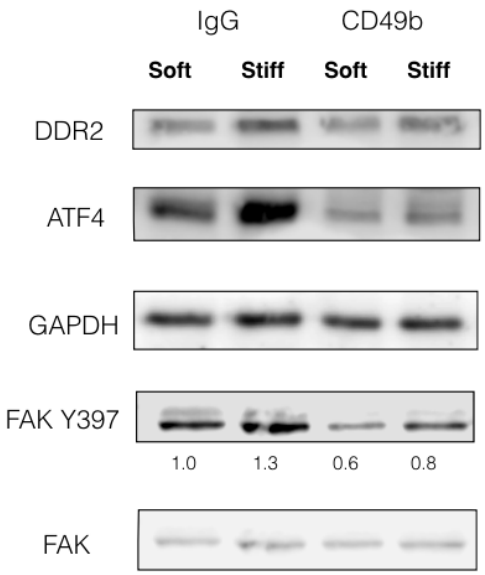
IgG
CD49b
Soft
Stiff
Soft
Stiff
DDR2
ATF4
GAPDH
FAK Y397
1.0
1.3
0.6
0.8
FAK

B)

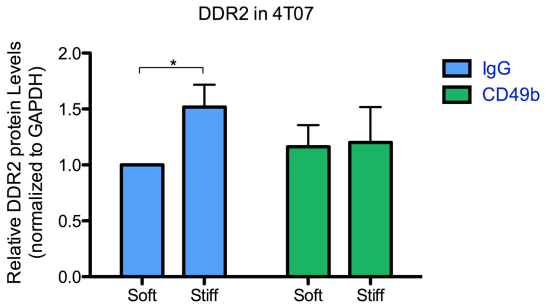
DDR2 in 4T07
Relative DDR2 protein Levels
(normalized to GAPDH)
2.0
1.5
1.0
0.5
0.0
*
Soft
Stiff
Soft
Stiff
IgG
CD49b

C)

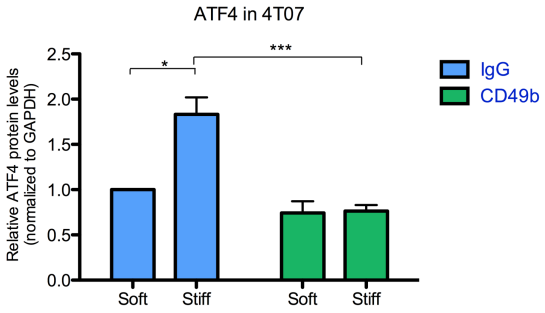
ATF4 in 4T07
Relative ATF4 protein levels
(normalized to GAPDH)
2.5
2.0
1.5
1.0
0.5
0.0
*
***
Soft
Stiff
Soft
Stiff
IgG
CD49b

Figure 3-3. DDR2 expression is controlled by modulating activity of FAK

A) Representative blot of DDR2 and p-FAK ± DMSO or PF-562,271 (10μM) and B) densitometry relative to GAPDH. C) Representative blot for TAE-226 (1μM) treatment and D) densitometry of protein production of DDR2 and ATF4 in 3D soft and stiff. E) Mock-transfected or SuperFAK cells were cultured in soft and stiff and lysed after 24h and F) densitometry is relative to GAPDH. $n \geq 3$, mean ±SEM,*$p<0.05$, **$p<0.01$,***$p<0.001$ vs respective control.

A)

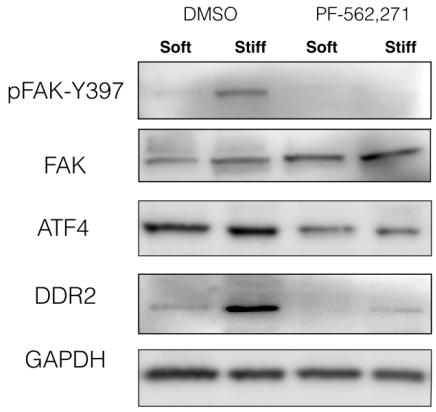
DMSO
PF-562,271
Soft
Stiff
Soft
Stiff
pFAK-Y397
FAK
ATF4
DDR2
GAPDH

B)

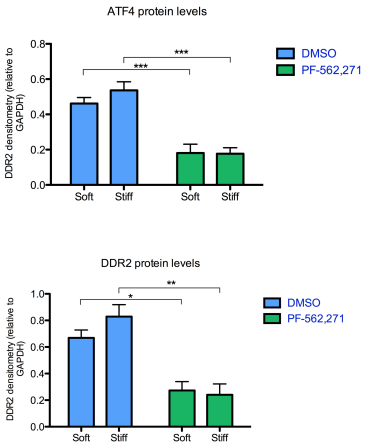
ATF4 protein levels
DDR2 densitometry (relative to GAPDH)
***
***
DMSO
PF-562,271
Soft
Stiff
Soft
Stiff
DDR2 protein levels
DDR2 densitometry (relative to GAPDH)
**
*
DMSO
PF-562,271
Soft
Stiff
Soft
Stiff

C)

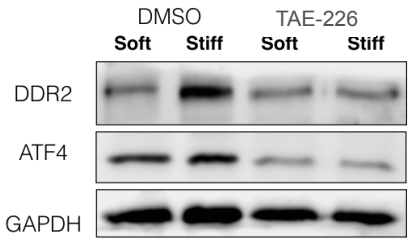
DMSO
TAE-226
Soft
Stiff
Soft
Stiff
DDR2
ATF4
GAPDH

D)

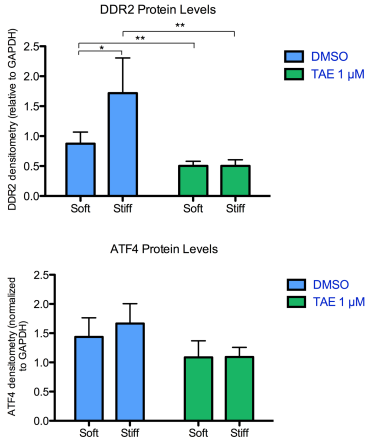
DDR2 Protein Levels
DDR2 densitometry (relative to GAPDH)
**
**
*
DMSO
TAE 1 μM
Soft
Stiff
Soft
Stiff
ATF4 Protein Levels
ATF4 densitometry (normalized to GAPDH)
DMSO
TAE 1 μM
Soft
Stiff
Soft
Stiff

E)

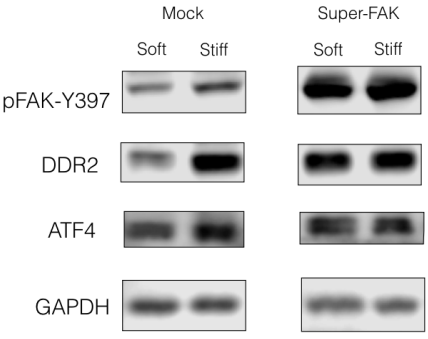
Mock
Super-FAK
Soft
Stiff
Soft
Stiff
pFAK-Y397
DDR2
ATF4
GAPDH

F)

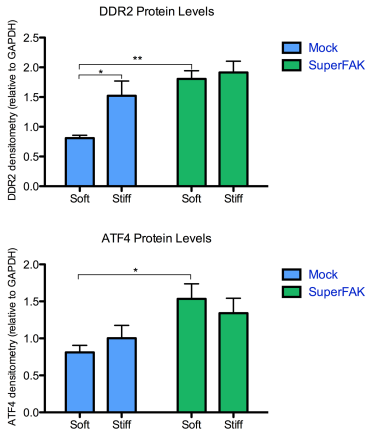
DDR2 Protein Levels
DDR2 densitometry (relative to GAPDH)
**
*
Mock
SuperFAK
Soft
Stiff
Soft
Stiff
ATF4 Protein Levels
ATF4 densitometry (relative to GAPDH)
*
Mock
SuperFAK
Soft
Stiff
Soft
Stiff

Figure 3-4. DDR2 expression is negatively regulated by p-ERK.

A) 4T07 and 4T1 cells were cultured in soft or stiff gels with ±U0126 (10μM) and ± PF-562,271 (10μM) for 24h before cell lysis. Assessment of DDR2, p-FAK, and p-ERK production by immunoblotting was measured by densitometry and normalized to GAPDH, total FAK, and total ERK, respectively. B) Representative immunoblots are displayed. n=4, ±SEM,**$p<0.01$.

A)

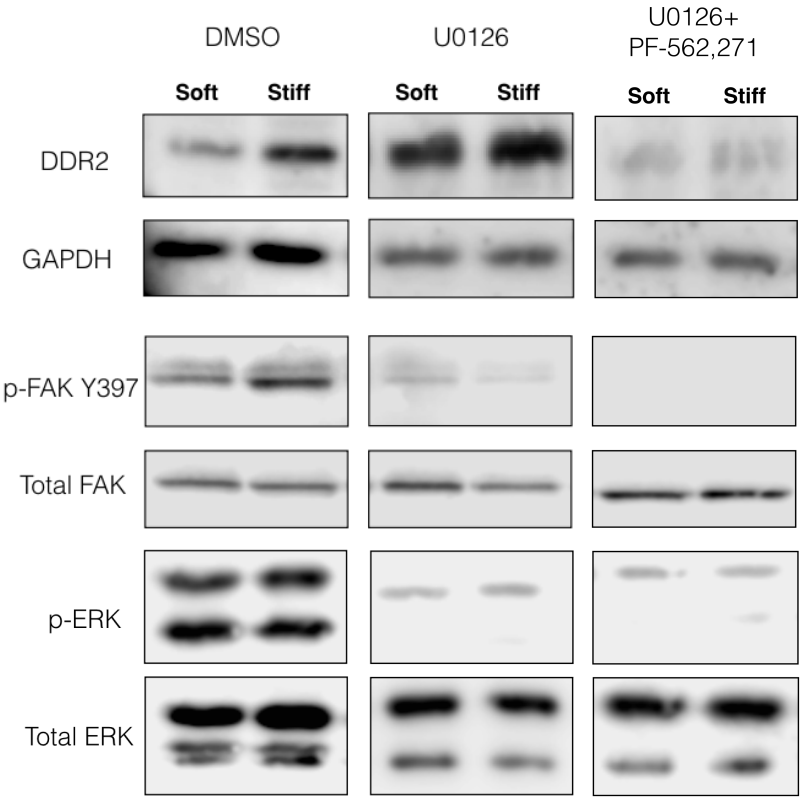
DMSO
U0126
U0126+
PF-562,271
Soft
Stiff
Soft
Stiff
Soft
Stiff
DDR2
GAPDH
p-FAK Y397
Total FAK
p-ERK
Total ERK

B)

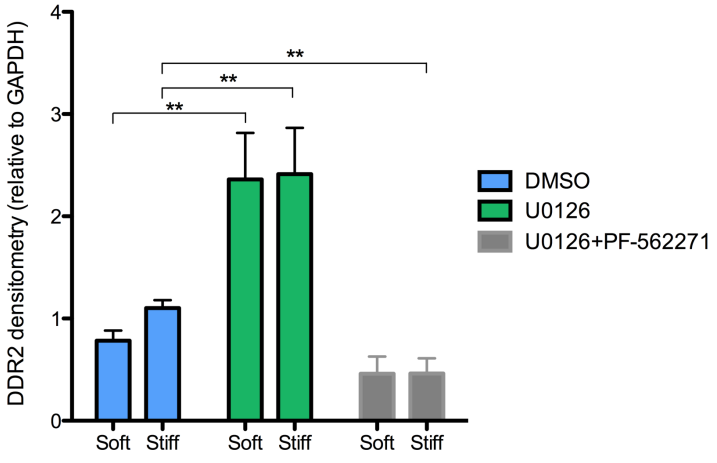
DDR2 densitometry (relative to GAPDH)
0
1
2
3
4
**
**
**
Soft
Stiff
Soft
Stiff
Soft
Stiff
DMSO
U0126
U0126+PF-562271

Figure 3-5. mRNA levels correlate with increased DDR2 protein in stiff matrices

A) Collagen gels were treated with DMSO, U0126 (10μM) and/or PF-562,271 (10μM) for 24h before RNA extraction and cDNA synthesis. qRT-PCR was performed using 18s rRNA as the normalizing gene to measure transcript levels. mRNA levels were then, normalized to soft untreated. The ΔΔCt method was used to calculate the relative quantity of gene expression levels. Ct is the threshold cycle where the amplification of template begins determined by the software. Relative levels= $2^{-\Delta\Delta Ct}$ and $\Delta\Delta C_t=(C_{t\ experimental} - C_{t\ 18s\ rRNA})-(C_{t\ control} - C_{t\ 18s\ rRNA})$. Data presented are the mean ± SEM, n=3, *p<0.05, ***p<0.001 vs. soft untreated.

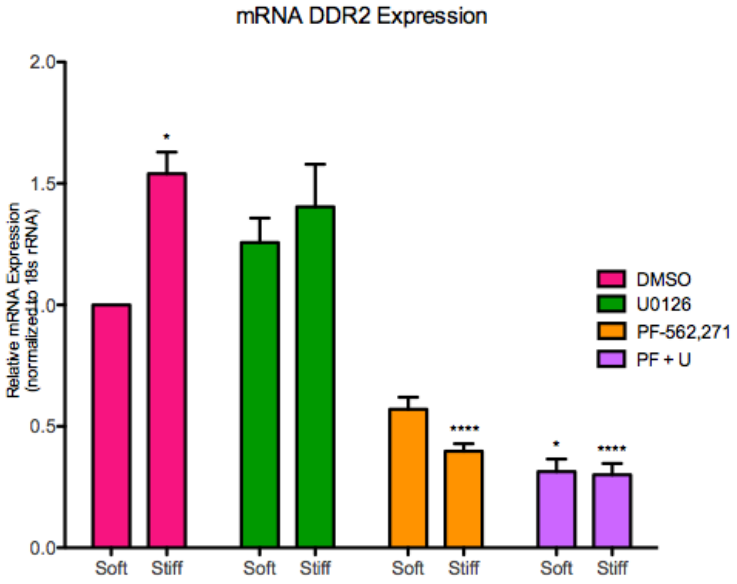
mRNA DDR2 Expression
Relative mRNA Expression (normalized to 18s rRNA)
2.0
1.5
1.0
0.5
0.0
*
****
*
****
Soft
Stiff
Soft
Stiff
Soft
Stiff
Soft
Stiff
DMSO
U0126
PF-562,271
PF + U

Figure 3-6. DDR1-depleted cells elevate DDR2 expression

MCF7 cells were stably transfected with shControl (pGIPZ) or shRNA-DDR1 and were cultured in 3D environments for 24h before cell lysis and immunoblotting. A) DDR1 protein levels are significantly reduced by shRNA and B) DDR2 levels show an increase in their protein amount, as well as ATF4. C) Representative immunoblots are shown to depict ATF4 and DDR2 up-regulation. Protein quantity was measured using densitometry and normalized to GAPDH. n=3, mean±SEM,**p<0.05,**p<0.01, ***p<0.001

A)

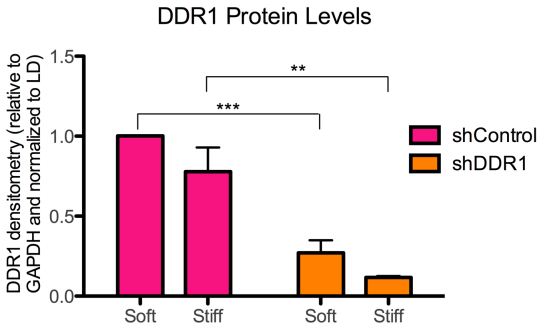
DDR1 Protein Levels
DDR1 densitometry (relative to GAPDH and normalized to LD)
1.5
1.0
0.5
0.0
**
***
shControl
shDDR1
Soft
Stiff
Soft
Stiff

B)


DDR2 Protein Levels
DDR2 densitometry (relative to GAPDH and normalized to LD)
6
4
2
0
*
*
*
shControl
shDDR1
Soft
Stiff
Soft
Stiff

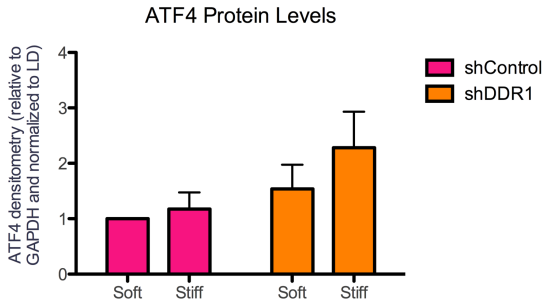
ATF4 Protein Levels
ATF4 densitometry (relative to GAPDH and normalized to LD)
4
3
2
1
0
shControl
shDDR1
Soft
Stiff
Soft
Stiff

C)

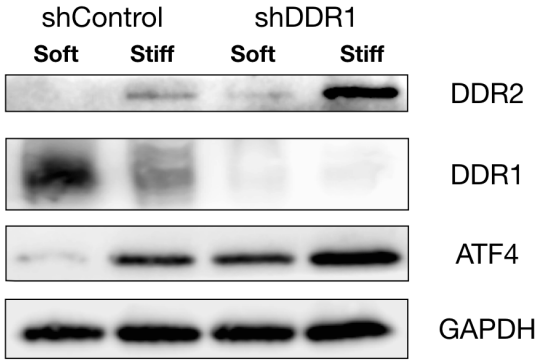
shControl
shDDR1
Soft
Stiff
Soft
Stiff
DDR2
DDR1
ATF4
GAPDH

Figure 3-7. Inhibiting DDR2's activity with WRG-28 enhances DDR2 protein production, increases p-FAK levels ,and reduces cell proliferation

-4T07 cells were treated with WRG-28 (5μM) for 24h before cell lysis and immunoblotting. Cells were cultured on either soft or stiff conditions. A) Densitometry was used to calculate DDR2 and p-FAK levels. B) Representative blot of 4T07 WRG-28 treated and DDR2 production assessment. C) 6-well gels with 300K were cultured for 48h ±WRG-28 on soft or stiff matrices and proliferation was quantified with fluorescence reading from Cyquant NF addition. D) Stably transfected DDR2 over-expressing and SuperFAK cells in soft or stiff matrices were quantified for proliferation with Cyquant NF. Raw numbers from each collagen gel were normalized per experiment to the values from the soft, untreated gels. n=3, mean ±SEM,*$p<0.05$,**$p<0.01$

A)

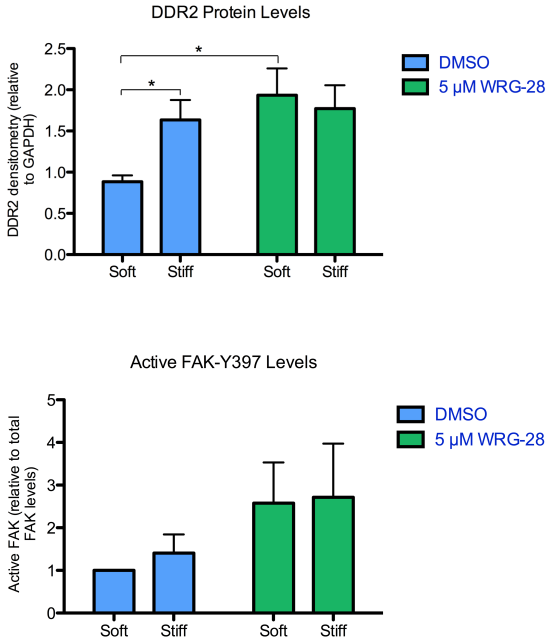
DDR2 Protein Levels
DDR2 densitometry (relative to GAPDH)
2.5
2.0
1.5
1.0
0.5
0.0
*
*
Soft
Stiff
Soft
Stiff
DMSO
5 μM WRG-28
Active FAK-Y397 Levels
Active FAK (relative to total FAK levels)
5
4
3
2
1
0
Soft
Stiff
Soft
Stiff
DMSO
5 μM WRG-28

B)

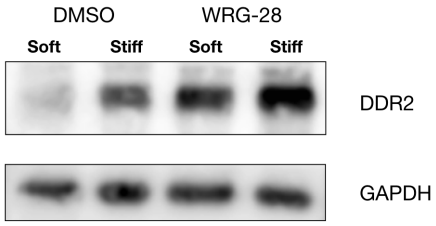
DMSO
WRG-28
Soft
Stiff
Soft
Stiff
DDR2
GAPDH

C)

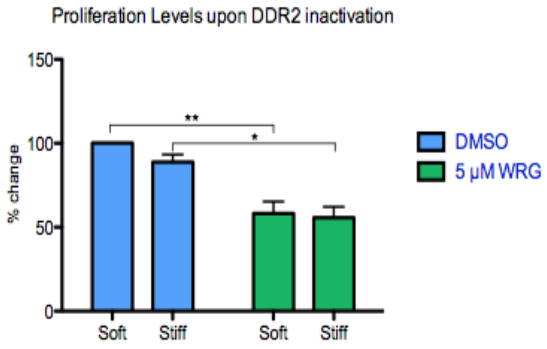
Proliferation Levels upon DDR2 inactivation
% change
150
100
50
0
**
*
Soft
Stiff
Soft
Stiff
DMSO
5 μM WRG

D)

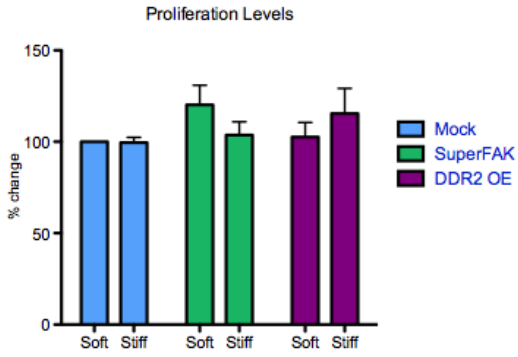
Proliferation Levels
% change
150
100
50
0
Soft
Stiff
Soft
Stiff
Soft
Stiff
Mock
SuperFAK
DDR2 OE

Figure 3-8. WRG-28 retards invasion and hinders collagen alignment

A cell plug of 20K of either 4T07 or 4T1 cells were seeded into a soft 3D collagen matrix (2mg/mL) ±WRG-28 and allowed to migrate for 48h for a time-lapse collection. After collection of time-lapse images, 3D plugs were fixed and SHG images were gathered, and CT-FIRE fiber re-construction was performed for angle measurement around the plug. Representative SHG images are displayed with CT-FIRE rendering for 4T07 (A) and 4T1 (B). (C,D) Three ROIs were taken from outside of the plug to quantify collagen alignment using CT-FIRE angle distribution parameter. (E,F) A low-magnification image was taken to assess total cell migration and (G,H) total distance traveled. n=5, mean is represented ±SEM, *$p<0.05$, **$p<0.01$, ***$p<0.001$. Scale bar 100 μm

A)

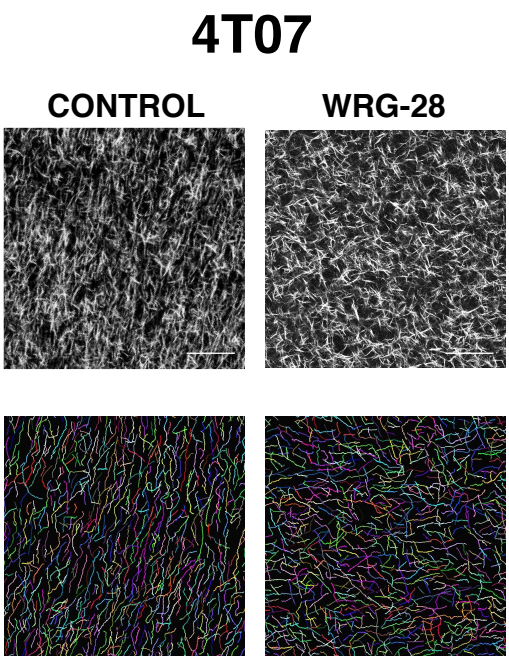
4T07
CONTROL
WRG-28

B)

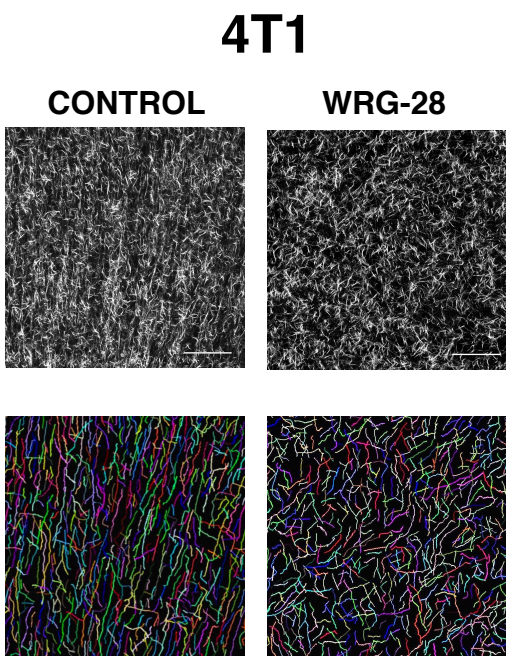
4T1
CONTROL
WRG-28

C)

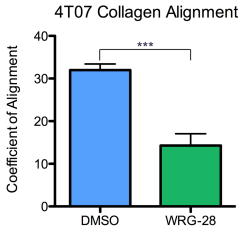
4T07 Collagen Alignment
Coefficient of Alignment
***
DMSO
WRG-28

D)

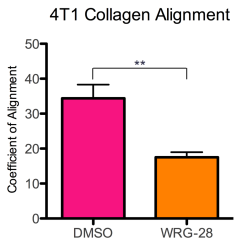
4T1 Collagen Alignment
Coefficient of Alignment
**
DMSO
WRG-28

E)

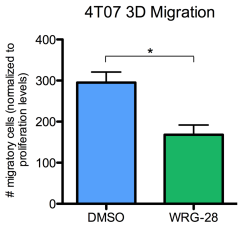
4T07 3D Migration
migratory cells (normalized to proliferation levels)
*
DMSO
WRG-28

F)

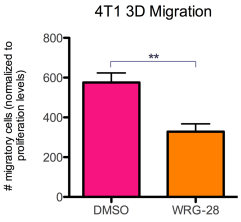
4T1 3D Migration
migratory cells (normalized to proliferation levels)
**
DMSO
WRG-28

G)

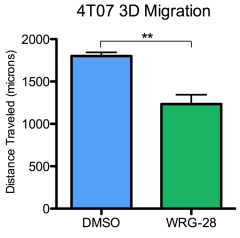
4T07 3D Migration
Distance Traveled (microns)
**
DMSO
WRG-28

H)

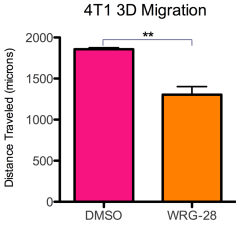
4T1 3D Migration
Distance Traveled (microns)
**
DMSO
WRG-28

Figure 3-9. Extracellular stiffness modulates DDR2 expression

As carcinoma mammary epithelial cells use DDR2 to align collagen and invade through a collagen matrix, stiffness in the microenvironment increases as fibers become more aligned. Alignment and high DDR2 expression drive cell invasion in highly active FAK cells.

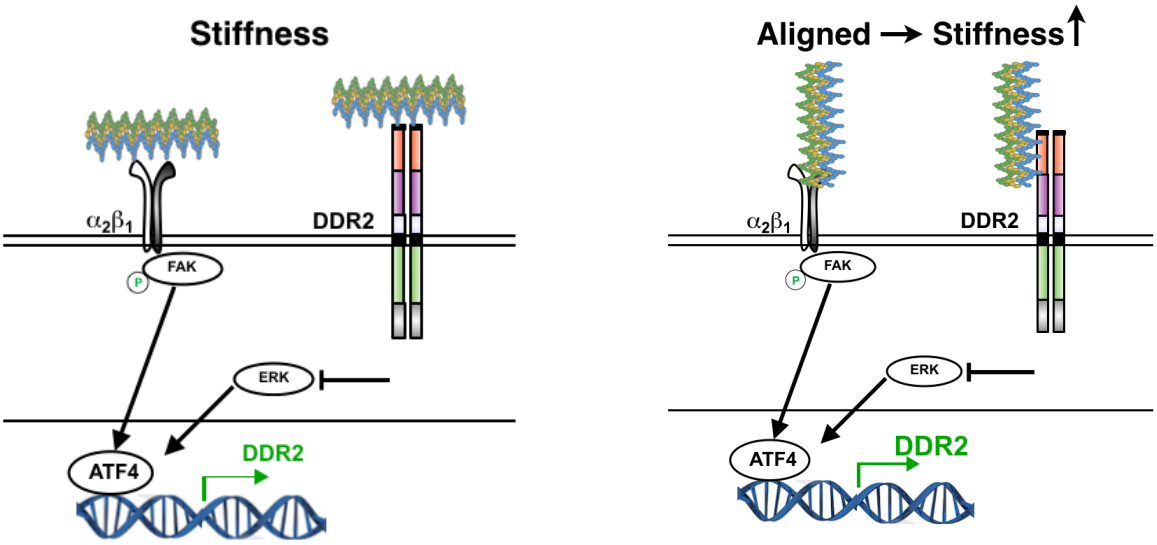
Stiffness
α2β1
DDR2
FAK
P
ERK
ATF4
DDR2
Aligned → Stiffness
α2β1
DDR2
FAK
P
ERK
ATF4
DDR2

DISCUSSION

Aligned collagen facilitates invasion out of primary tumors and is associated with poor patient outcome [11, 136]. Here, we find that stiff collagen matrices induce DDR2 expression (Figure 1). Increased DDR2 expression was downstream of the α2 integrin and FAK activation, and was negatively regulated by DDR1 and ERK (Figure 4, 6). Moreover, use of a novel inhibitor of DDR2 blocks cell-driven collagen alignment and subsequent invasion through 3D collagen matrices. Together, these findings suggest that extracellular matrix stiffness may drive a more invasive phenotype through DDR2.

Regulation of DDR2 is an important finding, as DDR2 levels are highly elevated in human breast tumors and, thus, linked to mammary tumor progression [60, 87, 129]. DDR2 functions as a collagen receptor and is expressed in mesenchymal cells. This, combined with its ability to facilitate invasiveness by regulating various matrix metalloproteinases (MMPs) suggests that control of DDR2 is an important aspect of breast cancer metastasis [47, 48, 137].

DDR1 is typically found in epithelial cells, while DDR2 is exclusively expressed in mesenchymal cells [43]. It may suggest that cells have the ability to acquire a different phenotype, similar to the observation that mesenchymal cells change from expressing E-cadherin to N-cadherin to promote migration. [138, 139]. By knocking-down DDR1, we measured an amplification of DDR2 leading us to believe that cancer cells compensate for the loss of a collagen-binding receptor, DDR1, by increasing the levels of another, DDR2. In this case, the shift in DDR expression also triggered to an invasive phenotype (Figure 6). However, we were unable to knock-down DDR2 to test if these mesenchymal cells increase DDR1 and revert to an epithelial, non-migratory phenotype.

Collagen also functions as a ligand for integrin binding and the resulting focal adhesion formation is required for FAK activation [34, 140]. We sought to understand whether collagen-binding integrins were upstream of this regulation and observed that using an antibody to α2 integrin blocks FAK phosphorylation and DDR2 up-regulation (Figure 2). Cancer cells that stably express SuperFAK, a pseudo-hyperphosphorylated FAK, demonstrate an increased downstream signaling effect and directly affected DDR2 (Figure 3). These findings shed light on how p-FAK senses mechanical tension and tightly regulates DDR2 and may be essential to understanding how cancer progression is associated with this pathway in a stiff microenvironment.

We identified ERK activation as a negative regulator of DDR2 levels, and that ERK functions on a pathway that is not apparently downstream of FAK in this system. This may explain the surprising observation that phosphorylation of ERK is decreased in stiff matrices, even though ERK is associated with proliferation and has been reported by us and others to be increased in stiff matrices [34, 140, 141]. It should be noted that here our time course differed from those studies, being much shorter (24h, rather than several days). While the relative quantities of mRNA between conditions resemble their protein levels, we discovered that ERK likely regulates DDR2 at the level of protein stability because inhibition with U0126 did not affect the the mRNA expression compared to vehicle-only samples (Figure 5).

ATF4 is a transcriptional regulator of DDR2, and thus it is striking that we observe that ATF4 regulation parallels DDR2 response to matrix stiffness [52]. Employing a transcriptome profiling approach, ATF4 was shown to be down-regulated by p38-MAPK signaling and thus, may contribute to a proliferation signature, like DDR2 [142]. Here, we show that ATF4 protein

levels are decreased after FAK activity is inhibited and when DDR1 is knocked-down, suggesting a transcriptional regulation by ATF4 (Figure 3 and 6). Upon U0126 addition, no changes in ATF4 protein were observed. miR-214 is a potential regulator in cancer cells that controls ATF4 protein stability as seen in gluconeogenesis and osteoblast activity, and its reduced levels contributes to tumorigenesis and proliferation in breast cancer cell lines [143-145]. We were not successful in reducing ATF4 mRNA expression via siRNA or shRNA in attempt to link ATF4 and DDR2. However, we performed the alternative by increasing the activity of ATF4 using an activator of endoplasmic reticulum stress, tunicamycin. By western blotting, we discovered that DDR2 levels were increased by this treatment (unpublished observation).

In summary, we find a novel pathway by which integrin-mediated activation of FAK leads to increased levels of DDR2. The subsequent increased cell proliferation and ability of the cells to align and migrate through collagen matrices suggest that this pathway may be important for breast cancer progression.

SUPPLEMENTARY FIGURES

Figure 3-S1. Varying stiffness on Polyacrylamide gels induces DDR2 expression

PA gels coated with collagen at 200μg/mL induces DDR2 up-regulation and phosphorylation of FAK is elevated by stiffness. We followed primarily [146] to produce PA gels of varying stiffness from soft (2kPa) to stiff (31kPa). 2.5 x10^5 cells were plated on top of the gel and allowed to adhere for 24h before cell lysis.

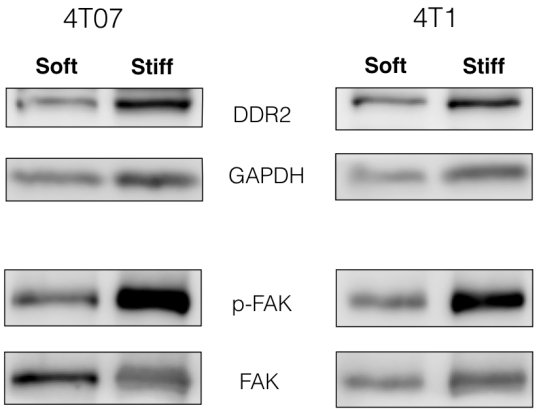

Figure 3-S2. DDR2 activity is increased matching DDR2 protein expression

Representative blot for phosphorylation of DDR2 (Y740) on either soft or stiff matrices showing that in 3D collagen environments DDR2 is constantly being phosphorylated but the pool of total protein in stiff matrices is higher than when cultured in soft.

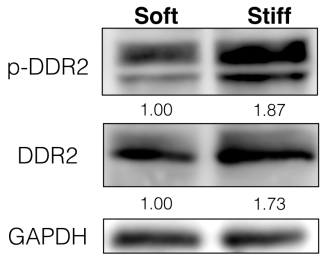

Figure 3-S3. Photos of collagen 3D invasion plugs after 48h of invasion

12-well non-tissue culture treated plates harbors 500µL of a 2mg/mL collagen gel and allowed to polymerize for 10min. 2.5 x10^4 4T07 and 4T1 cells were seeded in 5µL of a 2mg/mL plug. Sides of the dish were released and 500µL of media was added to the sides. Collagen gels were then either fixed or movies were taken.

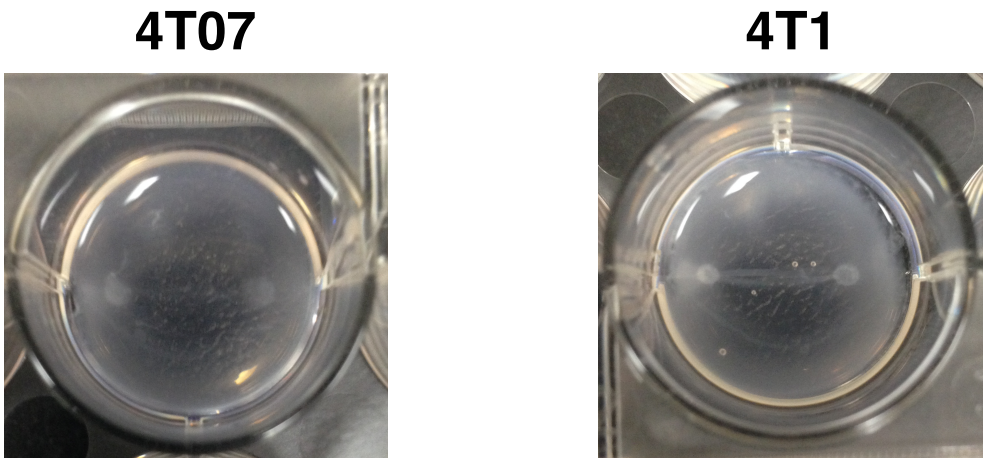

Figure 3-S4. Montage of SHG images ±WRG-28

4T07 and 4T1 cells ±WRG-28 after 48h treatment in 2mg/mL collagen gels. Three different regions of interest were chosen around the cell plug and imaged using a multiphoton microscope to gather the structures of collagen and by SHG. Scale bar 100μm

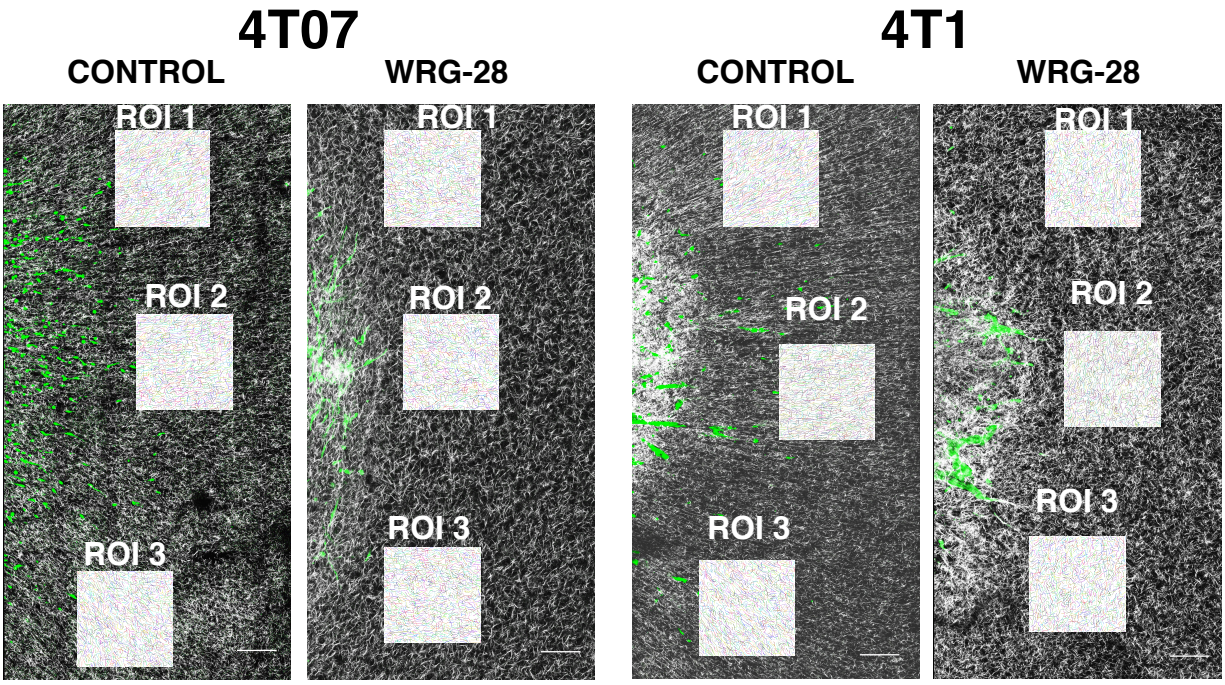

Supplementary Movies. Both A) 4T07 and B) 4T1 cancer cell lines were seeded into 5µL plugs of $5x10^4$ cells as shown in Supplementary Fig. S3 and were cultured at 37°C, 5%CO_2 for 48h, ± C, D) WRG-28, respectively. Bright-field acquisition images every 3min at 20X was taken by TE300 Nikon inverted microscope for 3h at different z-stacks. Movies were reconstructed using ImageJ as cells were migrating in different planes over time due to the thickness of the collagen gel. For measuring protrusions, invasion plugs were fixed after movies were taken. For each cell, the nucleus was identified and the length of a directional protrusion towards the other plug was measured.

A)

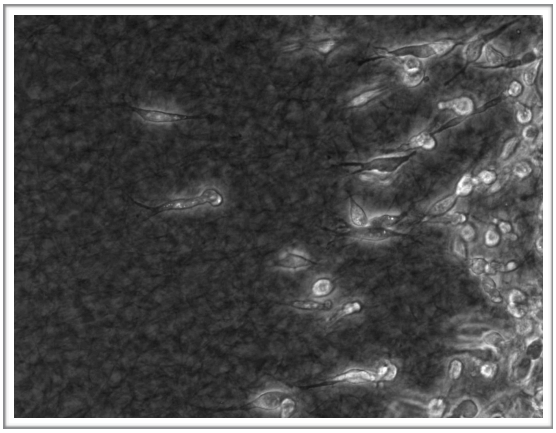

B)

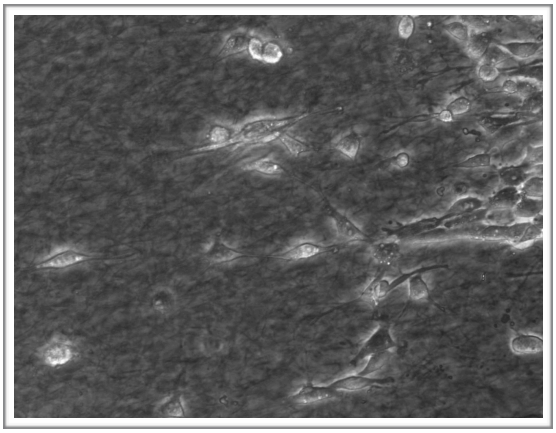

C)

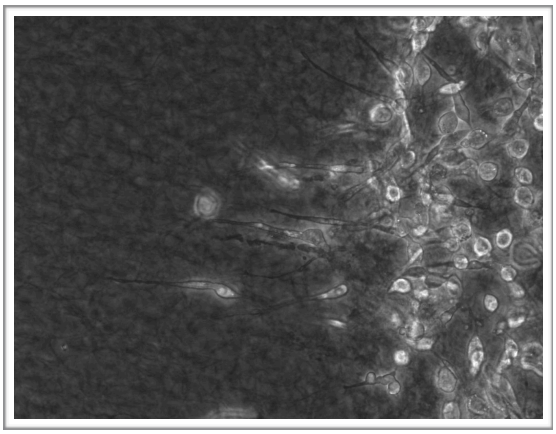

D)

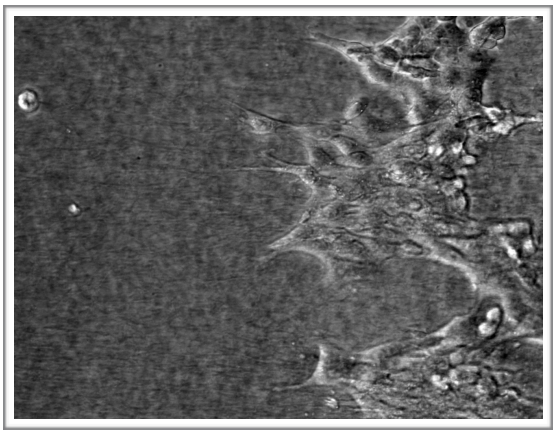

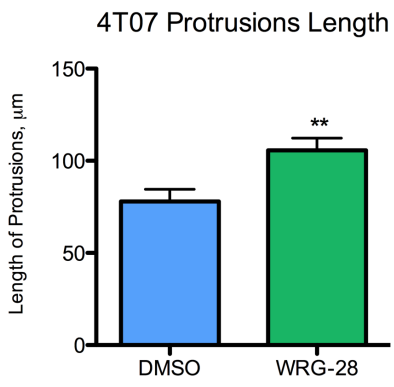
4T07 Protrusions Length
Length of Protrusions, µm
150
100
50
0
**
DMSO
WRG-28

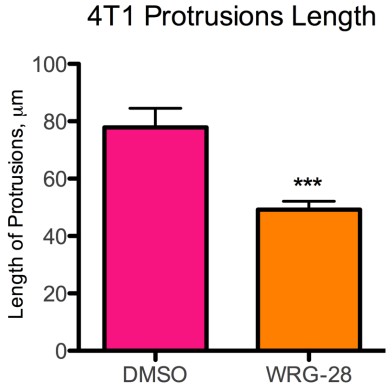
4T1 Protrusions Length
Length of Protrusions, µm
100
80
60
40
20
0
***
DMSO
WRG-28

MATERIAL AND METHODS

Cell lines and cell culture

Mouse 4T07 and 4T1 were used as mouse cell lines that demonstrate a quiescent or invasive phenotype, respectively. The MCF7 cell line was kindly provided by Dr. Linda Schuler (UW-Madison, Madison, WI). 4T07 and 4T1 were a kind gift by Dr. Julio Aguirre-Guiso, cultured in either cultured in either soft (2mg/ml, floating) or stiff conditions (2mg/ml, attached) in type I collagen gels as previously described [118]. In brief, rat tail collagen (Corning, 354249, Bedford, MA) was mixed thoroughly with a neutralization solution containing 100 mM Hepes and 2x PBS (pH 7.4) and placed briefly on ice to delay polymerization. Low-density (1 mg/ml) or high-density collagen in neutralized solutions were added to cells suspended in complete media and plated in 6-well non-tissue cultured treated plates (BD Falcon™, Franklin Lakes, NJ). All cell lines were cultured in RPMI 1640 (Gibco Life Technologies, Grand Island, NY) with 10% Fetal Bovine Serum (Gemini BioProducts, West Sacramento, CA). For gel 3D collagen gel pouring, cells and media were thoroughly mixed with neutralized collagen. A total volume of 1 ml cells/media/collagen was used per well/gel. After 10 mins, gels were incubated in 5% CO_2, 37°C for 2h. The gels were then either released from or left attached to the plate by gently sliding a 200 µl pipet tip around the outer edge of the gel and 2 mL of complete media was added to the gel prior to returning the plate to the incubator.

For drug treatment, cells were cultured overnight with 10µM FAK ATP inhibitor PF-562271, 1µM TAE226 (Selleckchem, Houston, TX),10 µM Src kinase inhibitor PP2 (Calbiochem/Millipore, Billerica, MA), 5 µM WRG-28 (DDR2 inhibitor, gift from Dr. Longmore at Washington University), U0126 10 µM MEK inhibitor (Promega, Madison,WI),

CD49b (BD Pharmingen, 558759). SuperFAK was a gift from Dr. Duperret at the University of Pennsylvania and p-FLRU-DDR2 (DDR2 O/E) was a kind gift from Dr. Greg Longmore at Washington University.

Immunoblots

Cells cultured in collagen gels were washed in ice-cold PBS and lysed in 200 µl 2X RIPA buffer (50 mM Tris [pH 7.4], 150 mM NaCl, 2 mM Na_2EDTA, 2% NP-40, 0.5% deoxycholic acid, 2 mM NaF, 1 mM Na_3VO_4). The lysate was repeatedly passed through an 18 gauge needle and centrifuged (15,800xg, 10min, 4°C) to clear the lysate. The supernatant solution was mixed with 10X sample buffer (100 mM Tris [pH 8], 7.5 mM EDTA, 100 mM dithiothreitol, 10% sodium dodecyl sulfate, 30% glycerol, 1% bromophenol blue) to a 1X sample buffer final concentration. Protein samples were boiled (8min), loaded onto an SDS-PAGE gel, transferred to a 0.45 mm Immobilion-P polyvinylidene difluoride membranes (Millipore). Blots were cut for multiple detection and incubated with antibodies raised against DDR2, p-DDR2, ATF4 (R&D Systems, AF2538, MAB25382, MAB7218), p-FAK(pY397) (Life Technologies, 44624G), total FAK (Millipore, 05-537), p44/42 MAPK, p-p44/42 MAPK (pT202/Y204) (Cell Signaling Technology, Beverly, MA), or GAPDH (Santa Cruz, sc-25778). Blots were washed and subsequently incubated with HRP-conjugated secondary antibodies (Jackson Immunolabs). Bound secondary antibody was visualized following incubation of the membrane with SuperSignal West chemiluminescent HRP substrate (Thermo Scientific Pierce) and using a LI-COR Odyssey (LI-COR) for imaging. Luminescence was quantified and evaluated using LI-COR's ImageStudio Software.

Immunofluorescence

Collagen and polyacrylamide gels were rinsed with TBST and then fixed with 1mL 4% paraformaldehyde for 15min. Followed by a wash with TBST, 1mL of 0.2% Triton was added. The plate incubated at RT for another 10min and was washed again with TBST. Following the removal of TBST, 1mL of blocking solution (1% Donkey Serum and 1% BSA in PBS) was added and allowed to incubate at 4°C overnight. Following the incubation, the blocking solution was removed from the plate, and fresh blocking serum containing the primary antibody was added. The gels were incubated at 4°C overnight. Next, gels were washed 3 times with TBST before adding fresh blocking serum containing the secondary antibodies. The plate incubated at RT for 1h. DAPI was added on the last wash step and incubated for 5min before extra washes with TBST. Then, the collagen gels were imaged using a 40X water or 60x oil objective on a TE300 Nikon inverted microscope (Nikon, Melville, NY) controlled by Slidebook software (Intelligent Imaging Innovations, Denver, CO).

RNA extraction from 3D collagen gels

Floating and attached collagen type I gels were plated with $7x10^5$ for both 4T1 and 4T07 cells. Gels were either treated with DMSO, U0126 and/or PF-562,271 overnight. After 24h, media was removed and washed quickly with ice-cold PBS. We followed the manufacturer's protocol for the extraction with RNeasy Fibrous tissue (QIAGEN, Valencia, CA) Briefly, β-Mercaptoethanol was added to Buffer RLT before use and 300µL was used per gel. Collagen gels were homogenized by pipetting. Added Proteinase K and incubated at 55°C for 10min. Transfer supernatant to new tube and perform washes. Performed DNase treatment in column.

RNA was eluted and its quality and concentration were measured using a NanoDrop spectrophotometer (Thermo Scientific).

Quantitative Real-time Polymerase Chain Reaction

After RNA extraction, 1µg of RNA was transcribed into cDNA using iScript cDNA Synthesis Kit (Bio-Rad) and followed the manufacturer's manual. Template was diluted 1:10 in RNase-free water after synthesis before amplification. Used Roche qPCR primer design for the majority of the primers used and were confirmed through *in silico* qPCR (genome.uscs.edu). Cycles to determine threshold of targets were normalized to 18s rRNA and then compared to Soft-Untreated to determine fold change. Blank and no template controls were also analyzed. Cycling protocol as follows: 30s at 95°C, 10s at 95°C and 30s at 52°C for 40 cycles. Melt-curve analysis was also performed after each experiment.

DDR2: Forward: 5- ATC CAG ACT GAT CCG AAA GC -3; Reverse: 5- GCT TCA CAA CAC CAC TGC AC -3

Snail1: Forward: 5- TCT GCA CGA CCT GTG GAA AG -3; Reverse: 5- TCA CAT CCG AGT GGG TTT GG -3

18s rRNA: Forward: 5-TTC GAA CGT CTG CCC TAT CAA -3; Reverse: 5-CTT CCT TGG ATG TGG TAG CCG -3

Cyquant Proliferation Assay

Cyquant NF Cell Proliferation Assay Kit was used (Life Technologies). Collagen gels were washed with PBS once for 5min each, 48h after being poured and treated. Meanwhile, 5X Hank's Balanced Salt Solution (HBSS) was mixed with DI water in a 2:3 ratio of HBSS to water. The solution was kept out of light. After the gels finished washing, the remaining PBS was

removed, and the gels were carefully spread in the well, avoiding folding. Then, in a 1:25 ratio, Cyquant Dye A was added to the HBSS and DI water mixture. 250 µL of this mixture were added to each well atop the gel, and the plate was covered with foil and incubated at 37°C for 30min. After this time, fluorescence was read on a Fluoroskan Ascent Plate Reader (Thermo Scientific) and proliferation levels were normalized to Soft-Untreated.

Collagen Plug Migration Assay

Using a 2mg/mL mix of media and neutralized collagen, gels were poured into 12-well, non-tissue culture treated plates. The gels were allowed to sit at RT for 10min. Next, a solution of 2mg/mL collagen in media with $1x10^7$ cells per mL was made. 5µL mixture of collagen solution and cells was then added to two opposite ends of the gels, allowing the droplet to sit atop the polymerizing gel. The gels incubated at RT for 5min and then were incubated at 37°C. After 1h, the gels were treated and released from the edges of the wells and left to incubate at 37°C overnight. After 48h, the plugs were carefully placed onto a glass bottom dish and allowed to settle for 15min before imaging. They were imaged using a 20X objective on a TE300 Nikon inverted microscope (Nikon, Melville, NY) controlled by Slidebook software (Intelligent Imaging Innovations, Denver, CO) for a 3D 3h time lapse. Images were taken every 3min, stacks every 5µm and processed using ImageJ software (National Institutes of Health).

Second Harmonic Generation

All imaging was done at the Laboratory for Optical and Computational Instrumentation (LOCI) at the University of Wisconsin-Madison. Upright intensity Multiphoton Microscopy was conducted on the Ultima IV (Bruker Nano Surfaces, Middleton, WI). Laser excitation on the Ultima IV was provided by the Insight (Spectra Physics, Palo Alto, CA) and detection by a

Hamamatsu multi-alkali photomultiplier detectors. Data acquisition and scanning control was provided by PrairieView (Bruker Nano Surfaces, Middleton, WI). Images were gathered with Zeiss 20X water 1.0 NA objective lens. Second Harmonic Generation images were gathered using 890nm excitation and 445/35 BP emission filter. Cell auto-fluorescence was gathered using 890nm excitation and 592/100 BP emission filter.

Statistical and Fiber Analysis

Statistical analysis was performed using GraphPad Prism 5 (GraphPad Software, La Jolla, CA) with an unpaired student's t test (two-tail), and two-way ANOVA using Bonferroni post-test method for comparison with multiple parameters. For fiber analysis of 3D cell plugs, we chose three different regions of interest (ROI) for each plug and measured angles perpendicular to the plug using default parameters on CT-FIRE software [147]. Angles were measured from 0° to 180° and any angle between 72° to 108° (90°±18) was deemed aligned and was normalized to the total number of fibers in that image using MATLAB (MathWorks, Natick, Massachusetts). Theses proportions were pooled and the mean was used for a two-tail unpaired student's t test.

CONCLUSIONS

The risk for developing breast carcinomas increases for women with high breast density [4, 5] When analyzing all the possible factors that may promote the development of breast cancer, breast density is the greatest independent risk factor [4]. In *in vivo* murine models, breast cancer cells metastasize onto aligned collagen fibers that are mechanically stiff [10, 121]. Understanding the cellular events and mechanisms that drive breast cancer progression is of vital importance because the number of deaths due to breast cancer remain significant. Although, there are signaling events that have been elucidated, it is still not well understood how a stiff tumor microenvironment can influence breast cancer progression. Previous work from our lab and others have established FAK activity as a mechanosensor that links ECM stiffness to the regulation of cell behavior [19, 34, 38]. It is known that the activity of FAK is modulated by stiffness, yet unproven as to what gene expression pathways are dependent on FAK.

The primary goal of this project was to identify pathways that were downstream of already known effectors to tissue stiffness. Both RhoA-GTP and p-FAK levels are greatly increased in cells embedded in a stiff matrix [19, 34]. In this study, RhoA activity correlates with the transcriptional activation of MRTF-A. In normal epithelial cells we measured that endogenous levels of MRTF-A targets were increased as well as observing high p-ERK levels in a stiff matrix. In cancer cells we find that this regulation is lost. Furthermore, FAK controls MRTF-A expression and thus, eliminates its transcriptional activity when FAK is inhibited. From previous *in vivo* studies FAK knock-out inhibits metastasis while it regulates an array of transcription factors [88]. Here, we also identified a transcription factor p53, a tumor suppressor, as being negatively regulated by FAK. Knock-down of p53 elevates the levels of MRTF-A

expression linking p53, FAK, and MRTF-A in the regulation of genes downstream of RhoA activation.

Moreover, the collagen receptor, DDR2, is regulated in a FAK-dependent manner, and DDR2 expression is linked to invasiveness and EMT. Matrix stiffness elevates both FAK activity and DDR2 expression. In carcinoma cells, p-ERK is down-regulated by matrix stiffness, and it negatively controls DDR2 expression. Furthermore, perturbing DDR2 activity by impeding its collagen binding reduces cell migration and collagen alignment, which are hallmarks of an invasive phenotype. While using drugs to inhibit FAK is a possible effective treatment alternative, breast cancer cells that are invasive express and exhibit high levels of DDR2 expression. Taken together, using a pharmacological inhibitor against DDR2 can be a more advantageous remedy due to its targeting of aggressive cancers.

FUTURE DIRECTIONS

Molecular mechanisms that drive tumorigenesis and metastatic disease are defined in countless studies. Breast cancer progression is in fact an extremely heterogeneous disease and not one treatment will mitigate this illness in every patient. Personalized therapies will be advantageous to patients' well-being as treatments become more efficient as we unveil more features and characteristics of the tumor niche and its microenvironment. In the tumor microenvironment, the ECM and neighboring cells that surround the breast ducts and lobules are necessary for proper development in ductal morphogenesis, but are also a decisive factor in carcinoma evolution [12, 14]. The ECM has proven to be of clinical relevance due to the pertinent finding that collagen remodeling in carcinoma bearing patients leads to a poor patient outcome [11]. This discovery developed from the notion that cells *in vitro* align collagen fibers to facilitate motility cont. This was further confirmed *in vivo* using a transgenic murine model in which collagen fibers aligned along with the progression of the tumor [10].

Breast carcinoma cells that migrate in a mesenchymal fashion extend protrusions while using proteolysis via MMPs to aid in their motility. In this type of migration, cells focalize integrins at sites of ECM binding [148]. Friedl *et al* (1999) conducted invasion experiments in melanoma cancer cells with a β1 integrin function-blocking antibody, and this presented a significant reduction in invasion, cell elongation, and force generation in a 3D collagen lattice [149]. This study suggested that patients be isolated while the treatment was administered since β1 is found in epithelial cell lines and is a major player in wound healing. We described here FAK inhibition, downstream of β1 integrin, as a potential target for chemotherapy since it controls MRTF-A (Tenascin-C) and DDR2. To our knowledge, PF-562,271, a pharmacological

inhibitor of FAK activity, has been evaluated in one *in vivo* study for breast cancer, and it is suggested from *in vitro* data that FAK inhibition blocks EMT even in the presence of transforming growth factor-β (TGF-β) [150, 151]. Interestingly, they observed reduced tumor growth in FAK-inhibited cells, but not in FAK-depleted cells compared to the controls, partially attributing this to the absence of macrophage recruitment in FAK-depleted 4T1 xenografts. On the other hand, metastases were greatly reduced from FAK-depleted tumors, but no change was observed in PF-562,271-treated 4T1 tumor xenografts after 4 weeks [150, 151]. Although it does so initially, these data indicate that FAK inhibition may not completely inhibit breast carcinoma invasiveness and may require combinational therapy or that the model of 4T1 xenografts needs to be reevaluated.

Human patients tumor arrays and *in vivo* knock-down of DDR2 have pinpointed DDR2 as molecule necessary for metastatic behavior, including EMT [58-60]. Since introduction of shRNA plasmids are not currently therapeutically available, a search for a selective inhibitor has been of crucial relevance. Longmore *et al.*, have developed a drug, WRG-28, that interferes with the binding of DDR2 to collagen that reduces DDR2 activation (manuscript in preparation). Taken into account what we already know about DDR2, collagen alignment, and invasiveness, it prompts us to investigate *in vivo* whether WRG-28 can inhibit tumor growth and metastasis. For this, we are interested in experimenting with both mouse and human cell lines that we have our disposal. We plan to test this in collaboration with the Longmore lab in a xenograft model using 4T1 cells in the Balb/C mouse strain and experimental metastasis with MCF10-Ca1d cells in athymic mice. Furthermore, we have observed that 4T1 cells in WRG-28-treated conditions did not migrate as single cells suggesting the regulation of E-cadherin, which is a molecule widely

used to measure EMT, and we plan to stain and immunoblot for this cell-cell adhesion marker to detect cell's mesenchymal transformation [59, 152]. We expect a significant reduction in the metastatic ability of these aggressive cell lines, as intend to also explore the impact of PF-562,271 and WRG-28 in these two models. Moreover, PF-562,271 in experimental metastasis has not been characterized in human breast cancer cell lines, and we propose to test this, as well.

We determined that PF-562,271 promotes p53 expression and believe this pathway, downstream of FAK, regulates proliferation rates and possibly invasion. Wendt *et al.* (2009) tested PF-562,271 in 4T1 xenografts; however, these cells are p53-deficient, and we ascribe this to the mild reduction in pulmonary metastasis after FAK-inhibition [150]. Lastly, we will assess whether PF-562,271 and/or WRG-28 are able to inhibit metastasis on PyVT/wt and PyVT/ Col1a1^{tm1Jae} (collagen dense) without orthotopic injections of immortalized cell lines.

With relation to MRTF-A and DDR2 protein levels, we are extremely interested in the regulation of these two molecules by FAK activity *in vivo.* We have already added PF-562,271 to our animal protocol and we are ready to probe whether this regulation is maintained in the animal. MCF10-Ca1d cells do not spontaneously metastasize when implanted in the mammary fat pad. Realizing that a collagen-dense tumor microenvironment promotes tumor growth and invasion, we propose to test that Ca1d cells can be forced to metastasize when are xenografted into a collagen-dense stroma in athymic mice.

To prove that DDR2 expression is relevant to metastasis, we will use *in vitro* and *in vivo* approaches. First, we propose to use DDR1-depleted cells to test for proliferation rates and the ability to migrate in 3D invasion plug assays since these cells carry striking elevated levels of

DDR2. Also, we intend to analyze Snail, E-Cadherin and Vimentin as markers of EMT in DDR1-deficient MECs. Once we have established that cancer cells increased their invasive potential when DDR1 is knocked-down, we aim to test this in a xenograft model with 4T07 and 4T1 cells.

For 4T1 cells, DDR1 depletion can indicate more aggressiveness than mock-transfected 4T1 cells. Of relevance, 4T07 cells disseminate out of the tumor, but fail to metastasize for unclear reasons. They serve a dormancy cancer cell model. We determined that a stiff matrix induces DDR2 up-regulation increasing the likelihood of EMT, therefore we plan to inject stably transfected 4T07 with either a mock vector, DDR2 O/E or shRNA-DDR1. These variants will be injected into the mammary fat pad of Balb/C mice to assess that DDR2 expression forces these dormant cells into a metastatic phenotype. To verify this change, we propose to assess the status on proliferation and EMT markers, as well as measuring tumor growth and pulmonary metastasis.

To understand MRTF-A regulation by FAK, we plan to conduct experiments that will confirm that p53 is a transcriptional repressor of MRTF-A. First, qPCR will be carried out on MCF10A p53-depleted cells and probe for MRTF-A, SRF, and TnC. Second, chromatin immunoprecipitation (ChIP) will be used to pull-down p53 from the region of the MRTF-A promoter. Lastly, Ca1d cells will be tested in the same manner to reinforce what we already know from MRTF-A protein analysis.

Aside from looking at DDR2 and its role in metastasis, we aspire to confirm that ATF4 is the transcription factor upstream of DDR2 and downstream of FAK. ATF4 down-regulation at the protein level can be credited to miR-214 [144]. miR-214 and ATF4 levels will be measured

using qPCR approaches in the presence and absence of PF-562,271. Also, over-expression of miR-214 will be introduced to analyze ATF4 and DDR2 mRNA/protein expression. Ultimately, it is unknown whether DDR2 colocalizes with integrins at sites of focal adhesion. Either FAK or β1 integrin along with DDR2 immunofluorescence protocols will help us comprehend where DDR2 localizes in a cancer cell within a 3D collagen environment.

Appendix I: Dormant cancer cells response to Cox-2 inhibition

Cyclooxygenase enzyme-2 (COX-2) is the protein responsible for carrying out the enzymatic reaction that turns arachidonic acid (AA) to Prostaglandin H_2 (PGH_2) to Prostaglandin E_2 (PGE_2) [153]. PGE_2 is the most abundant prostaglandin in the human body and its synthesis is driven by (COX)-2 [154]. While COX-1 is constitutively active, COX-2 production is induced by numerous stimuli, including cytokines, growth factors, and inflammation cues. It is transcriptionally controlled by NF-κB [155]. Increased expression levels of both COX-2 and PGE_2 are associated with many cancers including breast that prompted the use of pharmacological inhibitors to block PGE_2 production [156]. Celecoxib is a non-steroidal anti-inflammatory drug (NSAID) that selectively inhibits COX-2 activity [157]. Therefore, selective COX-2 NSAIDs may provide with anti tumor effects by inhibiting PGE_2 production making celecoxib treatment therapeutically relevant [158].

For instance, in colon cancer, PGE_2 levels are increased in human adenomas and are characterized by the loss or mutation of adenomatous polyposis coli protein (APC) [159]. APC loss enhances β-catenin stability and the formation of a complex with transcription factors that drive gene transcription upon nuclear β-catenin localization [159]. This study directly linked PGE_2 levels to β-catenin transcriptional activity, although, it is unknown whether celecoxib, a PGE_2 inhibitor, diminishes β-catenin nuclear accumulation and transcriptional activity. Furthermore, β-catenin expression was also reduced in celecoxib-treated osteosarcoma MG-63 cells and thus, reducing β-catenin transcriptional targets such as c-myc and Cyclin-D1 [160].

Here, high levels of β-catenin and PGE_2 are considered to be pro-tumorigenic. However, it is not unknown whether their regulation restarts proliferation, especially in dormant breast cancer cells.

Correspondence from a collaborator informed us that DDR2 immunoprecipitates with Cox-2 in murine mammary gland epithelial cells but their function is unknown. We sought to understand whether the modulation of Cox-2 alters DDR2 expression in 4T07 and 4T1 murine mammary gland cancer cells. After treatment with celecoxib (Sigma) for 24h to inhibit Cox-2 enzymatic action, we observed by immunoblotting a notable up-regulation of DDR2 in 4T07 cells, only, while 4T1 cells were not susceptible to this regulation (Figure 1A-D). This finding was also observed in a microarray performed in hepatocellular carcinoma (HCC) cell lines that were treated with celecoxib followed by the elevation of DDR2 mRNA levels by three-fold [161]. Expression levels of DDR2 correlate with high-proliferation rates and we decided to measure this in 3D collagen matrices after celecoxib treatment for 24h. We found that this treatment strongly increased the proliferation rates of 4T07, but did not influence 4T1 cells (Figure 1E,F). After addition of PGE_2, confirmed by an ELISA array, we observed no changes to the levels of DDR2 in 4T07 or 4T1 cells. We determined that celecoxib dramatically reduced PGE_2 levels on both cell lines suggesting that the increasing levels of PGE_2 do not influence DDR2, but rather its reduction. This discovery illustrates a possible negative feedback mechanism or that celecoxib affects DDR2 via another effector aside from PGE_2 levels (Figure 3A,B). To understand the contribution of celecoxib, we decided to explore other downstream possible targets of celecoxib that may be impinging in the DDR2 up-regulation including VEGF-A, calcium channels and β-catenin [157].

β-catenin, along with p120-, α-, and ɣ-catenin, bind to the cytoplasmic tail domain of E-cadherin aiding to actin cytoskeletal binding. E-cadherin localizes to the plasma membrane and stabilizes epithelial adherens junctions and its loss is considered as a central step in EMT by facilitating downstream signaling for metastasis [152, 162]. In stark contrast, 4T07 cells do not express E-cadherin, while 4T1 express E-cadherin regardless of substrate stiffness (Figure 2A, B). In E-cadherin-deficient cells, β-catenin translocates to the cytoplasm or nucleus depending on the action of APC and glycogen synthase kinase 3β (GSK3β). When it translocates to the nucleus, it binds to lymphoid enhancer binding factor/T-cell factor (LEF/TCF) family of transcription factors to initiate transcription of target genes such as Twist and Snail [163]. To determine whether DDR2 is regulated by β-catenin, 4T07 and 4T1 cells were plated in 3D soft or stiff matrices in the presence or absence of iCRT-14, a pharmacological inhibitor that interrupts the transcriptional activity of β-catenin by disrupting its attachment to TCF4 [164]. Here, iCRT14 treatment in dormant 4T07 cells drastically increased DDR2 similar to the original observation after celecoxib addition (Figure 2C, E). On the other hand, 4T1 cells do not up-regulate DDR2 as observed after celecoxib treatment (Figure 2D, F). We also measured β-catenin protein by immunoblotting to confirm that iCRT14-induction of DDR2 was a transcriptional activity effect and not due to degradation/protein stability (Figure 2C,D). From these early results we conclude that in 4T07 the loss of E-cadherin releases β-catenin into the nucleus to repress directly or indirectly the expression of DDR2 in dormant cells. In 4T1 cells, the presence of E-cadherin does not enable β-catenin to translocate to the nucleus, at least in this *in vitro* setup, to regulate transcription. Moreover, in non-metastatic 4T07 cells, once nuclear activity of β-catenin is blocked, repression on DDR2 is released allowing for its transcription and

possibly adding another layer of regulation to dormancy during breast cancer progression. As a result, the dual function of β-catenin in coordinating cell-cell adhesion and gene transcription may be of interest in tumor cell dormancy.

Figure A1-1. DDR2 expression and proliferation are increased after celecoxib treatment on dormant cells

A,C) Dormant 4T07 and B,D) metastatic 4T1 were cultured on either soft or stiff 3D collagen matrices for 24h before cell lysis and immunoblot detection. Gels were treated ±celecoxib (25μM) overnight. Representative immunoblots are displayed and quantification was performed using mean band densitometry. Proliferation rates were measured using Cyquant NF after 24h of treatment on E) 4T07 and F) 4T1 and raw numbers were normalized to soft, untreated in three independent experiments as percent change. n=3, mean±SEM, *$p<0.05$

A)

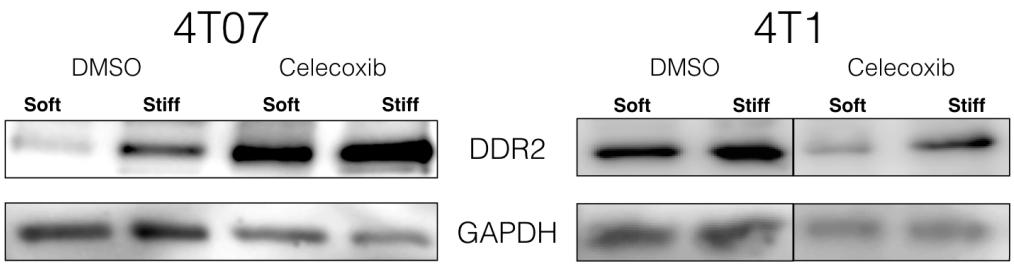
4T07
DMSO
Celecoxib
Soft
Stiff
Soft
Stiff
DDR2
GAPDH

B)

4T1
DMSO
Celecoxib
Soft
Stiff
Soft
Stiff

C)

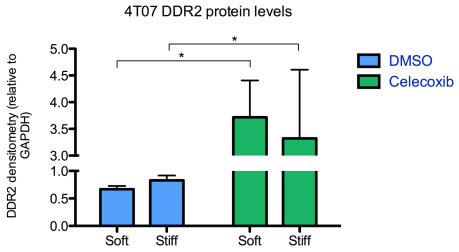
4T07 DDR2 protein levels
DDR2 densitometry (relative to GAPDH)
5.0
4.5
4.0
3.5
3.0
1.0
0.5
0.0
*
*
Soft
Stiff
Soft
Stiff
DMSO
Celecoxib

D)

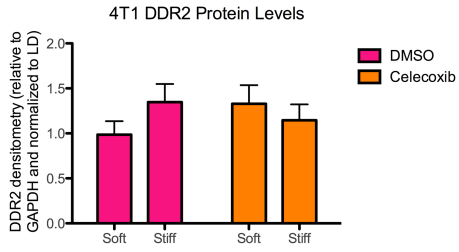
4T1 DDR2 Protein Levels
DDR2 densitometry (relative to GAPDH and normalized to LD)
2.0
1.5
1.0
0.5
0.0
Soft
Stiff
Soft
Stiff
DMSO
Celecoxib

E)

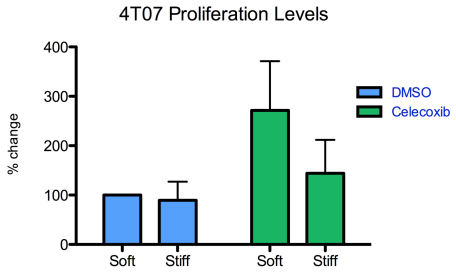
4T07 Proliferation Levels
% change
400
300
200
100
0
Soft
Stiff
Soft
Stiff
DMSO
Celecoxib

F)

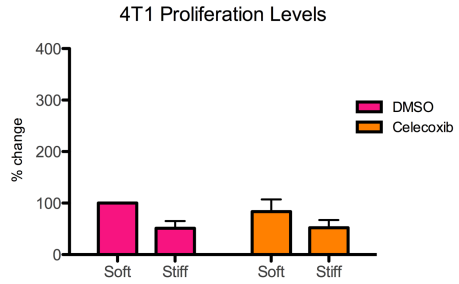
4T1 Proliferation Levels
% change
400
300
200
100
0
Soft
Stiff
Soft
Stiff
DMSO
Celecoxib

Figure A1-2. DDR2 expression is controlled by β-catenin activity on dormant cells

A,B) 4T07 and 4T1 expression of E-cadherin on soft or stiff conditions. C, E) Dormant 4T07 and D, F) metastatic 4T1 were cultured on either soft or stiff 3D collagen matrices for 24h before cell lysis and immunoblot detection after treatment with ±iCRT-14 (25μM). Representative immunoblots are displayed and quantification was performed using mean band densitometry. n=3, mean±SEM, *$p<0.05$.

A)

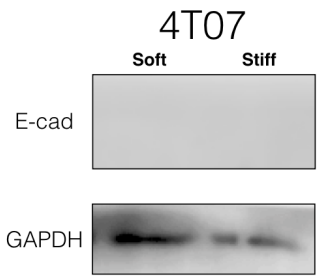
4T07
Soft
Stiff
E-cad
GAPDH

B)

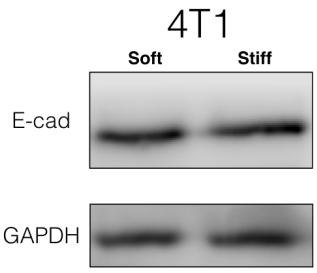
4T1
Soft
Stiff
E-cad
GAPDH

C)

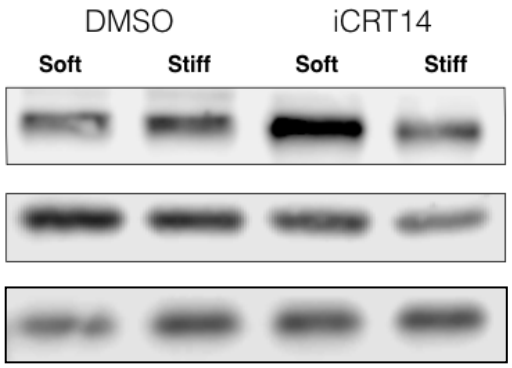
DMSO
iCRT14
Soft
Stiff
Soft
Stiff
DDR2
GAPDH
β-cat

D)

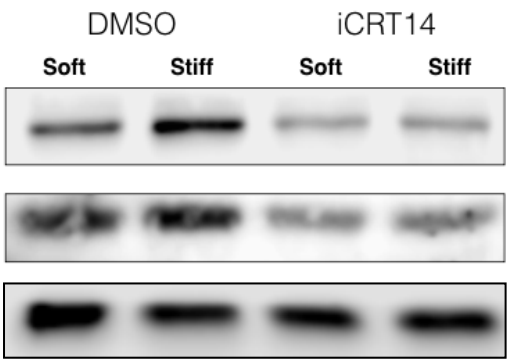
DMSO
iCRT14
Soft
Stiff
Soft
Stiff

E)

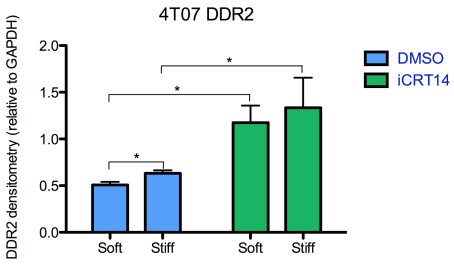
4T07 DDR2
DDR2 densitometry (relative to GAPDH)
2.0
1.5
1.0
0.5
0.0
Soft
Stiff
Soft
Stiff
DMSO
iCRT14

F)

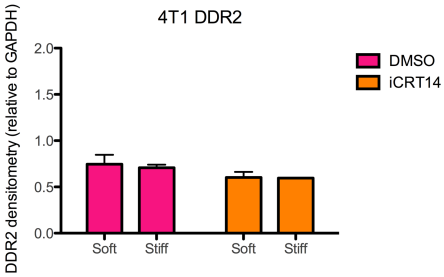
4T1 DDR2
DDR2 densitometry (relative to GAPDH)
2.0
1.5
1.0
0.5
0.0
Soft
Stiff
Soft
Stiff
DMSO
iCRT14

Figure A1-3. PGE_2 levels are reduced by celecoxib

A,B) Soft or stiff collagen gels of 4T07 and 4T1 cells were treated with either DMSO, celecoxib (25μM) or PGE_2 (10μM) and total PGE_2 levels were measured in an ELISA array. Raw numbers are shown after averaging duplicate wells from three independent experiments. n=3, mean ±SEM, *$p<0.05$, **$p<0.01$.

A)

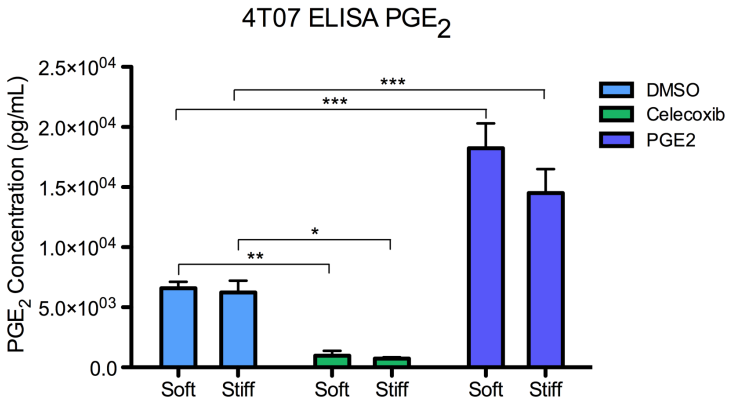
4T07 ELISA PGE2
PGE2 Concentration (pg/mL)
2.5×10^04
2.0×10^04
1.5×10^04
1.0×10^04
5.0×10^03
0.0
***
***
*
**
Soft
Stiff
Soft
Stiff
Soft
Stiff
DMSO
Celecoxib
PGE2

B)

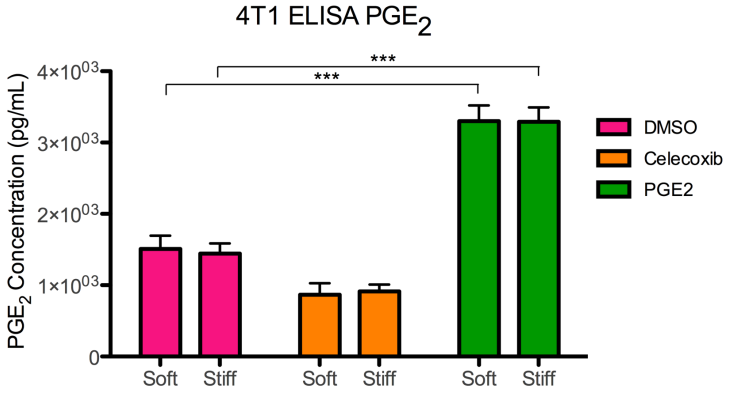
4T1 ELISA PGE2
PGE2 Concentration (pg/mL)
4×10^03
3×10^03
2×10^03
1×10^03
0
***
***
Soft
Stiff
Soft
Stiff
Soft
Stiff
DMSO
Celecoxib
PGE2

Appendix II: High-throughput siRNA screen

Breast cancer cell invasion *in vivo* occurs in a very complex environment. We have chosen to recreate that environment by using type I collagen gels as the *in vitro* model for a 3D migration assay [118]. Type I collagen is particularly relevant as it has been linked to breast density, which in turn has been associated with a higher risk of developing breast cancer [83]. To attain a better understanding at the gene level as to how cells invade in 3D collagen environments, we classified genes that may relevant by mining studies that profiled microarrays with breast cancer invasive signatures. First, we examined genes that were over-expressed in a tumor metastatic sub-population in a murine model [165]. We aligned these genes to another subset that were categorized as being down-regulated upon FAK-specific knock-out in the mammary gland of mice [88]. Animals with FAK -/- tumors showed growth, but a markedly reduced number of metastases were counted. Thus, we hypothesized these genes to be critical for invasion. From these studies, we categorized 68 target genes that were FAK regulated and highly-expressed in invasive tumors. In order to test this hypothesis, we initially tested a variety of invasion assays that were compared side by side. We tested length of assay, serum-conditions, cell-seeding numbers, cell line, ease of assay, and end result monitoring. After contrasting various commercial assays, we determined that iuvo plates from BellBrook Labs worked the best to monitor what genes perturb cell migration in 3D. This assay offers the ability to employ a novel 3D high-throughput migration assay using microchannels plates filled with type I collagen. To deplete gene expression we used an siRNA Block-IT (Dharmacon) supplied by an RNAi library through the UWCCC Small Molecule Screening Facility (UW-Madison). For our protocol we

plated $5x10^3$ MDA-MB-231 cells into each well of a 96-well plate on Day 0. On Day 1, we used using Lipofectamine RNAiMax (Life Technologies) and the RNAi library to transfect these oligos into MDA-MB-231cells. We included extra wells for positive, negative, blebbistatin, and transfection efficiency controls. After 24h of incubation, we transferred the cancer cells by adding each well with 15µL of 0.05% trypsin using a high-throughput liquid handler, CyBi (CyBio) (Figure 1A). CyBi transferred the cells to a V-bottom plate for centrifugation to remove trypsin after adding 15µL of regular growth media. Media was removed by CyBi, and cells were resuspended with 32µL of media with serum. CyBi aspirated 15µL and dispensed 6µL into duplicate ports of the invasion plate assay (Figure 1B). We allowed MDA-MB-231 cells to migrate into the 3D matrix for 5 days. The media was changed every day to avoid possible high-concentration of nutrients that could lead to cell death. Each plate was monitored daily and images of each port were taken using an inverted epifluorescence microscope. At the end of the assay cells were stained with a live-cell marker to discern cell death from non-migratory. Here, control, FAK, and blebbistatin treatment are shown (Figure 1C). The targets with the lowest proportion non-migratory cells are as follows: SAP18, KIF23, LIMK2, TWIST2, KIF18A, PAK1, and KIF11 (Figure 1C).

The end goal of this assay is to further understand the genes involved in breast cancer metastasis and the signaling pathways cancer cells employ to interact with the extracellular matrix. This high-throughput invasion assay allowed us to identify what genes, by knock-down, are vital for invasion using a well-documented carcinoma, highly invasive human cell line, MDA-MB-231.

Figure A2-1. High-throughput siRNA screen in a 3D matrix

A) CyBi robot shown dispensing resuspended 6μL of mixture of cells and media into B) input ports. In diagram, cells migrate out into the matrix and C) images were taken from the dashed square area at Day 5 with Calcein AM to detect live cells only.

A)

B)

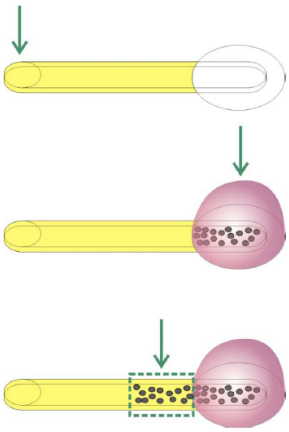

C)

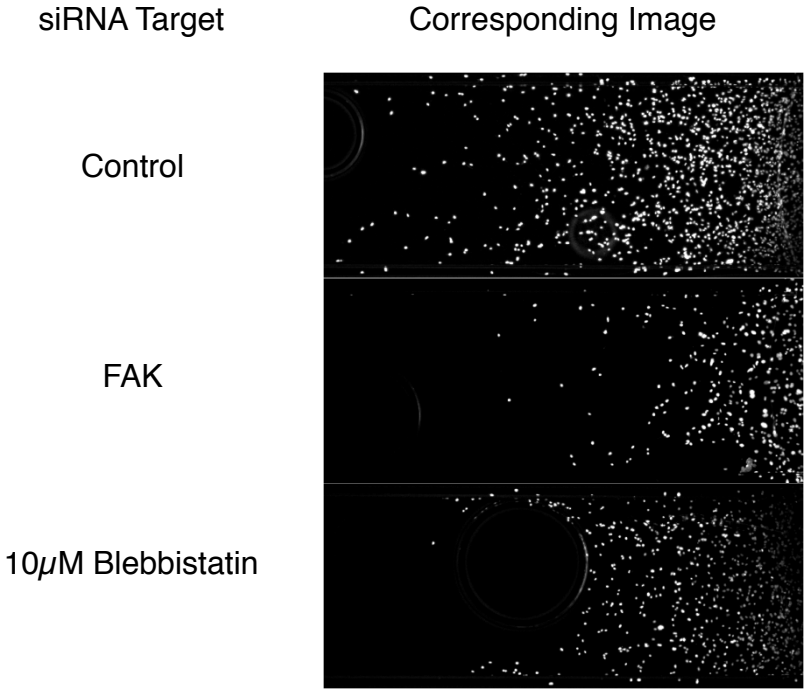

Appendix III: Collagen density regulates xenobiotic and hypoxic response of mammary epithelial cells.

This chapter is published as:

Colleen S. Curran; Esteban R. Carrillo; Suzanne M. Ponik; Patricia J. Keely. Environmental toxicology and pharmacology. 2015 , DOI: 10.1016/j.etap.2014.10.017, PMID: 25481308

ABSTRACT

Breast density, where collagen I is the dominant component, is a significant breast cancer risk factor. Cell surface integrins interact with collagen, activate focal adhesion kinase (FAK), and downstream cell signals associated with xenobiotics (AhR, ARNT) and hypoxia (HIF-1α, ARNT). We examined if mammary cells cultured in high density (HD) or low density (LD) collagen gels affected xenobiotic or hypoxic responses. ARNT production was significantly reduced by HD culture and in response to a FAK inhibitor. Consistent with a decrease in ARNT, AhR and HIF-1α reporter activation and VEGF production was lower in HD compared to LD. However, P450 production was enhanced in HD and induced by AhR and HIF-1α agonists, possibly in response to increased NF-κB activation. Thus, collagen density differentially regulates downstream cell signals of AhR and HIF-1α by modulating the activity of FAK, the release of NF-κB transcriptional factors, and the levels of ARNT.

BIBLIOGRAPHY

1. *What is Cancer?* Cancer.org 04/15/2015; Available from: http://www.cancer.org/cancer/cancerbasics/what-is-cancer.
2. NIH and Cancer.gov. *Breast Cancer*. 2013; Available from: http://report.nih.gov/nihfactsheets/ViewFactSheet.aspx?csid=73.
3. Lehmann, B.D., et al., Identification of human triple-negative breast cancer subtypes and preclinical models for selection of targeted therapies. J Clin Invest, 2011. **121**(7): p. 2750-67.
4. Boyd, N.F., et al., *Mammographic densities and breast cancer risk.* Cancer epidemiology, biomarkers & prevention : a publication of the American Association for Cancer Research, cosponsored by the American Society of Preventive Oncology, 1998. **7**(12): p. 1133-1144.
5. McCormack, V.A. and I. dos Santos Silva, Breast density and parenchymal patterns as markers of breast cancer risk: a meta-analysis. Cancer Epidemiol Biomarkers Prev, 2006. **15**(6): p. 1159-69.
6. Boyd, N.F., et al., Mammographic densities and breast cancer risk. Breast disease, 1998. **10**(3-4): p. 113-126.
7. Guo, Y.P., et al., *Growth factors and stromal matrix proteins associated with mammographic densities.* Cancer epidemiology, biomarkers & prevention : a publication of the American Association for Cancer Research, cosponsored by the American Society of Preventive Oncology, 2001. **10**(3): p. 243-248.
8. Alowami, S., et al., Mammographic density is related to stroma and stromal proteoglycan expression. Breast cancer research : BCR, 2003. **5**(5): p. 35.
9. Provenzano, P.P., et al., Collagen density promotes mammary tumor initiation and progression. BMC Medicine, 2008. **6**(1): p. 11.
10. Provenzano, P.P., et al., Collagen reorganization at the tumor-stromal interface facilitates local invasion. BMC Medicine, 2006. **4**(1): p. 38.
11. Conklin, M.W., et al., Aligned collagen is a prognostic signature for survival in human breast carcinoma. The American journal of pathology, 2011. **178**(3): p. 1221-1232.
12. Schedin, P. and P.J. Keely, Mammary Gland ECM Remodeling, Stiffness, and Mechanosignaling in Normal Development and Tumor Progression. Cold Spring Harbor Perspectives in Biology, 2011. **3**(1).
13. Liu, X., et al., A targeted mutation at the known collagenase cleavage site in mouse type I collagen impairs tissue remodeling. The Journal of cell biology, 1995. **130**(1): p. 227-237.
14. Wiseman, B.S. and Z. Werb, Stromal effects on mammary gland development and breast cancer. Science, 2002. **296**(5570): p. 1046-9.
15. Paszek, M.J. and V.M. Weaver, The Tension Mounts: Mechanics Meets Morphogenesis and Malignancy. Journal of Mammary Gland Biology and Neoplasia, 2004. **9**(4): p. 325-342.
16. Keely, P.J., Mechanisms by Which the Extracellular Matrix and Integrin Signaling Act to Regulate the Switch Between Tumor Suppression and Tumor Promotion. Journal of Mammary Gland Biology and Neoplasia, 2011. **16**(3): p. 205-219.
17. Wozniak, M.A. and P.J. Keely, Use of three-dimensional collagen gels to study mechanotransduction in T47D breast epithelial cells. Biological procedures online, 2005. **7**: p. 144-61.

18. Keely, P.J., et al., Alteration of collagen-dependent adhesion, motility, and morphogenesis by the expression of antisense alpha 2 integrin mRNA in mammary cells. J Cell Sci, 1995. **108 (Pt 2)**: p. 595-607.
19. Wozniak, M.A., et al., ROCK-generated contractility regulates breast epithelial cell differentiation in response to the physical properties of a three-dimensional collagen matrix. The Journal of Cell Biology, 2003. **163**(3): p. 583-595.
20. Provenzano, P.P., et al., Matrix density-induced mechanoregulation of breast cell phenotype, signaling and gene expression through a FAK-ERK linkage. Oncogene, 2009. **28**(49): p. 4326-43.
21. Ponik, S.M., et al., RhoA is down-regulated at cell-cell contacts via p190RhoGAP-B in response to tensional homeostasis. Molecular biology of the cell, 2013. **24**(11): p. 1688.
22. Santner, S.J., et al., Malignant MCF10CA1 Cell Lines Derived from Premalignant Human Breast Epithelial MCF10AT Cells. Breast Cancer Research and Treatment, 2001. **65**(2): p. 101110.
23. Aguirre-Ghiso, J.A., Models, mechanisms and clinical evidence for cancer dormancy. Nature Reviews Cancer, 2007. **7**(11): p. 834-846.
24. Karrison, T.G., D.J. Ferguson, and P. Meier, *Dormancy of mammary carcinoma after mastectomy.* Journal of the National Cancer Institute, 1999. **91**(1): p. 80-85.
25. Heppner, G.H., F.R. Miller, and P.M. Shekhar, *Nontransgenic models of breast cancer.* Breast cancer research : BCR, 2000. **2**(5): p. 331-334.
26. Aguirre Ghiso, J.A., K. Kovalski, and L. Ossowski, Tumor dormancy induced by downregulation of urokinase receptor in human carcinoma involves integrin and MAPK signaling. The Journal of cell biology, 1999. **147**(1): p. 89-104.
27. Schwartz, M.A., Integrins and extracellular matrix in mechanotransduction. Cold Spring Harbor perspectives in biology, 2010. **2**(12).
28. Hynes, R.O., Integrins: bidirectional, allosteric signaling machines. Cell, 2002. **110**(6): p. 673-687.
29. Choquet, D., D.P. Felsenfeld, and M.P. Sheetz, Extracellular matrix rigidity causes strengthening of integrin-cytoskeleton linkages. Cell, 1997. **88**(1): p. 39-48.
30. Katz, B.Z., et al., Physical state of the extracellular matrix regulates the structure and molecular composition of cell-matrix adhesions. Mol Biol Cell, 2000. **11**(3): p. 1047-60.
31. Galbraith, C.G., K.M. Yamada, and M.P. Sheetz, The relationship between force and focal complex development. J Cell Biol, 2002. **159**(4): p. 695-705.
32. Burridge, K. and M. Chrzanowska-Wodnicka, *FOCAL ADHESIONS, CONTRACTILITY, AND SIGNALING.* Annual Review of Cell and Developmental Biology, 1996. **12**(1): p. 463519.
33. Parsons, J.T., Focal adhesion kinase: the first ten years. Journal of Cell Science, 2003. **116**(8): p. 1409-1416.
34. Provenzano, P.P., et al., Matrix density-induced mechanoregulation of breast cell phenotype, signaling and gene expression through a FAK–ERK linkage. Oncogene, 2009. **28**(49): p. 4326-4343.
35. Yoav, D.S. and S. Rony, *The MEK/ERK cascade: From signaling specificity to diverse functions.* Biochimica et Biophysica Acta (BBA) - Molecular Cell Research, 2007. **1773**(8).

36. Howe, A.K. and R.L. Juliano, Distinct mechanisms mediate the initial and sustained phases of integrin-mediated activation of the Raf/MEK/mitogen-activated protein kinase cascade. The Journal of biological chemistry, 1998. **273**(42): p. 27268-27274.
37. Schlaepfer, D.D., K.C. Jones, and T. Hunter, Multiple Grb2-mediated integrin-stimulated signaling pathways to ERK2/mitogen-activated protein kinase: summation of both c-Src- and focal adhesion kinase-initiated tyrosine phosphorylation events. Molecular and cellular biology, 1998. **18**(5): p. 2571-2585.
38. Paszek, M., J., et al., Tensional homeostasis and the malignant phenotype. Cancer Cell, 2005. **8**(3).
39. Sieg, D.J., et al., FAK integrates growth-factor and integrin signals to promote cell migration. Nature Cell Biology, 2000. **2**(5): p. 249-256.
40. Abdulhussein, R., D.H.H. Koo, and W.F. Vogel, Identification of disulfide-linked dimers of the receptor tyrosine kinase DDR1. The Journal of biological chemistry, 2008. **283**(18): p. 12026-12033.
41. Leitinger, B., Molecular Analysis of Collagen Binding by the Human Discoidin Domain Receptors, DDR1 and DDR2 IDENTIFICATION OF COLLAGEN BINDING SITES IN DDR2. Journal of Biological Chemistry, 2003. **278**(19).
42. Vogel, W., et al., The Discoidin Domain Receptor Tyrosine Kinases Are Activated by Collagen. Molecular Cell, 1997. **1**(1).
43. Alves, F., et al., Distinct structural characteristics of discoidin I subfamily receptor tyrosine kinases and complementary expression in human cancer. Oncogene, 1995. **10**(3): p. 609-18.
44. Fu, H.-L.L., et al., Discoidin domain receptors: unique receptor tyrosine kinases in collagen-mediated signaling. The Journal of biological chemistry, 2013. **288**(11): p. 7430-7437.
45. Valiathan, R.R., et al., Discoidin domain receptor tyrosine kinases: new players in cancer progression. Cancer and Metastasis Reviews, 2012. **31**(1-2): p. 295-321.
46. Leitinger, B., *Transmembrane collagen receptors.* Cell and Developmental Biology, 2011. **27**(1): p. 265-290.
47. Olaso, E., et al., DDR2 receptor promotes MMP-2-mediated proliferation and invasion by hepatic stellate cells. The Journal of clinical investigation, 2001. **108**(9): p. 1369-1378.
48. Poudel, B., Y.-M.M. Lee, and D.-K.K. Kim, DDR2 inhibition reduces migration and invasion of murine metastatic melanoma cells by suppressing MMP2/9 expression through ERK/ NF-κB pathway. Acta biochimica et biophysica Sinica, 2015. **47**(4): p. 292-298.
49. Yasushi, S., et al., Collagen I–mediated up-regulation of N-cadherin requires cooperative signals from integrins and discoidin domain receptor 1. The Journal of Cell Biology, 2008. **180**(6).
50. Eswaramoorthy, R., et al., DDR1 regulates the stabilization of cell surface E-cadherin and E-cadherin-mediated cell aggregation. Journal of cellular physiology, 2010. **224**(2): p. 387-397.
51. Hsueh-Liang, F., et al., Shedding of Discoidin Domain Receptor 1 by Membrane-type Matrix Metalloproteinases. Journal of Biological Chemistry, 2013. **288**(17): p. 12114-12129.
52. Kuan−Liang, L., et al., Transcriptional upregulation of DDR2 by ATF4 facilitates osteoblastic differentiation through p38 MAPK−mediated Runx2 activation. Journal of Bone and Mineral Research, 2010. **25**(11): p. 2489-2503.

53. Vogel, W., et al., Discoidin domain receptor 1 is activated independently of beta(1) integrin. The Journal of biological chemistry, 2000. **275**(8): p. 5779-5784.
54. Xu, H., et al., Discoidin domain receptors promote α1β1- and α2β1-integrin mediated cell adhesion to collagen by enhancing integrin activation. PloS one, 2012. **7**(12).
55. Chen, S.-C.C., et al., Hypoxia induces discoidin domain receptor-2 expression via the p38 pathway in vascular smooth muscle cells to increase their migration. Biochemical and biophysical research communications, 2008. **374**(4): p. 662-667.
56. Sekiya, Y., et al., Suppression of hepatic stellate cell activation by microRNA-29b. Biochemical and biophysical research communications, 2011. **412**(1): p. 74-79.
57. Hammerman, P.S., et al., Mutations in the DDR2 Kinase Gene Identify a Novel Therapeutic Target in Squamous Cell Lung Cancer. Cancer Discovery, 2011. **1**(1): p. 78-89.
58. Ren, T., et al., Increased expression of discoidin domain receptor 2 (DDR2): a novel independent prognostic marker of worse outcome in breast cancer patients. Medical Oncology, 2013.
59. Ren, T., et al., Discoidin domain receptor 2 (DDR2) promotes breast cancer cell metastasis and the mechanism implicates epithelial-mesenchymal transition programme under hypoxia. The Journal of pathology, 2014. **234**(4): p. 526-537.
60. Zhang, K., et al., The collagen receptor discoidin domain receptor 2 stabilizes SNAIL1 to facilitate breast cancer metastasis. Nature cell biology, 2013. **15**(6): p. 677-687.
61. Burridge, K.W., K., Rho and Rac Take Center Stage. Cell, 2004. **116**: p. 13.
62. Amano, M.I., M.; Kimura, K.; Fukata, Y.; Chihara, K.; Nakano, T.; Matsuura, Y.; Kaibuchi, K.;, *Phosphorylation and activation of myosin by Rho-associated kinase (Rho-kinase)*. The Journal of Biological Chemistry, 1996. **271**(34): p. 4.
63. Kimura, K.I., M.; Amano, M.; Chihara, K.; Fukata, Y.; Nakafuku, M.; Yamamori, B.; Feng, J.; Nakano, T.; Okawa, K.; Iwamatsu, A.; Kaibuchi, K.;, *Regulation of myosin phosphatase by Rho and Rho-associated kinase (Rho-kinase)*. Science, 1996. **273**(5272): p. 4.
64. Paszek, M.J., et al., Tensional homeostasis and the malignant phenotype. Cancer cell, 2005. **8**(3): p. 241-54.
65. Ridley, A.J.H., A., The Small GTP-Binding Protein rho Regulates the Assembly of Focal Adhesions and Actin Stress Fibers in Response to Growth Factors. Cell, 1992. **70**: p. 11.
66. Athanassia, S., et al., Signal-Regulated Activation of Serum Response Factor Is Mediated by Changes in Actin Dynamics. Cell, 1999. **98**(2).
67. Hill, C.S.W., J.; Treisman, R., The Rho family GTPases RhoA, Rac1, and CDC42Hs regulate transcriptional activation by SRF. Cell, 1995. **81**(7): p. 1159-70.
68. Wang, D., et al., Activation of cardiac gene expression by myocardin, a transcriptional cofactor for serum response factor. Cell, 2001. **105**(7): p. 851-62.
69. Cen, B., A. Selvaraj, and R. Prywes, Myocardin/MKL family of SRF coactivators: key regulators of immediate early and muscle specific gene expression. Journal of cellular biochemistry, 2004. **93**(1): p. 74-82.
70. Miralles, F., et al., Actin dynamics control SRF activity by regulation of its coactivator MAL. Cell, 2003. **113**(3): p. 329-42.

71. Johansen, F.E. and R. Prywes, Identification of transcriptional activation and inhibitory domains in serum response factor (SRF) by using GAL4-SRF constructs. Mol Cell Biol, 1993. **13**(8): p. 4640-7.
72. Wang, D.-Z., et al., Potentiation of serum response factor activity by a family of myocardin-related transcription factors. Proc Natl Acad Sci USA, 2002. **99**(23): p. 14855-60.
73. Treisman, R., Ternary complex factors: growth factor regulated transcriptional activators. Curr Opin Genet Dev, 1994. **4**(1): p. 96-101.
74. Wang, Z., et al., Myocardin and ternary complex factors compete for SRF to control smooth muscle gene expression. Nature, 2004. **428**(6979): p. 185-9.
75. Johansen, F.E.P., R., Serum response factor: transcriptional regulation of genes induced by growth factors and differentiation. Biochimica et biophysica acta, 1995. **1242**(1): p. 10.
76. Susanne, M., et al., Serum-Induced Phosphorylation of the Serum Response Factor Coactivator MKL1 by the Extracellular Signal-Regulated Kinase 1/2 Pathway Inhibits Its Nuclear Localization. Molecular and Cellular Biology, 2008. **28**(20): p. 6302-6313.
77. Cen, B., et al., Megakaryoblastic Leukemia 1, a Potent Transcriptional Coactivator for Serum Response Factor (SRF), Is Required for Serum Induction of SRF Target Genes. Molecular and cellular biology, 2003. **23**(18): p. 6597-6608.
78. Du, K.L., et al., Myocardin Is a Critical Serum Response Factor Cofactor in the Transcriptional Program Regulating Smooth Muscle Cell Differentiation. Molecular and cellular biology, 2003. **23**(7): p. 2425-2437.
79. Li, S., et al., Requirement of a myocardin-related transcription factor for development of mammary myoepithelial cells. Molecular and cellular biology, 2006. **26**(15): p. 5797-808.
80. Chan, M.W.C., et al., Force-induced myofibroblast differentiation through collagen receptors is dependent on mammalian diaphanous (mDia). J Biol Chem, 2010. **285**(12): p. 9273-81.
81. Gomez, E.W., et al., Tissue geometry patterns epithelial-mesenchymal transition via intercellular mechanotransduction. Journal of cellular biochemistry, 2010. **110**(1): p. 44-51.
82. Lutz, R., T. Sakai, and M. Chiquet, Pericellular fibronectin is required for RhoA-dependent responses to cyclic strain in fibroblasts. Journal of Cell Science, 2010. **123**(Pt 9): p. 1511-21.
83. Boyd, N.F., et al., Mammographic density as a marker of susceptibility to breast cancer: a hypothesis. IARC Sci Publ, 2001. **154**: p. 163-9.
84. Wyckoff, J.B., et al., ROCK- and myosin-dependent matrix deformation enables protease-independent tumor-cell invasion in vivo. Curr Biol, 2006. **16**(15): p. 1515-23.
85. Rajeshwari, R.V., et al., Discoidin domain receptor tyrosine kinases: new players in cancer progression. Cancer and Metastasis Reviews, 2012. **31**(1-2): p. 295-321.
86. Lark, A.L., et al., High focal adhesion kinase expression in invasive breast carcinomas is associated with an aggressive phenotype. Modern pathology : an official journal of the United States and Canadian Academy of Pathology, Inc, 2005. **18**(10): p. 1289-1294.
87. Cerami, E., et al., The cBio cancer genomics portal: an open platform for exploring multidimensional cancer genomics data. Cancer Discov, 2012. **2**(5): p. 401-4.

88. Provenzano, P.P., et al., Mammary epithelial-specific disruption of focal adhesion kinase retards tumor formation and metastasis in a transgenic mouse model of human breast cancer. The American journal of pathology, 2008. **173**(5): p. 1551-1565.
89. Giaccia, A.J. and M.B. Kastan, The complexity of p53 modulation: emerging patterns from divergent signals. Genes & development, 1998. **12**(19): p. 2973-2983.
90. Vita, M.G., et al., p53 regulates FAK expression in human tumor cells. Molecular Carcinogenesis, 2008. **47**(5): p. 373-382.
91. Golubovskaya, V.M. and W. Cance, Focal adhesion kinase and p53 signal transduction pathways in cancer. … in bioscience: a journal and virtual …, 2010.
92. Lim, S.-T.T., et al., Nuclear FAK promotes cell proliferation and survival through FERM-enhanced p53 degradation. Molecular cell, 2008. **29**(1): p. 9-22.
93. Souhila, M., et al., Myocardin-related transcription factors and SRF are required for cytoskeletal dynamics and experimental metastasis. Nature Cell Biology, 2009. **11**(3): p. 257-268.
94. Xing-Hua, L., et al., MRTF-A and STAT3 synergistically promote breast cancer cell migration. Cellular Signalling, 2014. **26**(11): p. 23702380.
95. Zhang, C., et al., Myocardin-related transcription factor A is up-regulated by 17β-estradiol and promotes migration of MCF-7 breast cancer cells via transactivation of MYL9 and CYR61. Acta biochimica et biophysica Sinica, 2013. **45**(11): p. 921-927.
96. Richard, T., Identification of a protein-binding site that mediates transcriptional response of the c-fos gene to serum factors. Cell, 1986. **46**(4): p. 567574.
97. Da-Zhi, W., et al., Potentiation of serum response factor activity by a family of myocardin-related transcription factors. Proceedings of the National Academy of Sciences, 2002. **99**(23): p. 14855-14860.
98. Ahalya, S. and P. Ron, Expression profiling of serum inducible genes identifies a subset of SRF target genes that are MKL dependent. BMC Molecular Biology, 2004. **5**(1): p. 13.
99. Bo, C., S. Ahalya, and P. Ron, Myocardin/MKL family of SRF coactivators: Key regulators of immediate early and muscle specific gene expression. Journal of Cellular Biochemistry, 2004. **93**(1): p. 74-82.
100. Vartiainen, M.K., et al., Nuclear Actin Regulates Dynamic Subcellular Localization and Activity of the SRF Cofactor MAL. Science, 2007. **316**(5832): p. 1749-1752.
101. Johansen, F.E. and R. Prywes, Identification of transcriptional activation and inhibitory domains in serum response factor (SRF) by using GAL4-SRF constructs. Molecular and cellular biology, 1993. **13**(8): p. 4640-4647.
102. Caroline, S.H., W. Judy, and T. Richard, The Rho family GTPases RhoA, Racl , and CDC42Hsregulate transcriptional activation by SRF. Cell, 1995. **81**(7).
103. Rafał, P., et al., An actin−regulated importin α/β−dependent extended bipartite NLS directs nuclear import of MRTF−A. The EMBO Journal, 2010. **29**(20): p. 3448-3458.
104. Janknecht, R., W.H. Ernst, and V. Pingoud, *Activation of ternary complex factor Elk-1 by MAP kinases*. Activation of ternary complex factor Elk-1 by MAP kinases., 1993.
105. Whitmarsh, A.J., et al., Integration of MAP kinase signal transduction pathways at the serum response element. Science, 1995.

106. Treisman, R., Identification of a protein-binding site that mediates transcriptional response of the c-fos gene to serum factors. Cell, 1986. **46**(4): p. 567-74.
107. Selvaraj, A. and R. Prywes, Expression profiling of serum inducible genes identifies a subset of SRF target genes that are MKL dependent. BMC molecular biology, 2004. **5**: p. 13.
108. Muehlich, S., et al., Serum-Induced Phosphorylation of the Serum Response Factor Coactivator MKL1 by the Extracellular Signal-Regulated Kinase 1/2 Pathway Inhibits Its Nuclear Localization. Molecular and Cellular Biology, 2008. **28**(20): p. 6302-6313.
109. Dean, P.S., et al., Nuclear RhoA signaling regulates MRTF-dependent SMC-specific transcription. American Journal of Physiology - Heart and Circulatory Physiology, 2014. **307**(3).
110. Olson, E.N. and A. Nordheim, Linking actin dynamics and gene transcription to drive cellular motile functions. Nature Reviews Molecular Cell Biology, 2010. **11**(5): p. 353-365.
111. Bo, C., et al., Megakaryoblastic Leukemia 1, a Potent Transcriptional Coactivator for Serum Response Factor (SRF), Is Required for Serum Induction of SRF Target Genes. Molecular and Cellular Biology, 2003. **23**(18): p. 6597-6608.
112. Asparuhova, M.B., L. Gelman, and M. Chiquet, Role of the actin cytoskeleton in tuning cellular responses to external mechanical stress. Scandinavian Journal of Medicine & Science in Sports, 2009. **19**(4): p. 490-499.
113. Thordur, O., et al., Breast cancer cells produce tenascin C as a metastatic niche component to colonize the lungs. Nature Medicine, 2011. **17**(7): p. 867-874.
114. Matys, V., et al., TRANSFAC and its module TRANSCompel: transcriptional gene regulation in eukaryotes. Nucleic acids research, 2006. **34**(Database issue): p. 10.
115. Golubovskaya, V., A. Kaur, and W. Cance, Cloning and characterization of the promoter region of human focal adhesion kinase gene: nuclear factor kappa B and p53 binding sites. Biochimica et biophysica acta, 2004. **1678**(2-3): p. 111-125.
116. Ahalya, S. and P. Ron, Megakaryoblastic Leukemia-1/2, a Transcriptional Co-activator of Serum Response Factor, Is Required for Skeletal Myogenic Differentiation. Journal of Biological Chemistry, 2003. **278**(43): p. 41977-41987.
117. Jayanta, D., K.M. Senthil, and S.B. Joan, Morphogenesis and oncogenesis of MCF-10A mammary epithelial acini grown in three-dimensional basement membrane cultures. Methods, 2003. **30**(3).
118. Wozniak, M.A. and P.J. Keely, Use of three-dimensional collagen gels to study mechanotransduction in T47D breast epithelial cells. Biological Procedures Online, 2005. **7**.
119. Curran, C.S., et al., Collagen density regulates xenobiotic and hypoxic response of mammary epithelial cells. Environmental toxicology and pharmacology, 2015. **39**(1): p. 114-124.
120. Levental, K.R., et al., Matrix crosslinking forces tumor progression by enhancing integrin signaling. Cell, 2009. **139**(5): p. 891-906.
121. Riching, K.M., et al., 3D collagen alignment limits protrusions to enhance breast cancer cell persistence. Biophysical journal, 2014. **107**(11): p. 2546-2558.
122. Provenzano, P.P., et al., Contact guidance mediated three-dimensional cell migration is regulated by Rho/ROCK-dependent matrix reorganization. Biophysical journal, 2008. **95**(11): p. 5374-5384.
123. Michele, A.W., et al., *Focal adhesion regulation of cell behavior.* Biochimica et Biophysica Acta (BBA) - Molecular Cell Research, 2004. **1692**.

124. Provenzano, P.P. and P.J. Keely, The role of focal adhesion kinase in tumor initiation and progression. Cell adhesion & migration, 2009. **3**(4): p. 347-350.
125. Wolfgang, V., et al., The Discoidin Domain Receptor Tyrosine Kinases Are Activated by Collagen. Molecular Cell, 1997. **1**(1).
126. Leitinger, B., Discoidin domain receptor functions in physiological and pathological conditions. International review of cell and molecular biology, 2014. **310**: p. 39-87.
127. Vogel, W., *Discoidin domain receptors: structural relations and functional implications.* FASEB journal : official publication of the Federation of American Societies for Experimental Biology, 1999. **13 Suppl**: p. 82.
128. Herrera-Herrera, M.L. and R. Quezada-Calvillo, DDR2 plays a role in fibroblast migration independent of adhesion ligand and collagen activated DDR2 tyrosine kinase. Biochemical and biophysical research communications, 2012. **429**(1-2): p. 39-44.
129. Zhang, S., et al., A host deficiency of discoidin domain receptor 2 (DDR2) inhibits both tumour angiogenesis and metastasis. The Journal of pathology, 2014. **232**(4): p. 436-448.
130. Azemikhah, M., et al., Evaluation of discoidin domain receptor-2 (DDR2) expression level in normal, benign, and malignant human prostate tissues. Research in pharmaceutical sciences, 2015. **10**(4): p. 356-363.
131. Keely, P.J., et al., Alteration of collagen-dependent adhesion, motility, and morphogenesis by the expression of antisense alpha 2 integrin mRNA in mammary cells. Journal of cell science, 1995. **108 (Pt 2)**: p. 595-607.
132. Gabarra-Niecko, V., P.J. Keely, and M.D. Schaller, Characterization of an activated mutant of focal adhesion kinase: 'SuperFAK'. The Biochemical journal, 2002. **365**(Pt 3): p. 591-603.
133. Maeyama, M., et al., Switching in discoid domain receptor expressions in SLUG-induced epithelial-mesenchymal transition. Cancer, 2008. **113**(10): p. 2823-2831.
134. Logan, A.W., N. Ali, and M. Damian, Discoidin domain receptor 2 is a critical regulator of epithelial-mesenchymal transition. Matrix biology : journal of the International Society for Matrix Biology, 2011. **30**(4): p. 243-247.
135. Labrador, J.P., et al., The collagen receptor DDR2 regulates proliferation and its elimination leads to dwarfism. EMBO reports, 2001. **2**(5): p. 446-452.
136. Tingting, R., et al., Increased expression of discoidin domain receptor 2 (DDR2): a novel independent prognostic marker of worse outcome in breast cancer patients. Medical Oncology, 2013.
137. Olaso, E., et al., Discoidin domain receptor 2 regulates fibroblast proliferation and migration through the extracellular matrix in association with transcriptional activation of matrix metalloproteinase-2. The Journal of biological chemistry, 2002. **277**(5): p. 3606-3613.
138. Andrew, J.E., et al., Collective Epithelial Migration and Cell Rearrangements Drive Mammary Branching Morphogenesis. Developmental Cell, 2008. **14**(4).
139. Vesuna, F., et al., Twist is a transcriptional repressor of E-cadherin gene expression in breast cancer. Biochemical and biophysical research communications, 2008. **367**(2): p. 235-241.
140. Matthew, J.P., et al., Tensional homeostasis and the malignant phenotype. Cancer Cell, 2005. **8**(3).

141. Bragado, P., et al., *Microenvironments dictating tumor cell dormancy.* Recent results in cancer research. Fortschritte der Krebsforschung. Progrès dans les recherches sur le cancer, 2012. **195**: p. 25-39.
142. Adam, A.P., et al., Computational Identification of a p38SAPK-Regulated Transcription Factor Network Required for Tumor Cell Quiescence. Cancer Research, 2009. **69**(14): p. 5664-5672.
143. Derfoul, A., et al., Decreased microRNA-214 levels in breast cancer cells coincides with increased cell proliferation, invasion and accumulation of the Polycomb Ezh2 methyltransferase. Carcinogenesis, 2011. **32**(11): p. 1607-1614.
144. Wang, X., et al., miR-214 targets ATF4 to inhibit bone formation. Nature medicine, 2013. **19**(1): p. 93-100.
145. Li, K., et al., MicroRNA-214 suppresses gluconeogenesis by targeting activating transcriptional factor 4. The Journal of biological chemistry, 2015. **290**(13): p. 8185-8195.
146. Ishihara, S., et al., Substrate stiffness regulates temporary NF-κB activation via actomyosin contractions. Experimental cell research, 2013. **319**(19): p. 2916-2927.
147. Bredfeldt, J.S., et al., Computational segmentation of collagen fibers from second-harmonic generation images of breast cancer. Journal of biomedical optics, 2014. **19**(1): p. 16007.
148. Wolf, K. and P. Friedl, Molecular mechanisms of cancer cell invasion and plasticity. The British journal of dermatology, 2006. **154 Suppl 1**: p. 11-15.
149. Maaser, K., et al., Functional hierarchy of simultaneously expressed adhesion receptors: integrin alpha2beta1 but not CD44 mediates MV3 melanoma cell migration and matrix reorganization within three-dimensional hyaluronan-containing collagen matrices. Molecular biology of the cell, 1999. **10**(10): p. 3067-3079.
150. Wendt, M.K. and W.P. Schiemann, Therapeutic targeting of the focal adhesion complex prevents oncogenic TGF-β signaling and metastasis. Breast Cancer Research, 2009. **11**(5).
151. Wendt, M.K., J.A. Smith, and W.P. Schiemann, Transforming growth factor-β-induced epithelial–mesenchymal transition facilitates epidermal growth factor-dependent breast cancer progression. Oncogene, 2010. **29**(49): p. 6485-6498.
152. Wendt, M.K., et al., Down-regulation of epithelial cadherin is required to initiate metastatic outgrowth of breast cancer. Molecular Biology of the Cell, 2011. **22**(14): p. 2423-2435.
153. Reader, J., D. Holt, and A. Fulton, Prostaglandin E2 EP receptors as therapeutic targets in breast cancer. Cancer metastasis reviews, 2011. **30**(3-4): p. 449-463.
154. Hoellen, F., et al., Impact of cyclooxygenase-2 in breast cancer. Anticancer research, 2011. **31**(12): p. 4359-4367.
155. Jobin, C., et al., Specific NF-kappaB blockade selectively inhibits tumour necrosis factor-alpha-induced COX-2 but not constitutive COX-1 gene expression in HT-29 cells. Immunology, 1998. **95**(4): p. 537-543.
156. Howe, L.R., Inflammation and breast cancer. Cyclooxygenase/prostaglandin signaling and breast cancer. Breast cancer research : BCR, 2007. **9**(4): p. 210.
157. Gong, L., et al., Celecoxib pathways: pharmacokinetics and pharmacodynamics. Pharmacogenetics and genomics, 2012. **22**(4): p. 310-318.

158. Arber, N., et al., Celecoxib for the prevention of colorectal adenomatous polyps. … England Journal of …, 2006.
159. Castellone, M.D., et al., Prostaglandin E2 promotes colon cancer cell growth through a Gs-axin-beta-catenin signaling axis. Science (New York, N.Y.), 2005. **310**(5753): p. 1504-1510.
160. Xia, J.J.J., et al., Celecoxib inhibits β-catenin-dependent survival of the human osteosarcoma MG-63 cell line. The Journal of international medical research, 2010. **38**(4): p. 1294-1304.
161. Lee, N.O., et al., Dual action of a selective cyclooxygenase-2 inhibitor on vascular endothelial growth factor expression in human hepatocellular carcinoma cells: novel involvement of discoidin domain receptor 2. Journal of cancer research and clinical oncology, 2012. **138**(1): p. 73-84.
162. Onder, T.T., et al., Loss of E-cadherin promotes metastasis via multiple downstream transcriptional pathways. Cancer research, 2008. **68**(10): p. 3645-3654.
163. Larsen, M., M.L. Tremblay, and K.M. Yamada, Phosphatases in cell-matrix adhesion and migration. Nature reviews. Molecular cell biology, 2003. **4**(9): p. 700-711.
164. Mathur, R., et al., Targeting Wnt pathway in mantle cell lymphoma-initiating cells. Journal of hematology & oncology, 2015. **8**: p. 63.
165. Weigang, W., et al., Identification and Testing of a Gene Expression Signature of Invasive Carcinoma Cells within Primary Mammary Tumors. Cancer Research, 2004. **64**(23): p. 8585-8594.